APPENDIX G

EXPERIMENTAL DATA BASE FOR THE APPLICATION OF CSAU TO AN LBLOCA IN A WESTINGHOUSE FOUR-LOOP PWR

APPENDIX G

EXPERIMENTAL DATA BASE FOR THE APPLICATION OF CSAU TO AN LBLOCA IN A WESTINGHOUSE FOUR-LOOP PWR

The subject data base is described in Tables G-1 (SETs), G-2 (IETs), and G-3 (Facility Description).

The first two tables identify each test in the first two columns, followed by a description of the tests use in the CSAU procedure in the third through seventh columns. An entry in any one of these columns signifies the corresponding use, and additionally, cross-references the section, table, and/or figure in Part B that further describes its use.

Table G-3 defines facility-specific information important to the use shown in the first two tables.

Table G-1. Primary CSAU application for SET

FACILITY	TEST	PIRT	SCALING	PARAMETER RANGING	NODALIZATION	CODE & EXP ACCURACY	TEST REFERENCE
BCL	262XX		4.3.1	3.3.7	3.2.2		"Baseline Plenum Filing Behavior In a 2/15 Scale Model of a Four Loop PWR, Topical Report," R.A. Cudnit et al., NUREG/CR-0069, April 1978.
BCL	263XX		4.3.1	3.3.7	3.2.2		"Baseline Plenum Filing Behavior In a 2/15 Scale Model of a Four Loop PWR, Topical Report," R.A. Cudnit et al., NUREG/CR-0069, April 1978.
BCL	265XX		4.3.1	3.3.7			"Baseline Plenum Filing Behavior In a 2/15 Scale Model of a Four Loop PWR, Topical Report," R.A. Cudnit et al., NUREG/CR-0069, April 1978.
BCL	29111		4.3.1	3.3.7	3.2.2		"Baseline Plenum Filing Behavior In a 2/15 Scale Model of a Four Loop PWR, Topical Report," R.A. Cudnit et al., NUREG/CR-0069, April 1978.
BCL (60 psi)	ID 101 THRU 1212		4.3.1	3.3.7			R. A. Cudnik, et al.,"Penetration Behavior in a 1/15 Scale Model of a Four Loop Pressurized Water Reactor," BMI-NUREG-1973, June 1977.
BCL (60 psi)	ID 1301 THRU 1708		4.3.1	3.3.7			R. A. Cudnik, et al.,"Penetration Behavior in a 1/15 Scale Model of a Four Loop Pressurized Water Reactor," BMI-NUREG-1973, June 1977.
BCL (60 psi)	ID 1801 THRU 2008		4.3.1	3.3.7			R. A. Cudnik, et al.,"Penetration Behavior in a 1/15 Scale Model of a Four Loop Pressurized Water Reactor," BMI-NUREG-1973, June 1977.
BCL (60 psi)	ID 2101 THRU 2328		4.3.1	3.3.7			R. A. Cudnik, et al.,"Penetration Behavior in a 1/15 Scale Model of a Four Loop Pressurized Water Reactor," BMI-NUREG-1973, June 1977.
BCL (60 psi)	ID 2401 THRU 2621		4.3.1	3.3.7			R. A. Cudnik, et al.,"Penetration Behavior in a 1/15 Scale Model of a Four Loop Pressurized Water Reactor," BMI-NUREG-1973, June 1977.

Table G-1. (continued)

FACILITY	TEST	PIRT	SCALING	PARAMETER RANGING	NODALIZATION	CODE & EXP ACCURACY	TEST REFERENCE
BCL (60 psi)	ID 2701 THRU 3329		4.3.1	3.3.7			R. A. Cudnik, et al.,"Penetration Behavior in a 1/15 Scale Model of a Four Loop Pressurized Water Reactor," BMI-NUREG-1973, June 1977.
BCL (60 psi)	ID 3401 THRU 3710		4.3.1	3.3.7			R. A. Cudnik, et al.,"Penetration Behavior in a 1/15 Scale Model of a Four Loop Pressurized Water Reactor," BMI-NUREG-1973, June 1977.
BCL (60 psi)	ID 3801 THRU 3542		4.3.1	3.3.7			R. A. Cudnik, et al.,"Penetration Behavior in a 1/15 Scale Model of a Four Loop Pressurized Water Reactor," BMI-NUREG-1973, June 1977.
BECKER	248-277			Fig. 22			K.M. Becker et al., "An Experimental Investigation of Post-Dryout Heat Transfer," KTH-NEL-33, May 1983.
BECKER	309-334			Fig. 22			K.M. Becker et al., "An Experimental Investigation of Post-Dryout Heat Transfer," KTH-NEL-33, May 1983.
BECKER	424,425, 431-443			Fig. 22			K.M. Becker et al., "An Experimental Investigation of Post-Dryout Heat Transfer," KTH-NEL-33, May 1983.
BECKER	453-472			Fig. 22			K.M. Becker et al., "An Experimental Investigation of Post-Dryout Heat Transfer," KTH-NEL-33, May 1983.
BENNETT	5240-42,5261 ,5262,5283			Fig. 22			A.W. Bennett et al.,"Heat Transfer to Steam-Water Mixtures Flowing in Uniformly Heated Tubes in Which the Critical Heat Flux Has Been Exceeded," AERE-RE373,
BENNETT	5304,05,45-4 7,23-25,52			Fig. 22			A.W. Bennett et al.,"Heat Transfer to Steam-Water Mixtures Flowing in Uniformly Heated Tubes in Which the Critical Heat Flux Has Been Exceeded," AERE-RE373,

Table G-1. (continued)

FACILITY	TEST	PIRT	SCALING	PARAMETER RANGING	NODALIZATION	CODE & EXP ACCURACY	TEST REFERENCE
BENNETT	5355,58,64,68,69,			Fig. 22			A.W. Bennett et al.,"Heat Transfer to Steam-Water Mixtures Flowing in Uniformly Heated Tubes in Which the Critical Heat Flux Has Been Exceeded," AERE-RE373,
BENNETT	5417,34,44			Fig. 22			A.W. Bennett et al.,"Heat Transfer to Steam-Water Mixtures Flowing in Uniformly Heated Tubes in Which the Critical Heat Flux Has Been Exceeded," AERE-RE373,
CCTF	C1-01 (010)	2.3					"Quick Look Report On Large Scale Reflood Test-01 - CCTF Test C1-01 (Run 010)," JAERI-memo-8453, August 1979.
CCTF	C1-02 (011)	2.3					"Quick Look Report On Large Scale Reflood Test-02 - CCTF Test C1-02 (Run 011)," JAERI-memo-8530, October 1979.
CCTF	C1-03 (012)	2.3					"Quick Look Report On Large Scale Reflood Test-03 - CCTF Test C1-03 (Run 012)," JAERI-memo-8539, November 1979.
CCTF	C1-04 (013)	2.3					"Quick Look Report On Large Scale Reflood Test-04 - CCTF Test C1-04 (Run 013)," JAERI-memo-8685, February 1980.
CCTF	C1-05 (014)	2.3					"Quick Look Report On Large Scale Reflood Test-05 - CCTF Test C1-05 (Run 014)," JAERI-memo-8696, February 1980.
CCTF	C1-06 (015)	2.3	Fig. 31				"Quick Look Report On Large Scale Reflood Test-06 - CCTF Test C1-06 (Run 015)," JAERI-memo-8990, July 1980.
CCTF	C1-07 (016)	2.3					"Quick Look Report On Large Scale Reflood Test-07 - CCTF Test C1-07 (Run 016)," JAERI-memo-8991, July 1980.

Table G-1. (continued)

FACILITY	TEST	PIRT	SCALING	PARAMETER RANGING	NODALIZATION	CODE & EXP ACCURACY	TEST REFERENCE
CCTF	C1-08 (017)	2.3					"Quick Look Report On Large Scale Reflood Test-08 - CCTF Test C1-08 (Run 017)," JAERI-memo-8972, July 1980.
CCTF	C1-09 (018)	2.3	Fig 3.1				"Quick Look Report On Large Scale Reflood Test-09 - CCTF Test C1-09 (Run 018)," JAERI-memo-9125, September 1980.
CCTF	C1-10 (019)	2.3					"Quick Look Report On Large Scale Reflood Test-10 - CCTF Test C1-10 (Run 019)," JAERI-memo-9207, November 1980.
CCTF	C1-11 (020)	2.3	Fig. 31				"Quick Look Report On Large Scale Reflood Test-11 - CCTF Test C1-11 (Run 020)," JAERI-memo-9208, November 1980.
CCTF	C1-12 (021)	2.3					"Quick Look Report On Large Scale Reflood Test-12 - CCTF Test C1-12 (Run 021)," JAERI-memo-9270, January 1981.
CCTF	C1-13 (022)	2.3	Fig. 31				"Quick Look Report On Large Scale Reflood Test-13 - CCTF Test C1-13 (Run 022)," JAERI-memo-9282, January 1981.
CCTF	C1-14 (023)	2.3	Fig. 31				"Quick Look Report On Large Scale Reflood Test-14 - CCTF Test C1-14 (Run 023)," JAERI-memo-9305, February 1981.
CCTF	C1-15 (024)	2.3					"Quick Look Report On Large Scale Reflood Test-15 - CCTF Test C1-15 (Run 024)," JAERI-memo-9329, February 1981.
CCTF	C1-16 (025)	2.3	Fig. 31				"Quick Look Report On Large Scale Reflood Test-16 - CCTF Test C1-16 (Run 025)," JAERI-memo-9349, March 1981.

Table G-1. (continued)

FACILITY	TEST	PIRT	SCALING	PARAMETER RANGING	NODALIZATION	CODE & EXP ACCURACY	TEST REFERENCE
CCTF	C1-18 (037)	2.3					"Quick Look Report On Large Scale Reflood Test-18 - CCTF Test C1-18 (Run 037)," JAERI-memo-9713, October 1981.
CCTF	C1-19 (038)	2.3					"Quick Look Report On Large Scale Reflood Test-19 - CCTF Test C1-19 (Run 038)," JAERI-memo-9767, November 1981.
CCTF	C1-20 (039)	2.3					"Quick Look Report On Large Scale Reflood Test-20 - CCTF Test C1-20 (Run 039)," JAERI-memo-9768, November 1981.
CCTF	C1-21 (040)	2.3	Fig. 31				"Quick Look Report On Large Scale Reflood Test-21 - CCTF Test C1-21 (Run 040)," JAERI-memo-9903, January 1982.
CCTF	C1-SH5(009)	2.3	Fig. 31				"Quick Look Report On Large Scale Reflood Test-09 - CCTF Test C1-SH5 (Run 009)," JAERI-memo-8933, June 1980.
CCTF	C2-01 (055)	2.3					"Quick Look Report On CCTF Core-II Reflood Test, C2-1 (Run 55)," JAERI-memo-57-392, December 1982.
CCTF	C2-02 (056)	2.3					"Quick Look Report On CCTF Core-II Reflood Test, C2-2 (Run 56)," JAERI-memo-57-393, December 1982.
CCTF	C2-03 (061)	2.3					"Quick Look Report On CCTF Core-II Reflood Test, C2-3 (Run 61)," JAERI-memo-58-460, January 1984.
CCTF	C2-04 (062)	2.3	Fig. 31				"Quick Look Report On CCTF Core-II Reflood Test, C2-4 (Run 62)," JAERI-memo-58-479, January 1984.

Table G-1. (continued)

FACILITY	TEST	PIRT	SCALING	PARAMETER RANGING	NODALIZATION	CODE & EXP ACCURACY	TEST REFERENCE
CCTF	C2-05 (063)	2.3	Fig. 31				"Quick Look Report On CCTF Core-II Reflood Test, C2-5 (Run 63)," JAERI-memo-59-046, February 1984.
CCTF	C2-06 (064)	2.3	Fig. 31				"Quick Look Report On CCTF Core-II Reflood Test, C2-6 (Run 64)," JAERI-memo-59-012, February 1984.
CCTF	C2-07 (065)	2.3					"Quick Look Report On CCTF Core-II Reflood Test, C2-7 (Run 65)," JAERI-memo-59-047, February 1984.
CCTF	C2-08 (067)	2.3	Fig. 31				"Quick Look Report On CCTF Core-II Reflood Test, C2-8 (Run 67)," JAERI-memo-59-028, February 1984.
CCTF	C2-09 (068)	2.3	Fig. 31				"Quick Look Report On CCTF Core-II Reflood Test, C2-9 (Run 68)," JAERI-memo-59-048, February 1984.
CCTF	C2-10 (069)	2.3	Fig. 31				"Quick Look Report On CCTF Core-II Reflood Test, C2-10 (Run 69)," JAERI-memo-59-029, February 1984.
CCTF	C2-11 (070)	2.3	Fig. 31				"Quick Look Report On CCTF Core-II Reflood Test, C2-11 (Run 70)," JAERI-memo-59-013, February 1984.
CCTF	C2-12 (071)	2.3		3.3		Fig. 28	"Quick Look Report On CCTF Core-II Reflood Test, C2-12 (Run 71)," JAERI-memo-59-326, October 1984.
CCTF	C2-13 (072)	2.3				Fig. 28	"Quick Look Report On CCTF Core-II Reflood Test, C2-13 (Run 72)," JAERI-memo-59-416, January 1985.

Table G-1. (continued)

FACILITY	TEST	PIRT	SCALING	PARAMETER RANGING	NODALIZATION	CODE & EXP ACCURACY	TEST REFERENCE
CCTF	C2-14 (074)	2.3					"Quick Look Report On CCTF Core-II Reflood Test, C2-14 (Run 74)," JAERI-memo-59-352, October 1984.
CCTF	C2-15 (075)	2.3	Fig. 31	3.3			"Quick Look Report On CCTF Core-II Reflood Test, C2-15 (Run 75)," JAERI-memo-60-255, September 1985.
CCTF	C2-16 (076)	2.3				Fig. 28	"Quick Look Report On CCTF Core-II Reflood Test, C2-16 (Run 76)," JAERI-memo-60-142, June 1985.
CCTF	C2-17 (077)	2.3					"Quick Look Report On CCTF Core-II Reflood Test, C2-17 (Run 77)," JAERI-memo-61-136, May 1986.
CCTF	C2-18 (078)	2.3				Fig. 28	"Quick Look Report On CCTF Core-II Reflood Test, C2-18 (Run 78)," JAERI-memo-60-372, December 1985.
CCTF	C2-AA1(057)	2.3					"Quick Look Report On CCTF Core-II Reflood Test, C2-AA1 (Run 57)," JAERI-memo-58-415, November 1983.
CCTF	C2-AA2(058)	2.3					"Quick Look Report On CCTF Core-II Reflood Test, C2-AA2 (Run 58)," JAERI-memo-58-386, October 1983.
CE	209-214			3.3.2			"PUMP TWO-PHASE PERFORMANCE PROGRAM," Combustion Engineering, Inc., ERPI NP-1556, September 1980.
CE	403-406			3.3.2			"PUMP TWO-PHASE PERFORMANCE PROGRAM," Combustion Engineering, Inc., ERPI NP-1556, September 1980.

Table G-1. (continued)

FACILITY	TEST	PIRT	SCALING	PARAMETER RANGING	NODALIZATION	CODE & EXP ACCURACY	TEST REFERENCE
CREARE	2.5032 thru 2.5046	2.3		3.3.7			"1/5 Scale Counter Current Flow Data Presentation and Discussion," C.J. Crowley, P.H. Rothe, R.B. Sam, NUREG/CR-2106, November 1981.
CREARE	2.5047 THRU 2.5059	2.3					"1/5 Scale Counter Current Flow Data Presentation and Discussion," C.J. Crowley, P.H. Rothe, R.B. Sam, NUREG/CR-2106, November 1981.
CREARE	2.5062 thru 2.5070	2.3					"1/5 Scale Counter Current Flow Data Presentation and Discussion," C.J. Crowley, P.H. Rothe, R.B. Sam, NUREG/CR-2106, November 1981.
CREARE	2.5104 thru 2.5117	2.3					"1/5 Scale Counter Current Flow Data Presentation and Discussion," C.J. Crowley, P.H. Rothe, R.B. Sam, NUREG/CR-2106, November 1981.
CREARE	2.5122 thru 2.5232	2.3					"1/5 Scale Counter Current Flow Data Presentation and Discussion," C.J. Crowley, P.H. Rothe, R.B. Sam, NUREG/CR-2106, November 1981.
CREARE	2.5133 thru 2.5141	2.3					"1/5 Scale Counter Current Flow Data Presentation and Discussion," C.J. Crowley, P.H. Rothe, R.B. Sam, NUREG/CR-2106, November 1981.
CREARE PF	Runs A1 THRU A49	2.3		3.3.7			"ECC Delivery Study: Experimental Results and Discussion," Crowley, C.T., Block, J.A., CREARE TN-217, October 1975.
CREARE PF	Runs B1 THRU B35	2.3		3.3.7			"ECC Delivery Study: Experimental Results and Discussion," Crowley, C.T., Block, J.A., CREARE TN-217, October 1975.
CREARE PF	Runs D1 THRU D21	2.3		3.3.7			"ECC Delivery Study: Experimental Results and Discussion," Crowley, C.T., Block, J.A., CREARE TN-217, October 1975.

Table G-1. (continued)

FACILITY	TEST	PIRT	SCALING	PARAMETER RANGING	NODALIZATION	CODE & EXP ACCURACY	TEST REFERENCE
CREARE (PUMP)	1145		3.3.2	3.3.2			"Model Pump Performance Program," W.L. Swift, EPRI-NP-2379 (May 1982).
CREARE (PUMP)	1232		3.3.2	3.3.2			"Model Pump Performance Program," W.L. Swift, EPRI-NP-2379 (May 1982).
DARTMOUTH	EXPER. 1				3.2		H.J. Richter, et al., "Effect of Scale On Two-Phase Countercurrent Flow Flooding," NUREG/CR-0312, June 1979.
DARTMOUTH	EXPER. 2				3.2		H.J. Richter, et al., "Effect of Scale On Two-Phase Countercurrent Flow Flooding," NUREG/CR-0312, June 1979.
DHIR				Fig. 22			V.K. Dhir et al., "Subcooled Film Boiling Heat Transfer from Spheres," Nuc. Eng. Des., 47, 1978, pp. 49-66.
FLECHT	1002		Fig. 31				F.F. Cadek et al.,"PWR FLECHT FINAL REPORT," WCAP-7665, April 1971.
FLECHT	11003		Fig. 31				E.R. Rosal et al., "FLECHT Low Flooding Rate Skewed Test Series Data Report," WCAP-9108, May 1977.
FLECHT	13404		Fig. 31				E.R. Rosal et al., "FLECHT Low Flooding Rate Skewed Test Series Data Report," WCAP-9108, May 1977.
FLECHT	15305		Fig. 31				E.R. Rosal et al., "FLECHT Low Flooding Rate Skewed Test Series Data Report," WCAP-9108, May 1977.

Table G-1. (continued)

FACILITY	TEST	PIRT	SCALING	PARAMETER RANGING	NODALIZATION	CODE & EXP ACCURACY	TEST REFERENCE
FLECHT	15423		Fig. 31				E.R. Rosal et al., "FLECHT Low Flooding Rate Skewed Test Series Data Report," WCAP-9108, May 1977.
FLECHT	17201		Fig. 31		3.2		E.R. Rosal et al., "FLECHT Low Flooding Rate Skewed Test Series Data Report," WCAP-9108, May 1977.
FLECHT	17302		Fig. 31				E.R. Rosal et al., "FLECHT Low Flooding Rate Skewed Test Series Data Report," WCAP-9108, May 1977.
FLECHT	4831				3.2		"FLECHT LOW FLOODING RATE COSINE TEST SERIES DATA REPORT," Rosal, E.R. et al., WCAP-8651, December 1975.
FLECHT-SEASET	30619	2.3					M.J. Loftus et al., "PWR FLECHT-SEASET Unblocked Bundle Forced and Gravity Reflood Task Data Report," NUREG/CR-1532, Vols. 1 and 2, WCAP-9699,
FLECHT-SEASET	30817	2.3	Fig. 31				M.J. Loftus et al., "PWR FLECHT-SEASET Unblocked Bundle Forced and Gravity Reflood Task Data Report," NUREG/CR-1532, Vols. 1 and 2, WCAP-9699,
FLECHT-SEASET	31203	2.3					M.J. Loftus et al., "PWR FLECHT-SEASET Unblocked Bundle Forced and Gravity Reflood Task Data Report," NUREG/CR-1532, Vols. 1 and 2, WCAP-9699,
FLECHT-SEASET	31302	2.3					M.J. Loftus et al., "PWR FLECHT-SEASET Unblocked Bundle Forced and Gravity Reflood Task Data Report," NUREG/CR-1532, Vols. 1 and 2, WCAP-9699,
FLECHT-SEASET	31504	2.3	Fig. 31		3.2		M.J. Loftus et al., "PWR FLECHT-SEASET Unblocked Bundle Forced and Gravity Reflood Task Data Report," NUREG/CR-1532, Vols. 1 and 2, WCAP-9699,

Table G-1. (continued)

FACILITY	TEST	PIRT	SCALING	PARAMETER RANGING	NODALIZATION	CODE & EXP ACCURACY	TEST REFERENCE
FLECHT-SEASET	31701	2.3	Fig. 31				M.J. Loftus et al., "PWR FLECHT-SEASET Unblocked Bundle Forced and Gravity Reflood Task Data Report," NUREG/CR-1532, Vols. 1 and 2, WCAP-9699,
FLECHT-SEASET	31805	2.3					M.J. Loftus et al., "PWR FLECHT-SEASET Unblocked Bundle Forced and Gravity Reflood Task Data Report," NUREG/CR-1532, Vols. 1 and 2, WCAP-9699,
JANSEN	301-310			Fig. 22			E. Jansen and J.A. Kervinen, "Film Boiling and Rewetting," Nedo-20975, 75 NED 50, General Electric, August 1975.
JANSEN	601-610			Fig. 22			E. Jansen and J.A. Kervinen, "Film Boiling and Rewetting," Nedo-20975, 75 NED 50, General Electric, August 1975.
LEHIGH UNIVERSITY	100			Fig. 22			D.G. Evans, et al., "Measurement of Axially Varying Nonequilibrium in Post-Critical-Heat-Flux Boiling in a Vertical Tube." NUREG/CR-3363 TS-831-1, Lehigh
LEHIGH UNIVERSITY	124			Fig. 22			D.G. Evans, et al., "Measurement of Axially Varying Nonequilibrium in Post-Critical-Heat-Flux Boiling in a Vertical Tube," NUREG/CR-3363 TS-831-1, Lehigh
MARVIKEN	12			Fig. 21			"The Marviken Full Scale Critical Flow Tests, Volume 1: Summary Report," EPRI-NP-2370 (MAY 1982).
MARVIKEN	13			Fig. 21	3.2		"Results From Test 13, The Marviken Full Scale Critical Flow Tests," Joint Reactor Safety Experiment in the Marviken Power Station, Sweden, Marviken report
MARVIKEN	15			Fig. 21			"The Marviken Full Scale Critical Flow Tests, Volume 1: Summary Report," EPRI-NP-2370 (MAY 1982).

Table G-1. (continued)

FACILITY	TEST	PIRT	SCALING	PARAMETER RANGING	NODALIZATION	CODE & EXP ACCURACY	TEST REFERENCE
MARVIKEN	16			Fig. 21			"The Marviken Full Scale Critical Flow Tests, Volume 1: Summary Report," EPRI-NP-2370 (MAY 1982).
MARVIKEN	17			Fig. 21			"The Marviken Full Scale Critical Flow Tests, Volume 1: Summary Report," EPRI-NP-2370 (MAY 1982).
MARVIKEN	18, 19, 21, 25			Fig. 21			"The Marviken Full Scale Critical Flow Tests, Volume 1: Summary Report," EPRI-NP-2370 (MAY 1982).
MARVIKEN	20			Fig. 21	3.2		"Results From Test 20, The Marviken Full Scale Critical Flow Tests," Joint Reactor Safety Experiment in the Marviken Power Station, Sweden, Marviken report
MARVIKEN	22			Fig. 21	3.2		"Results From Test 22, The Marviken Full Scale Critical Flow Tests," Joint Reactor Safety Experiment in the Marviken Power Station, Sweden, Marviken report
MARVIKEN	24			Fig. 21	3.2		"Results From Test 24, The Marviken Full Scale Critical Flow Tests," Joint Reactor Safety Experiment in the Marviken Power Station, Sweden, Marviken report
MARVIKEN	4				3.2		"Results From Test 4, The Marviken Full Scale Critical Flow Tests," Joint Reactor Safety Experiment in the Marviken Power Station, Sweden, Marviken report
NEPTUNUS	Y05				3.2		"TRAC-PF1/MOD1 Independent Assessment: NEPTUNUS Pressurizer Test Y05," A.C. Peterson, NUREG/CR-3919, SAND84-1534, December 1984.
NORTHWESTERN UNIVERSITY	ALL TESTS				3.2		I. Dilber, et al., "Countercurrent Steam/Water Flow Above a Perforated Plate-Vertical Injection of Water," NUREG/CR-2323, September 1981.

Table G-1. (continued)

FACILITY	TEST	PIRT	SCALING	PARAMETER RANGING	NODALIZATION	CODE & EXP ACCURACY	TEST REFERENCE
ORNL	3.07.9 K-M, P			Fig. 22			G.L. Yoder et al., "Dispersed Flow Film Boiling in Rod Bundle Geometry--Steady State Heat Transfer Data and Correlation Comparisons," NUREG/CR-2435,
ORNL	3.07.9 N, X			Fig. 22			G.L. Yoder et al., "Dispersed Flow Film Boiling in Rod Bundle Geometry--Steady State Heat Transfer Data and Correlation Comparisons," NUREG/CR-2435,
PBF-LLR	LLR-3		Fig. 30				D.J. Varacalle, jr., R.W. Garner, "PBF/LOFT Lead Rod Program Tests LLR-3, -4, -5 Quick Look Report," TFBP-TR-315, April 1979.
PBF-LLR	LLR-4		Fig. 30				D.J. Varacalle, jr., R.W. Garner, "PBF/LOFT Lead Rod Program Tests LLR-3, -4, -5 Quick Look Report," TFBP-TR-315, April 1979.
PBF-LLR	LLR-4R		Fig. 30				D.J. Varacalle, jr., R.W. Garner, "PBF/LOFT Lead Rod Program Test LLR-4A Quick Look Report," TFBP-TR-320, June 1979.
PBF-LLR	LLR-5		Fig. 30				D.J. Varacalle, jr., R.W. Garner, "PBF/LOFT Lead Rod Program Tests LLR-3, -4, -5 Quick Look Report," TFBP-TR-315, April 1979.
SCTF	S1-01 (507)	2.3					"Data Report on Large Scale Reflood Test, SCTF Test S1-01 (Run 507)," JAERI-memo-9976, March 1982.
SCTF	S1-02 (508)	2.3					"Data Report on Large Scale Reflood Test, SCTF Test S1-02 (Run 508)," JAERI-memo-9977, March 1982.
SCTF	S1-03 (509)	2.3					"Data Report on Large Scale Reflood Test, SCTF Test S1-03 (Run 509)," JAERI-memo-57-318, November 1982.

Table G-1. (continued)

FACILITY	TEST	PIRT	SCALING	PARAMETER RANGING	NODALIZATION	CODE & EXP ACCURACY	TEST REFERENCE
SCTF	S1-04 (510)	2.3					"Data Report on Large Scale Reflood Test, SCTF Test S1-04 (Run 510)," JAERI-memo-57-319, November 1982.
SCTF	S1-05 (511)	2.3					"Data Report on Large Scale Reflood Test, SCTF Test S1-05 (Run 511)," JAERI-memo-57-320, November 1982.
SCTF	S1-06 (512)	2.3					"Data Report on Large Scale Reflood Test, SCTF Test S1-06 (Run 512)," JAERI-memo-57-350, November 1982.
SCTF	S1-07 (513)	X					"Data Report on Large Scale Reflood Test, SCTF Test S1-07 (Run 513)," JAERI-memo-57-351, November 1982.
SCTF	S1-08 (514)	2.3					"Data Report on Large Scale Reflood Test, SCTF Test S1-08 (Run 514)," JAERI-memo-57-354, November 1982.
SCTF	S1-09 (515)	2.3					"Data Report on Large Scale Reflood Test, SCTF Test S1-09 (Run 515)," JAERI-memo-57-355, November 1982.
SCTF	S1-10 (516)	2.3					"Data Report on Large Scale Reflood Test, SCTF Test S1-10 (Run 516)," JAERI-memo-57-365, December 1982.
SCTF	S1-11 (517)	2.3					"Data Report on Large Scale Reflood Test, SCTF Test S1-11 (Run 517)," JAERI-memo-57-372, December 1982.
SCTF	S1-12 (518)	2.3					"Data Report on Large Scale Reflood Test, SCTF Test S1-12 (Run 518)," JAERI-memo-57-380, December 1982.

Table G-1. (continued)

FACILITY	TEST	PIRT	SCALING	PARAMETER RANGING	NODALIZATION	CODE & EXP ACCURACY	TEST REFERENCE
SCTF	S1-13 (519)	2.3	Fig. 31				"Data Report on Large Scale Reflood Test, SCTF Test S1-13 (Run 519)," JAERI-memo-57-401, December 1982.
SCTF	S1-14 (520)	2.3					"Data Report on Large Scale Reflood Test, SCTF Test S1-14 (Run 520)," JAERI-memo-57-381, December 1982.
SCTF	S1-15 (521)	2.3					"Data Report on Large Scale Reflood Test, SCTF Test S1-15 (Run 521)," JAERI-memo-57-382, December 1982.
SCTF	S1-16 (522)	2.3					"Data Report on Large Scale Reflood Test, SCTF Test S1-16 (Run 522)," JAERI-memo-57-384, December 1982.
SCTF	S1-17 (523)	2.3					"Data Report on Large Scale Reflood Test, SCTF Test S1-17 (Run 523)," JAERI-memo-57-385, December 1982.
SCTF	S1-18 (524)	2.3					"Data Report on Large Scale Reflood Test, SCTF Test S1-18 (Run 524)," JAERI-memo-57-402, December 1982.
SCTF	S1-19 (525)	2.3					"Data Report on Large Scale Reflood Test, SCTF Test S1-19 (Run 525)," JAERI-memo-57-403, December 1982.
SCTF	S1-20 (530)	2.3					"Data Report on Large Scale Reflood Test, SCTF Test S1-20 (Run 530)," JAERI-memo-58-298, September 1983.
SCTF	S1-22 (532)	2.3					"Data Report on Large Scale Reflood Test, SCTF Test S1-22 (Run 532)," JAERI-memo-58-299, September 1983.

Table G-1. (continued)

FACILITY	TEST	PIRT	SCALING	PARAMETER RANGING	NODALIZATION	CODE & EXP ACCURACY	TEST REFERENCE
SCTF	S1-23 (536)	2.3					"Data Report on Large Scale Reflood Test, SCTF Test S1-23 (Run 536)," JAERI-memo-58-300, September 1983.
SCTF	S1-24 (537)	2.3	Fig. 31				"Data Report on Large Scale Reflood Test, SCTF Test S1-24 (Run 537)," JAERI-memo-58-301, September 1983.
SCTF	S1-BH3 (528)	2.3					"Data Report on Large Scale Reflood Test, SCTF Test S2-BH3 (Run 528)," JAERI-memo-58-296, September 1983.
SCTF	S1-BH4 (529)	2.3					"Data Report on Large Scale Reflood Test, SCTF Test S1-BH4 (Run 529)," JAERI-memo-58-297, September 1983.
SCTF	S2-01 (606)	2.3					"Data Report on Large Scale Reflood Test, SCTF Test S2-01 (Run 606)," JAERI-memo-59-288, September 1984.
SCTF	S2-02 (607)	2.3					"Data Report on Large Scale Reflood Test, SCTF Test S2-02 (Run 607)," JAERI-memo-59-283, September 1984.
SCTF	S2-03 (608)	2.3					"Data Report on Large Scale Reflood Test, SCTF Test S2-03 (Run 608)," JAERI-memo-59-432, January 1985.
SCTF	S2-04 (609)	2.3					"Data Report on Large Scale Reflood Test, SCTF Test S2-04 (Run 609)," JAERI-memo-59-433, January 1985.
SCTF	S2-05 (610)	2.3					"Data Report on Large Scale Reflood Test, SCTF Test S2-05 (Run 610)," JAERI-memo-59-434, January 1985.

Table G-1. (continued)

FACILITY	TEST	PIRT	SCALING	PARAMETER RANGING	NODALIZATION	CODE & EXP ACCURACY	TEST REFERENCE
SCTF	S2-06 (611)	2.3		3.3		Fig. 28	"Data Report on Large Scale Reflood Test, SCTF Test S2-06 (Run 611)," JAERI-memo-59-435, February 1985.
SCTF	S2-07 (612)	2.3	Fig. 31				"Data Report on Large Scale Reflood Test, SCTF Test S2-07 (Run 612)," JAERI-memo-59-436, February 1985.
SCTF	S2-08 (613)	2.3	Fig. 31	3.3		Fig. 28	"Data Report on Large Scale Reflood Test, SCTF Test S2-08 (Run 613)," JAERI-memo-59-437, February 1985.
SCTF	S2-09 (614)	2.3				Fig. 28	"Data Report on Large Scale Reflood Test, SCTF Test S2-09 (Run 614)," JAERI-memo-59-438, February 1985.
SCTF	S2-10 (615)	2.3					"Data Report on Large Scale Reflood Test, SCTF Test S2-10 (Run 615)," JAERI-memo-60-110, May 1985.
SCTF	S2-11 (616)	2.3	Fig. 31				"Data Report on Large Scale Reflood Test, SCTF Test S2-11 (Run 616)," JAERI-memo-60-111, May 1985.
SCTF	S2-12 (617)	2.3	Fig. 31				"Data Report on Large Scale Reflood Test, SCTF Test S2-12 (Run 617)," JAERI-memo-60-112, May 1985.
SCTF	S2-13 (618)	2.3					"Data Report on Large Scale Reflood Test, SCTF Test S2-13 (Run 618)," JAERI-memo-60-113, May 1985.
SCTF	S2-14 (619)	2.3	Fig. 31				"Data Report on Large Scale Reflood Test, SCTF Test S2-14 (Run 619)," JAERI-memo-60-114, May 1985.

Table G-1. (continued)

FACILITY	TEST	PIRI	SCALING	PARAMETER RANGING	NODALIZATION	CODE & EXP ACCURACY	TEST REFERENCE
SCTF	S2-15 (620)	2.3	Fig. 31				"Data Report on Large Scale Reflood Test, SCTF Test S2-15 (Run 620)," JAERI-memo-60-258, October 1985.
SCTF	S2-16 (621)	2.3	Fig. 31				"Data Report on Large Scale Reflood Test, SCTF Test S2-16 (Run 621)," JAERI-memo-60-259, October 1985.
SCTF	S2-17 (622)	2.3	Fig. 31				"Data Report on Large Scale Reflood Test, SCTF Test S2-17 (Run 622)," JAERI-memo-60-260, October 1985.
SCTF	S2-18 (623)	2.3	Fig. 31				"Data Report on Large Scale Reflood Test, SCTF Test S2-18 (Run 623)," JAERI-memo-60-268, October 1985.
SCTF	S2-19 (624)	2.3					"Data Report on Large Scale Reflood Test, SCTF Test S2-19 (Run 624)," JAERI-memo-60-269, October 1985.
SCTF	S2-21 (626)	2.3	Fig. 31				"Data Report on Large Scale Reflood Test, SCTF Test S2-21 (Run 626)," JAERI-memo-60-270, October 1985.
SCTF	S2-AC1 (601)			3.3			"Study on ECC Injection Modes In Reflood Tests With SCTF Core II," Akira Ohnuki et al., JAERI memo 61-115, March 1986.
SCTF	S2-BH1 (604)	2.3		3.3		Fig. 28	"Data Report on Large Scale Reflood Test, SCTF Test S2-BH1 (Run 604)," JAERI-memo-59-282, September 1984.
SCTF	S2-BH2 (605)	2.3		3.3		Fig. 28	"Data Report on Large Scale Reflood Test, SCTF Test S2-BH2 (Run 605)," JAERI-memo-59-287, September 1984.

Table G-1. (continued)

FACILITY	TEST	PIRT	SCALING	PARAMETER RANGING	NODALIZATION	CODE & EXP ACCURACY	TEST REFERENCE
SCTF	S3-01 (705)	2.3					"Data Report on Large Scale Reflood Test, SCTF Test S3-01 (Run 705)," JAERI-memo-62-117, March 1987.
SCTF	S3-02 (706)	2.3					"Data Report on Large Scale Reflood Test, SCTF Test S3-02 (Run 706)," JAERI-memo-62-118, March 1987.
SCTF	S3-03 (707)	2.3					"Data Report on Large Scale Reflood Test, SCTF Test S3-03 (Run 707)," JAERI-memo-62-119, March 1987.
SCTF	S3-04 (708)	2.3					"Data Report on Large Scale Reflood Test, SCTF Test S3-04 (Run 708)," JAERI-memo-62-120, March 1987.
SCTF	S3-05 (709)	2.3					"Data Report on Large Scale Reflood Test, SCTF Test S3-05 (Run 709)," JAERI-memo-62-121, March 1987.
SCTF	S3-06 (710)	2.3					"Data Report on Large Scale Reflood Test, SCTF Test S3-06 (Run 710)," JAERI-memo-62-122, March 1987.
SCTF	S3-07 (711)	2.3					"Data Report on Large Scale Reflood Test, SCTF Test S3-07 (Run 711)," JAERI-memo-62-123, March 1987.
SCTF	S3-08 (712)	2.3					"Data Report on Large Scale Reflood Test, SCTF Test S3-08 (Run 712)," JAERI-memo-62-124, March 1987.
SCTF	S3-09 (713)	2.3					"Data Report on Large Scale Reflood Test, SCTF Test S3-09 (Run 713)," JAERI-memo-62-125, March 1987.

Table G-1. (continued)

FACILITY	TEST	PIRT	SCALING	PARAMETER RANGING	NODALIZATION	CODE & EXP ACCURACY	TEST REFERENCE
SCTF	S3-10 (714)	2.3	Fig. 31				"Data Report on Large Scale Reflood Test, SCTF Test S3-10 (Run 714)," JAERI-memo-62-125, March 1987.
SCTF	S3-SH1 (703)	2.3					"Data Report on Large Scale Reflood Test, SCTF Test S3-SH1 (Run 703)," JAERI-memo-62-115, March 1987.
SCTF	S3-SH2 (704)	2.3					"Data Report on Large Scale Reflood Test, SCTF Test S3-SH2 (Run 704)," JAERI-memo-62-116, March 1987.
SEMISCALE	S-03-1 AND S-03-3	2.3	Fig. 30				"Experimental Data Report For Semiscale MOD-1 Tests S-03-1, Thru S-03-4 (REFLOOD HEAT TRANSFER TESTS)," H. Crapo, M. Jensen, K. Sackett,
SEMISCALE	S-03-2 AND S-03-4	2.3	Fig. 30				"Experimental Data Report For Semiscale MOD-1 Tests S-03-1, Thru S-03-4 (REFLOOD HEAT TRANSFER TESTS)," H. Crapo, M. Jensen, K. Sackett,
SEMISCALE	S-03-5 Thru S-03-8	2.3					"Experimental Data Report For Semiscale MOD-1 Tests S-03-5, S-03-6, S-03-7, and S-03-8 (REFLOOD HEAT TRANSFER TESTS)," H. Crapo et al., ANCR-NUREG-1307,
SEMISCALE	S-03-A THRU S-03-D	2.3	Fig. 30				"Experimental Data Report For Semiscale MOD-1 Tests S-03-A, S-03-B, S-03-C, S-03-D (REFLOOD HEAT TRANSFER TESTS)," H. Crapo, M. Jensen, K. Sackett,
SEMISCALE	S-07-4		Fig. 30		3.2		"Experimental Data Report For Semiscale MOD-3 Reflood Heat transfer Test S-07-4," R. Billins, K. Sackett, K. Stanger, NUREG/CR-0254, August 1978.
THTF	151		Fig. 30				D.M. Leon et al.,"PWR Blowdown Heat Transfer Seperate Effects Program THTF Experimental Data Report for Test 151," ORNL/NUREG/TM-188.

Table G-1. (continued)

FACILITY	TEST	PIRT	SCALING	PARAMETER RANGING	NODALIZATION	CODE & EXP ACCURACY	TEST REFERENCE
THTF	153		Fig. 30				D.M. Leon et al.,"PWR Blowdown Heat Transfer Seperate Effects Program THTF Experimental Data Report for Test 153," NUREG/CR-0278.
THTF	161		Fig. 30				W.G. Craddick et al.,"PWR Blowdown Heat Transfer Seperate Effects Program THTF Experimental Data Report for Test 161," NUREG/CR-0731.
THTF	162		Fig. 30				W.G. Craddick et al.,"PWR Blowdown Heat Transfer Seperate Effects Program THTF Experimental Data Report for Test 162," NUREG/CR-0732.
UPTF	10		Fig. 30				TO BE PUBLISHED
UPTF	5			3.3.6			TO BE PUBLISHED
UPTF	6		4.3	3.3.6			TO BE PUBLISHED

********** SUMMARY **********

TOTAL TESTS USED FOR NODALIZATION	TOTAL TESTS USED FOR SCALING	TOTAL TESTS USED FOR PIRT	TOTAL PARAMETER RANGING TESTS
16	67	120	53

TOTAL TEST USED FOR CODE AND EXPERIMENTAL ACCURACY

9

Table G-2. Primary CSAU application for IET)

FACILITY	TEST	PIRT	SCALING	PARAMETER RANGING	NODALIZATION	CODE & EXP ACCURACY	TEST REFERENCE
LOBI	A1-04		Fig.30				L. Piplies and W. Kolar, "Quick Look Report on LOBI Test A1-04R," Communication LOC 80-03, Commission of the European Communities, J.R.C.-IspraEUR-6969
LOBI	A1-07		Fig.30				L. Piplies and W. Kolar, "Quick Look Report on LOBI Test A1-04R," Communication LOC 80-03, Commission of the European Communities, J.R.C.-IspraEN, June
LOBI	A1-4R		Fig.30		3.2.2		L. Piplies and W. Kolar, "Quick Look Report on LOBI Test A1-04R," Communication LOC 80-03, Commission of the European Communities, J.R.C.-Ispra
LOBI	A1-66		Fig.30				L. Piplies and W. Kolar, "Quick Look Report on LOBI Test A1-04R," Communication LOC 80-03, Commission of the European Communities, J.R.C.-Ispra
LOFT	L2-2	2.3	Fig.30		3.2.2		S.M Modro, S.N. Aksan, V.T. Berta, A.B. Wahba, "Review Of Loft Large Break Experiments," OECD LOFT-T-3900 (MARCH 1988).
LOFT	L2-3	2.3	Fig.30		3.2.2		S.M Modro, S.N. Aksan, V.T. Berta, A.B. Wahba, "Review Of Loft Large Break Experiments," OECD LOFT-T-3900 (MARCH 1988).
LOFT	L2-5	2.3	Fig.30		3.2.2		S.M Modro, S.N. Aksan, V.T. Berta, A.B. Wahba, "Review Of Loft Large Break Experiments," OECD LOFT-T-3900 (MARCH 1988).
LOFT	LP-02-6		Fig.30		3.2.2	Fig. 29	S.M Modro, S.N. Aksan, V.T. Berta, A.B. Wahba, "Review Of Loft Large Break Experiments," OECD LOFT-T-3900 (MARCH 1988).
LOFT	LP-LB-1		Fig.30				S.M Modro, S.N. Aksan, V.T. Berta, A.B. Wahba, "Review Of Loft Large Break Experiments," OECD LOFT-T-3900 (MARCH 1988).

Table G-2. (continued)

FACILITY	TEST	PIRT	SCALING	PARAMETER RANGING	NODALIZATION	CODE & EXP ACCURACY	TEST REFERENCE
PKL	IIB-5		Fig.30				"Ergebnisse des Versuches IIB-5 aus der Testserie PKL IIB," R13/85/15, 8/9/85.
PKL	K9				3.2.2		B. Brand, R. Mandl and H. Schmidt, "PKL Refill and Reflood Experiment-Selected Results From Test K9," Kraftwerk Union report R51/22/79, December 14, 1979.
SEMISCALE	S-02-2	2.3	Fig. 30				K.E. Sackett, H.S. Crapo, M.S. Jensen, "Experimental Data Report For Semiscale Mod-I Test S-02-2," ANCR-1232, August 1975.
SEMISCALE	S-02-3	2.3	Fig. 30				K.E. Sackett, H.S. Crapo, M.S. Jensen, "Experimental Data Report For Semiscale Mod-I Test S-02-3," ANCR-1233, September1975.
SEMISCALE	S-02-4		Fig. 30				K.E. Sackett, H.S. Crapo, M.S. Jensen, "Experimental Data Report For Semiscale Mod-I Test S-02-4,(Blowdown Heat Transfer Test)," ANCR-1234, November 1975.
SEMISCALE	S-02-5		Fig. 30				K.E. Sackett, H.S. Crapo, M.S. Jensen, "Experimental Data Report For Semiscale Mod-I Test S-02-5,(Blowdown Heat Transfer Test)," ANCR-1235, December 1975.
SEMISCALE	S-02-7	2.3	Fig. 30				K.E. Sackett, H.S. Crapo, M.S. Jensen, "Experimental Data Report For Semiscale Mod-I Test S-02-7,(Blowdown Heat Transfer Test)," ANCR-1237, November 1975.
SEMISCALE	S-02-8				3.2.2		"Quick Look Report On Semiscale Mod-I Test S-02-8," T.K. Larson, B.W. Johnson, M.A. Langerman, August 1976.
SEMISCALE	S-02-9		Fig. 30				K.E. Sackett, H.S. Crapo, M.S. Jensen, "Experimental Data Report For Semiscale Mod-I Test S-02-9 and 9A,(Blowdown Heat Transfer Test)," ANCR-1236, January 1976.

Table G-2. (continued)

FACILITY	TEST	PIRT	SCALING	PARAMETER RANGING	NODALIZATION	CODE & EXP ACCURACY	TEST REFERENCE
SEMISCALE	S-02-9A		Fig. 30				K.E. Sackett, H.S. Crapo, M.S. Jensen, "Experimental Data Report For Semiscale Mod-I Test S-02-9 and 9A,(Blowdown Heat Transfer Test)," ANCR-1236, January 1976.
SEMISCALE	S-04-1	2.3	Fig. 30				K.E. Sackett, H.S. Crapo, B. Collins, "Experimental Data Report For Semiscale Mod-I Test S-04-1,(Baseline ECC Test)," NUREG-ANCR-1330, September 1976
SEMISCALE	S-04-2	2.3	Fig. 30				K.E. Sackett, H.S. Crapo, B. Collins, "Experimental Data Report For Semiscale Mod-I Test S-04-2,(Baseline ECC Test)," NUREG-ANCR-1331, September 1976
SEMISCALE	S-04-3	2.3	Fig. 30				K.E. Sackett, H.S. Crapo, B. Collins, "Experimental Data Report For Semiscale Mod-I Test S-04-3,(Baseline ECC Test)," TREE-NUREG-1002, October 1976.
SEMISCALE	S-04-4	2.3	Fig. 30				K.E. Sackett, H.S. Crapo, B. Collins, "Experimental Data Report For Semiscale Mod-I Test S-04-4,(Baseline ECC Test)," TREE-NUREG-1003, October 1976.
SEMISCALE	S-04-5	2.3	Fig. 30		3.2.2		"Quick Look Report On Semiscale MOD-I Test S-04-5, (Baseline ECC Test Series)," J.M. Cozzuol, October 1976.
SEMISCALE	S-04-6	2.3	Fig. 30				"Quick Look Report On Semiscale MOD-I Test S-04-6, (Baseline ECC Test Series)," J.M. Cozzuol, October 1976.
SEMISCALE	S-06-1		Fig. 30				"Quick Look Report On Semiscale MOD-I Test S-06-1, (LOFT Counterpart Test Series)," J.M. Cozzuol, W.W. Tingle, April 1977.
SEMISCALE	S-06-2		Fig. 30				"Quick Look Report On Semiscale MOD-I Test S-06-2, (LOFT Counterpart Test Series)," J.M. Cozzuol, W.W. Tingle, April 1977.

Table G-2. (continued)

FACILITY	TEST	PIRT	SCALING	PARAMETER RANGING	NODALIZATION	CODE & EXP ACCURACY	TEST REFERENCE
SEMISCALE	S-06-3		Fig. 30		3.2.2		"Quick Look Report On Semiscale MOD-1 Test S-06-3, (LOFT Counterpart Test Series)," M.A. Langerman, May 1978.
SEMISCALE	S-07-1	2.3	Fig. 30				"Experimental Data Report For Semiscale MOD-3 Blowdown Heat Transfer Test S-07-1," D. Collins, K. Sackett, K. Stanger, NUREG/CR-0281, September 1978.
SEMISCALE	S-07-6		Fig. 30				"Experimental Operating Specification Tests S-07-1 through S-07-7 Semiscale MOD-3 Baseline Test Series, WR-S-78-002, MARCH 1978.
SEMISCALE	S-07-9	2.3					"Experimental Data Report For Semiscale MOD-3 Lower Plenum Injection Test S-07-9," R. Gillins, K. Sackett, D.R. Pack, NUREG/CR-0814, June 1979.
SEMISCALE	S-28-1				3.2.2		"Experimental Data Report For Semiscale MOD-1 Test S-28-1 (Steam Generator U-Tube Rupture Test)," R. Gillins, K. Sackett, C.E. Coppin, March 1978.
SEMISCALE	S-28-10				3.2.2		"Experimental Data Report For Semiscale MOD-1 Test S-28-9,10,11 (Steam Generator U-Tube Rupture Test)," R. Gillins, V. Esparza, K. Sackett, C.E. Coppin, March

********** SUMMARY **********

TOTAL TESTS USED FOR NODALIZATION	TOTAL TESTS USED FOR SCALING	TOTAL TESTS USED FOR PIRT	TOTAL PARAMETER RANGING TESTS
11	28	14	0

TOTAL TEST USED FOR CODE AND EXPERIMENTAL ACCURACY
1

Table G-3. Facility description

FACILITY	PRIMARY SCALING CRITERION	VOLUME SCALE	SET/IET	HEATING TYPE	MLHGR	CORE LENGTH	REFERENCE
BCL (60 psi)	GEOMETRY	1/15	SET	STEAM INJECT	N/A	20.5 in.	R.A. Cudnik, et al.,"Penetration Behavior In a 1/15-Scale Model Of a Four-Loop Pressurized Water Reactor," BMI-NUREG-1973, June 1977.
BCL (low press)	GEOMETRY	2/15	SET	STEAM INJECT	N/A	45 in.	"Baseline Plenum Filling Behavior In a 2/15 Scale Model of a Four Loop PWR, Topical Report," R.A. Cundit et al., NUREG/CR-0069, April 1978.
CCTF	CORE AREA	1/21	SET	ELECTRIC	0.5 KW/FT	144 in.	K. Hiranao, et al., "Quick Look Report On Large Scale Reflood Test-6," JAERI-memo-8990, July 1980.
CE (PUMP)	GEOMETRY	1/5	SET	N/A	N/A	45 in.	"Pump Two-Phase Performance Program," Combustion Engineering Inc., September 1980.
CREARE (CCF)	GEOMETRY	1/15	SET	STEAM INJECT	N/A		"ECC Delivery Study: Experimental Results and Discussion," Crowley, C.J.; Block, J.A., CREARE-TN-217, October 1975.
CREARE (CCF) (1/5)	GEOMETRY	1/5	SET	STEAM INJECT	N/A		"1/5 Scale Countercurrent Flow Data Presentation and Discussion," C.J. Crowley, P.H. Rothe, R.B. Sam, NUREG/CR-2106, November 1981.
CREARE (PF)	GEOMETRY	1/15	SET	STEAM INJECT	N/A		"ECC Delivery Study: Experimental Results and Discussions," Crowley C.J.; Block, J.A., Creare-TN-217, October 1975.
CREARE (PUMP)	GEOMETRY	1/20	SET	N/A	N/A	N/A	"1/20 Scale Model Pump Test Program: Facility Description Report," Runstadler, P.W., March 1977.
DARTMOUTH			SET	N/A	N/A	N/A	"EFFECT OF SCALE ON TWO-PHASE COUNTERCURRENT FLOW FLOODING," H.J. Richter et al., NUREG/CR-0312, June 1979.

Table G-3. (continued)

FACILITY	PRIMARY SCALING CRITERION	VOLUME SCALE	SET/IET	HEATING TYPE	MLHGR	CORE LENGTH	REFERENCE
FLECHT	VOLUME	1/400	SET	ELECTRIC	1.4 KW/FT	144 in.	"PWR FLECHT Final Test Plan," WCAP-7288, January 1969.
FLECHT-SEASET	1/400	VOLUME	SET	ELECTRIC	1.0 KW/FT	144 in.	"PWR FLECHT SEASET UNBLOCKED BUNDLE, FORCED AND GRAVITY REFLOOD TASK DATA REPORT," M.J. Loftus, et al., EPRI-NP-1459, September 1981.
LOBI	POWER-VOLUME	1/700	IET	ELECTRIC	0.5 KW/FT	153.5 in.	W.L. Riebolt et al.,"LOBI Experimental Programme Results and Plans: Status Sept. 1982," NUREG/CP-0041, October 1982.
LOFT	POWER-VOLUME	1/48	IET	NUCLEAR	16 KW/FT	66 in.	D.L. Reeder, "LOFT System and Test Description," NUREG/CR-0247, July 1978.
MARVIKEN	N/A	N/A	SET	N/A	N/A	N/A	"Marviken Full-Scale Critical Flow Tests. Vol. 4: Description of the test facility," Studsvik Energiteknik AB, May 1982.
NEPTUNUS	VOLUME	1/40	SET	ELECTRIC	N/A	N/A	"TRAC-PF1/MOD1 Independent Assessment: NEPTUNUS Pressurizer Test Y05," A.C. Peterson, NUREG/CR-3919, December 1984.
NORTHWESTERN UNIVERSITY			SET	N/A	N/A	N/A	I. Dilber, "Countercurrent Steam/Water Flow Above a Perforated Plate-Vertical Injection of Water," NUREG/CR-2323, September 1981.
PBF	N/A	N/A	IET	NUCLEAR	16 KW/FT	36 in.	"PBF/LOFT Lead Rod Test Series Test Results Report," D. Varaculle,Jr. et al., NUREG/CR-1538, July 1980.
PKL	POWER-VOLUME	1/134	IET	ELECTRIC		153.5 in.	"Ergebnissedesversuches IIB-5 aus der Testserie PKL IIB," R 513/85/15, 8/9/85.

Table G-3. (continued)

FACILITY	PRIMARY SCALING CRITERION	VOLUME SCALE	SET/IET	HEATING TYPE	MLHGR	CORE LENGTH	REFERENCE
SCTF	CORE FLOW AREA	1/21	SET	ELECTRIC	0.4 KW/FT	144 in.	T. Okubo, et al.,"Data Report On Large Scale Reflood Test-102," JAERI-memo-60-268, October 1985.
SEMISCALE	FULL HEIGHT/VOLUME	1/1705	IET	ELECTRIC	15 KW/FT	66/144 in.	L.J. Ball et al.,"Semiscale Program Description,"EG&G Idaho, Inc., Tree-NUREG-1212, July 1978.
THTF	POWER-VOLUME	1/500	SET	ELECTRIC	17 KW/FT	144 in.	"Project Description: ORNL PWR Blowdown Heat Transfer Seperate-Effects Program, THTF," ORNL, NUREG/CR-0104, October 1978.
UPTF	FULL SCALE	1/1	SET	STEAM INJECT	N/A	N/A	"2D/3D Program. Upper Plenum Test Facility Test No. 1," Kraftwerk Union A.G., Erlangen Abt. Verfahrenstechnik, January 1987.

****
****
****

There are 22 facilities currently present in this portion of the Data Base.

APPENDIX H

NODALIZATION OF TRAC ASSESSMENT AND PLANT ANALYSES

APPENDIX H

NODALIZATION OF TRAC ASSESSMENT AND PLANT ANALYSES

The tables presented here contain nodalization information from previous TRAC assessment calculations, as compiled by Ms. J. Jacobson (INEL).

The three tables contain nodalization information from TRAC assessment calculations. The three types of assessments that are described include:

1. Separate-effects tests related to LBLOCA,

2. LBLOCA integral-effects tests, and

3. LBLOCA plant simulations.

Each table identifies the calculation and report, the code version used, and a breakdown of the major components. Calculations from TRAC-PF1 are of primary interest; however, nodalization information is also reported from previous versions of the code. In the tables, a single value represents the number of cells in a component; and values presented in the #/#/# form represent numbers of axial nodes, radial nodes, and azimuthal segments for three-dimensional components. The reports that have an asterisk above them have incomplete information, such as nodalization diagrams with no indication of cell divisions.

CALCULATIONS/REPORTS

		REFERENCE NUMBER		
EG&G	1/9	1	IET	Semiscale MOD1/S-04-5 and S-28-1
EG&G	2/9	1	IET	Semiscale MOD1/S-28-1, S-28-10
EG&G	3/9	1	SET	Semiscale MOD3/S-07-4, reflood
EG&G	4/9	1	SET	KWU PKL/K5A, refill, reflood
EG&G	5/9	2	IET	Semiscale MOD2C/S-FS-6B, S-FS-7, S-FS-11
EG&G	6/9	3	IET	ROSA-IV/LSTF
EG&G	7/9	4	Plant	200% LBLOCA - cold leg
EG&G	8/9	5	Plant	200% LBLOCA - hot leg
EG&G	9/9	6	Plant	200% LBLOCA - cold leg
LANL	1/21	7	SET	Edward's pipe
LANL	2/21	7	SET	CISE/4 and R
LANL	3/21	7	SET	Marviken CF/4.24
LANL	4/21	7	SET	THTF
LANL	5/21	7	SET	Bennett tube/5336, 5431, 5442
LANL	6/21	7	SET	Creare CCF/low and high subcooling
LANL	7/21	7	SET	FLECHT/4831, 17201
LANL	8/21	8	SET	Marviken CF/4, 13, 20, 22, 24
LANL	9/21	8	SET	BCL/262XX, 263XX, 29111
LANL	10/21	8	SET	FLECHT-SEASET/31504
LANL	11/21	7	SET	Dartmouth, air-water CCF
LANL	12/21	7	IET	Semiscale MOD1/S-02-8
LANL	13/21	7	IET	Semiscale MOD1/S-06-3 (LOFT L2-3)
LANL	14/21	7	IET	LOFT/L1-4
LANL	15/21	7	IET	LOFT/L2-2
LANL	16/21	8	IET	PKL/K9 and K54A
LANL	17/21	8	IET	LOFT/L2-3
LANL	18/21	8	IET	LOFT/L2-5
LANL	19/21	9	IET	Semiscale MOD1/S-06-3
LANL	20/21	9	IET	LOFT/L2-2
LANL	21/21	10	IET	LOFT/LP-02-6
Sandia	1/12	11-13	Plant	LBLOCA, fine node, coarse node
Sandia	2/12	14-17	Plant	LBLOCA with UHI
Sandia	3/12	20-24	Plant	Zion 1 LBLOCA
Sandia	4/12	25	Plant	LBLOCA, 2-loop with UPI
Sandia	5/12	26-27	SET	Creare ECC injection bypass
Sandia	6/12	28-31	SET	Dartmouth air-water CCF
Sandia	7/12	32-33	SET	Northwestern CCFL
Sandia	8/12	34-37	IET	Semiscale MOD2A/S-IB-3
Sandia	9/12	38-41	IET	LOBI/B-RIM
Sandia	10/12	42-45	IET	LOBI/AI-04R
Sandia	11/12	46-47	IET	LOFT/L2-5
Sandia	12/12	48	SET	NEPTUNUS pressurizer test Y05

SET - Separate effect tests related to LBLOCA
IET - LBLOCA integral tests
Plant - LBLOCA plant tests

TRAC-P MODALIZATION OF SEPARATE EFFECT TESTS RELATED TO LBLOCA

COMPONENTS	EPRI 3/9	* EPRI 4/9	LANL 1/21	LANL 2/21	* LANL 3/21	LANL 4/21	LANL 5/21	LANL 6/21	LANL 7/21	LANL 8/21	LANL 9/21	LANL 10/21	LANL 11/21	Sandia 5/12	Sandia 6/12	Sandia 7/12	Sandia 12/18					
REACTOR VESSEL	10/2/2					10/2/1		7/2/8	13	15	8/2/6	18		5/2/2	9/1/3	9/1/2						
UPPER HEAD	3/1/2					3/2/1																
UPPER PLENUM	5/2/2					1/1/1							2									
CORE	7/2/2					12/1/1			9			15	1									
LOWER PLENUM	3/2/2					2/2/1				15			1									
DOWNCOMER	9/1/2					14/1/1		4			5											
HOT LEG - BROKEN			46	38			24															
- INTACT																						
PRESSURIZER																	13/4					
PRIMARY LOOP STEAM GENERATOR - BROKEN																						
- INTACT																						
SECONDARY LOOP STEAM GENERATOR - BROKEN																						
- INTACT																						
COLD LEG - BROKEN																						
- INTACT											4											
PUMP - BROKEN																						
- INTACT																						
ACCUMULATOR - BROKEN																						
- INTACT																						
BREAK/FILL			1/1	1/1			1/1	1/1	1/1		7/3	1/1	1/1									
CODE VERSION	PD2	PD2	PD2	PD2	PD2	PD2	PD2	PD2	PD2	PD2	PD2	PD2	PF1	PD2	PF1	PF1	PF1					

A SINGLE VALUE REPRESENTS THE NUMBER OF CELLS. VALUES PRESENTED IN #/#/# FORM REPRESENT NUMBERS OF AXIAL NODES, RADIAL NODES, AND AZIMUTHAL SEGMENTS RESPECTIVELY.

* - INCOMPLETE INFORMATION AVAILABLE

TRAC-P MODALIZATION OF LBLOCA INTEGRAL TESTS

COMPONENTS	REPORTS																				
	* EG&G 1/9	* EG&G 2/9	EG&G 5/9	EG&G 6/9	LANL 12/21	LANL 13/21	LANL 14/21	LANL 15/21	* LANL 16/21	LANL 17/21	LANL 18/21	LANL 19/21	LANL 20/21	* LANL 21/21	* Sandia 8/12	* Sandia 9/12	* Sandia 10/12	Sandia 11/12			
REACTOR VESSEL	18/2/2	18/2/2	34/1/2	15/2/2	13/2/2	13/2/2	9/2/4	12/4/4	9/3/4	12/4/4	12/4/4	11	12/4/4	12/4/4	24/1/2	13/3/2	13/3/2				
UPPER HEAD			8/1/2	3/2/2			4/2/4	4/4/4	1/3/4	4/4/4	4/4/4		4/4/4	1/4/4							
UPPER PLENUM	1/2/2	1/2/2	8/1/2	3/2/2					2/2/4			2		3/3/4							
CORE	10/1/2	10/1/2	12/1/2	7/2/2	6/2/2	6/2/2	5/2/4	5/4/4	3/2/4	5/4/4	5/4/4	8	5/4/4	5/4/4							
LOWER PLENUM	4/2/2	4/2/2	4/1/2	7/2/2			2/2/4	2/4/4	3/2/4	2/4/4	2/4/4		2/4/4	3/4/4							
DOWNCOMER			12				1/1/4	1/1/4	6/1/1	1/1/4	1/1/4	13	1/1/4	9/1/4							
HOT LEG - BROKEN			8	10	21	21	45	45		45	45	34	45								
- INTACT			10	9	6	9	8	8		8	8	11	8								
PRESSURIZER	5	5	17	11	9	2	5	5		5	5	12	5								
PRIMARY LOOP STEAM GENERATOR - BROKEN	6	6	16	16																	
- INTACT			16	16	12	12	7	10		10	10	34	10								
SECONDARY LOOP STEAM GENERATOR - BROKEN			29	9																	
- INTACT			30	10						14				21							
COLD LEG - BROKEN			6	23	5	5	32	32		32	32	18	32								
- INTACT			10	22	11	9	8	8		8	8	3	8								
PUMP - BROKEN			10	2																	
- INTACT			10	2	2	2	4	4		4	4	8	4								
ACCUMULATOR - BROKEN	4	4		1																	
- INTACT				1		13	9	9		9	9	13	9								
BREAK			1	1	1	2	4	4		4	4	2	4								
CODE VERSION	PD2	PD2	PF1	PF1	PF1	PD2	PD2	PD2	PD2	PD2	PD2	PF1	PF1	PD2 & PF1	PF1	PF1	PF1	PF1			

A SINGLE VALUE REPRESENTS THE NUMBER OF CELLS. VALUES PRESENTED IN #/#/# FORM REPRESENT NUMBERS OF AXIAL NODES, RADIAL NODES, AND AZIMUTHAL SEGMENTS RESPECTIVELY.

* - INCOMPLETE INFORMATION AVAILABLE

TRAC-P MODALIZATION OF LBLOCA PLANT TESTS

COMPONENTS	REPORTS: *EG&G 7/9	*EG&G 8/9	EG&G 9/9	Sandia 1/13	*Sandia 2/13	*Sandia 3/13	*Sandia 4/13
REACTOR VESSEL	12/3/8	12/3/8	17/4/8	520/156	13/3/4		13/2/3
UPPER HEAD	1/3/8	1/3/8	1/4/8				
UPPER PLENUM	3/3/8	3/3/8	3/3/8				
CORE	5/2/8	5/2/8	5/2/8				
LOWER PLENUM	3/3/8	3/3/8	3/4/8				
DOWNCOMER	6/1/8	6/1/8	13/1/8				
HOT LEG - BROKEN			6	256/164			
- INTACT			6				
PRESSURIZER	6	6	10				
PRIMARY LOOP STEAM GENERATOR - BROKEN			41				
- INTACT			40				
SECONDARY LOOP STEAM GENERATOR - BROKEN			3				
- INTACT			3				
COLD LEG - BROKEN			10				
- INTACT			12				
PUMP - BROKEN			2				
- INTACT			2				
ACCUMULATOR - BROKEN			21				
- INTACT			21				
BREAK			5				
CODE VERSION	PIA	PIA	PF1	PF1	PF1	PF1	PF1

A SINGLE VALUE REPRESENTS THE NUMBER OF CELLS. VALUES PRESENTED IN #/#/# FORM REPRESENT NUMBERS OF AXIAL NODES, RADIAL NODES, AND AZIMUTHAL SEGMENTS RESPECTIVELY.

* - INCOMPLETE INFORMATION AVAILABLE

REFERENCES

1. M. E. Waterman, Overview of TRAC-PD2 Assessment Calculations, NUREG/CR-4195, EGG-2380, November 1985.

2. D. G. Hall and J. C. Watkins, An Evaluation of TRAC-PF1/MOD1 Computer Code Performance During Posttest Simulations of Semiscale Mod-2c Feedwater Line Break Transients, NUREG/CR-4802, EGG-2486, January 1987.

3. R. R. Schultz et al., "Single and Two-Phase Natural Circulation in Westinghouse Pressurized Water Reactor Simulators: Phenomena, Analysis and Scaling," The Winter Annual Meeting of the American Society of Mechanical Engineers, Boston, Massachusetts, December 13-18, 1987, pp. 59-70.

4. P. D. Wheatley and M. A. Bolander, TRAC-P1A Calculations for a 200%, 0.25 m-diameter, and 0.10 m-diameter Cold Leg Break in a Pressurized Water Reactor, EGG-CAAP-5190, June 1980.

5. M. A. Bolander, TRAC-P1A Calculations for a 200% Hot Leg Break Simultaneous with a Rupture of 16 Steam Generator Tubes in a Pressurized Water Reactor, EGG-CAAP-5191, June 1980.

6. G. E. Gruen and J. E. Fisher, TRAC-PF1/MOD1 US/Japanese PWR Conservative LOCA Prediction, NUREG/CR-4965, EGG-2513, July 1987.

7. T. D. Knight and V. Metzger, TRAC-PD2 Developmental Assessment, NUREG/CR-3208, LA-9700-MS, January 1985.

8. T. D. Knight, TRAC-PD2 Independent Assessment, NUREG/CR-3866, LA-10166-MS, December 1984.

9. B. E. Boyak, TRAC-PF1 Developmental Assessment, NUREG/CR-3280, LA-9704-M, July 1983.

10. T. D. Knight, TRAC Analysis of LOFT LP-02-6, LA-UR-85-3723, October 17, 1985, pp. 13-17, 59-60.

11. T. J. Bartel, Calculations Conducted in Developing an Audit Capability for ECCS Analysis, NUREG/CR-1470, SAND80-1149, December 1981.

12. L. D. Buxton, letter report to G. N. Lauben of NRC/NRR, Sandia National Laboratories, February 10, 1983.

13. D. Dobranich, L. D. Buxton, C. C. Wong, TRAC-PF1 LOCA Calculations Using Fine-Node and Course-Node Input Models, NUREG/CR-4044, SAND84-2305, May 1985.

14. D. Dobranich, letter report to D. Langford of NRC, Sandia National Laboratories, December 12, 1985.

15. D. Dobranich, LOCA Calculations for Upper Head Injection Plants, letter report to J. Watt of RSB, Sandia National Laboratories, January 29, 1986.

16. D. Dobranich, LOCA Calculations for a UHI PWR with the UHI System, letter report to J. Watt of RSB, Sandia National Laboratories, March 17, 1986.

17. T. E. Guidotti, M. J. Thurgood, J. M. Kelly, A COBRA/TRAC, Best Estimate Analysis of a Large-Break Accident in a PWR Equipped with Upper Head Injection, FATE-83-137, June 1982.

18. T. E. Guidotti and M. J. Thurgood, A COBRA/TRAC, Best Estimate Analysis of a Large-Break Accident in a PWR Equipped with Upper Head Injection, FATE-83-137, December 1983.

19. Seabrook Safety Evaluation Report, NUREG-0896, March 1983, Appendix E.

20. Light Water Reactor Safety Research Program Quarterly Report, October-December 1979, NUREG/CR-1469, SAND80-0927, September 1980, Vol. 14.

21. Thermal/Hydraulic Analysis Research Program Quarterly Report, January-March 1980, NUREG/CR-1157/1 of 4, SAND80-1091/1 of 4, May 1980.

22. Thermal/Hydraulic Analysis Research Program Quarterly Report, April-June 1980, NUREG/CR-1157/1 of 4, SAND80-1091/1 of 4, August 1980.

23. Thermal/Hydraulic Analysis Research Program Quarterly Report, July-September 1980, NUREG/CR-1157/1 of 4, SAND80-1091/1 of 4, November 1980.

24. Thermal/Hydraulic Analysis Research Program Quarterly Report, October-December 1980, NUREG/CR-1157/1 of 4, SAND80-1091/1 of 4, May 1981.

25. D. Dobranich and L. D. Buxton, Large Break LOCA Analysis for Two-Loop PWRs with Upper-Plenum Injection, NUREG/CR-3639, SAND84-0040, May 1984.

26. L. N. Kmetyk, L. D. Buxton, R. K. Cole, Jr., Analyses of 1/15 Scale Creare Bypass Transient Experiments, NUREG/CR-2606, SAND81-1932, September 1982.

27. C. J. Crowley et al., Downcomer Effects in a 1/15-Scale PRW Geometry-Experimental Data Report, NUREG-0281, May 1977.

28. C. R. Clark III, H. J. Richter, G. B. Wallis, D. Bharathan, Flooding in Multi-Path Vertical Countercurrent Air-Water Flow, NRC-0193-5, September 1978.

29. D. Dobranich, TRAC-PF1/MOD1 Independent Assessment: Dartmouth College Air-Water Counter-Current Flow Tests, NUREG/CR-4337, SAND85-1594, December 1985.

30. Brookhaven National Laboratory Quarterly Progress Report, July 1 - September 30, 1982, NUREG/CR-2331, BNL-NUREG-51454, Vol. 2, No. 3.

31. Brookhaven National Laboratory Quarterly Progress Report, October 1 - December 31, 1982, NUREG/CR-2331, BNL-NUREG-51454, Vol. 2, No. 4.

32. I. Dilber, S. G. Bankoff, R. S. Tankin, M. C. Yuen, Countercurrent Steam/Water Flow Above a Perforated Plate - Vertical Injection of Water, NUREG/CR-2323, September 1981.

33. D. Dobranich, TRAC-PF1/MOD1 Independent Assessment: Northwestern University Perforated-Plate CCFL Tests, NUREG/CR-4155, SAND85-0172, February 1985.

34. T. J. Boucher, Experimental Operating Specification for Semiscale Mod-2A Experiment S-IB-3, EGG-SEMI-5787, February 1982.

35. T. J. Boucher and M. T. Leonard, Quick Look Report for Semiscale Intermediate Break Test S-IB-3, EGG-SEMI-6013, August 1982.

36. K. E. Sackett and L. B. Clegg, Experiment Data Report for Semiscale Mod-2A Intermediate Break Test Series (S-IB-3), NUREG/CR-2738, EGG-2198, June 1982.

37. L. N. Kmetyk, TRAC-PF1/MOD1 Independent Assessment: Semiscale Mod-2A Intermediate Break Test S-IB-3, NUREG/CR-4465, SAND85-2563, February 1986.

38. C. Addabbo, G. De Santi, L. Piplies, Quick Look Report on LOBI Test B-R1M, Communication LQC 82-08, Commission of the European Communities, J.R.C.-Ispra, March 1982.

39. T. Fortescue, LOBI Test B-R1M: Preliminary Data Report, Technical Note No. I.06.01.81.153, Commission of the European Communities, J.R.C.-Ispra, December 1981.

40. E. Ohlmer and J. Sanders, Experimental Data Report on LOBI Test B-R1M, LEC 82-08, Commission of the European Communities, J.R.C.-Ispra, April 1982.

41. L. N. Kmetyk, TRAC-PF1/MOd1 Independent Assessment: LOBI Intermediate Break Test B-R1M, NUREG/CR-3970, SAND85-2264, February 1986.

42. L. Piplies and W. Kolar, Quick Look Report on LOBI Test A1-04R, Communication LQC 80-03, Commission of the European Communities, J.R.C.-Ispra, December 1980.

43. E. Ohlmer et al., Experimental Data Report on LOBI Test A1-04R, Communication LEC 80-03, Commission of the European Communities, J.R.C.-Ispra, December 1980.

44. L. N. Kmetyk, RELAP5 Assessment: LOBI Large Break Transients, NUREG/CR-3075, SAND82-2525, March 1983.

45. L. N. Kmetyk, TRAC-PF1/MOD1 Independent Assessment: LOBI Large Break Transient A1-04R, NUREG/CR-4171, SAND85-0442, December 1985.

46. J. P. Adams, Quick-Look Report on LOFT Nuclear Experiment L2-5, EGG-LOFT-5912, June 1982.

47. P. B. Bayless and J. M. Divine, Experiment Data Report for LOFT Large Break Loss-of-Coolant Experiment L2-5, NUREG/CR-2826, EGG-2210, August 1982.

48. A. C. Peterson, TRAC-PF1/MOD1 Independent Assessment: NEPTUNUS Pressurizer Test Y05, NUREG/CR-3919, SAND84-1534, December 1984.

APPENDIX I

HOT CHANNEL ANALYSIS

APPENDIX I

HOT CHANNEL ANALYSIS

This appendix describes an evaluation of the impact of a hot channel hydraulics, compared to an average channel, on peak cladding temperature. The data supporting the analysis are also reported.

HOT CHANNEL ANALYSIS

At the January 13-14, 1988, Peer Review Group Meeting, Westinghouse representatives stated that the hydraulic conditions in a reactor hot bundle region may be significantly different than that of an average bundle; and consequently, the peak cladding temperatures could be higher than our calculations have shown. They noted that in the present application of the CSAU methodology no hot bundle was simulated, only a hot rod with average fluid conditions of the hottest (innermost) ring. Therefore, the results of the CSAU study may have a lower peak cladding temperature than a study that included a hot bundle in the inner ring.

INEL proposed that the effect of a hot channel be investigated by adding a small central ring to the CSAU model. This ring would include four hot bundles, one for each of the four azimuth sectors. Calculations with the hot channel model, when compared to the innermost ring of the base model, indicate the differences in peak clad temperatures. It was proposed that this difference be included in the analysis as a bias.

INEL modified the base input deck to include a hot channel, and four calculations were performed through the reflood period. The results of these calculations were presented at the June 1988 TPG Meeting.

S. Levy Inc. has taken the data from the two hot channel runs and the same two cases without the hot channel and performed a statistical analysis that included linear and full second-order fits. The analysis was then compared against the previous base analysis (eight plant calculations for blowdown). Results of these analyses are as follows:

	Temperatures in Degrees Fahrenheit					
	Base		2 Runs Old 3 Ring		2 Runs New 4 Ring	
	μ	T_{05}	μ	T_{05}	μ	T_{05}
Linear	1112	1418	1072	1452	1155	1480
Full 2nd	1147	1430	1072	1502	1137	1547

From this analysis, using data from the full second-order response surface analysis (i.e. most conservative penalty for T_{05}), the blowdown bias that should be included for hot channel effects is:

Mean value difference ($\Delta\mu$) = 63°F
Temperature difference at 95% (ΔT_{05}) = 45°F

Similar calculations for early and late reflood PCT yield:

	Early Reflood, °F	Late Reflood, °F
Mean value difference	25	-14
Temperature at 95%	-54	-157

The decrease in the bias (becoming a benefit) is unexpected; although some evidence exists for such effects, it was decided to use the mean bias uniformly over the probability distribution function.

A three-ring model was used because the current application is a demonstration of the methodology and not a rigorous licensing application. In this context, it was decided to take a conservative penalty, rather than perform a more refined and costly analysis to reduce the penalty.

As a matter of interest to the TPG, the cost difference between an analysis using the four-ring model (including hot channel) and three-ring model is about 6 to 8 Cray computer hours ($4000) per run. For the required calculations, the total cost of using the hot channel model would increase the analysis cost by about $50,000.

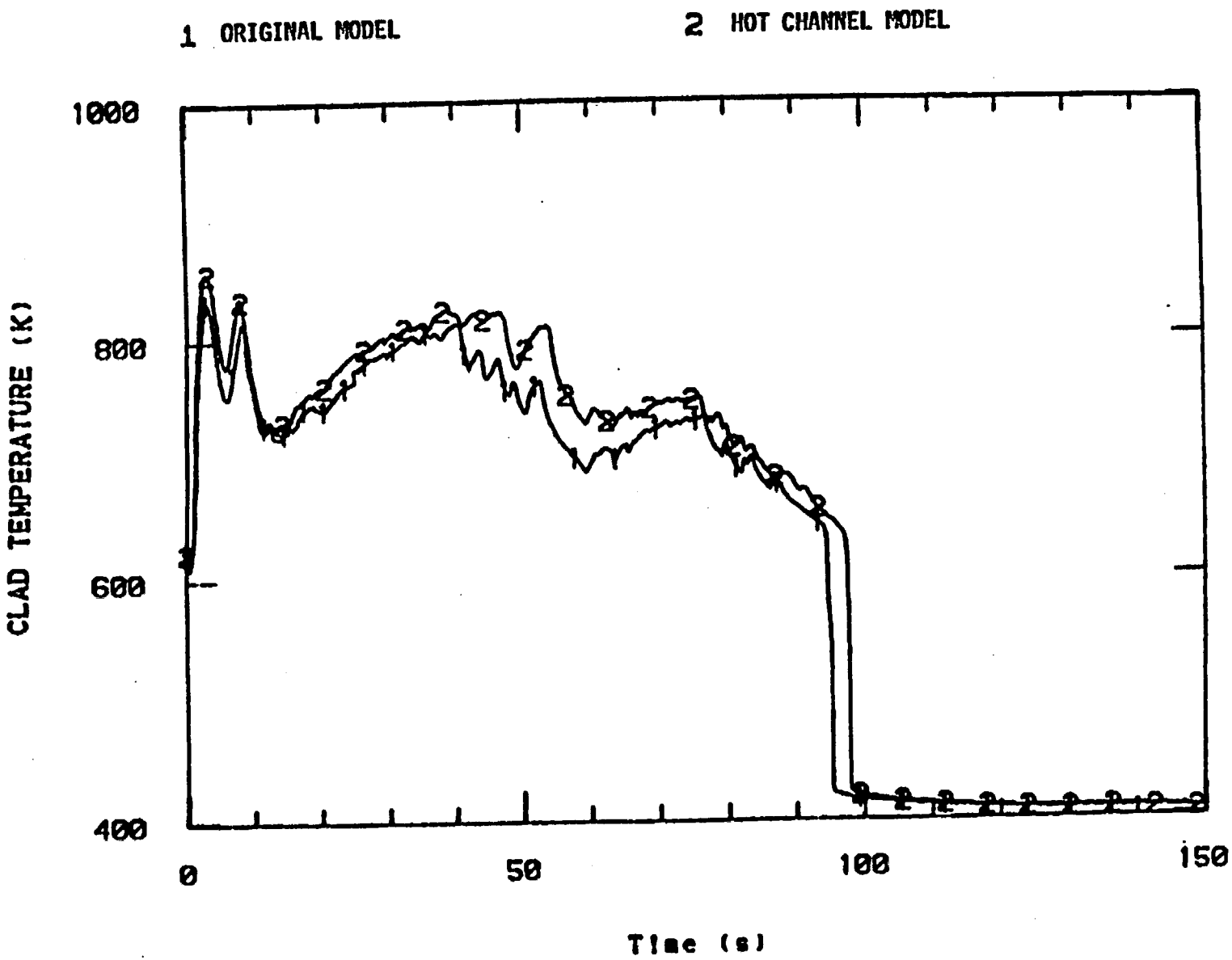

BASE CASE AND HØT CHANNEL CØMPARISØN

APPENDIX J

CODE UPDATES FOR CSAU UNCERTAINTY EVALUATION

APPENDIX J

CODE UPDATES FOR CSAU UNCERTAINTY EVALUATION

Code updates used to perform CSAU uncertainty studies and input multipliers for sensitivity calculations are documented in the appendix. These updates were provided by LANL in support of the study. The updates are limited to the coding necessary to vary the effects of the models selected to reflect the variability in important phenomena. That is, they do not constitute code improvements.

```
 1 *id uncert
 2 */
 3 */  Developed by Jay W.Spore   9/87
 4 */     Modified by Ralph Nelson  1/88
 5 */     Modified by Jay Spore 2/88
 6 */     Modified by Ralph Nelson  4/88
 7 */  No q/c as requested by Dr. Zuber NRC.
 8 */  This of course means no peer review and no test problem
 9 */  checks and no documentation and no comment cards.
10 */
11 */  Just a few notes to the user of this update
12 */
13 */  The number of rod multiplier factors to be input (NMROD)
14 */ must be input as the fifth number on main contrl card 2.  Example given
15 */ below.
16 */
17 */      numtcr       ieos       inopt      nmat       nmrod
18 */         2          0          1          0          16
19 */
20 */  Sixteen is the largest number allowed for nmrod.  It is easy to
21 */ change this limit, if you desire.
22 */
23 */ NMROD multiplier factors must be input right after
24 */ the iorder array.  NMROD and the factors must be input on each
25 */ restart.  Please note that the multipliers can be changed
26 */ on restart.  Therefore a steady-state can be run with say an hgap
27 */ multiplier of 1.0, then the transient could be restarted with
28 */ the hgap multiplier of 0.9, or something.
29 */
30 */  An example of the multiplier input is given below,
31 */
32 */  This update adds three new namelist variables,
33 */    icfz = 0 no cfzmul input or no modification to interfacial shear
34 */    icfz = 1 cfzmul is input and interfacial shear is modified.
35 */    dltmin = adder for tmin
36 */    rosenm = multiplier applied to the rosen interfacial sharpner
37 */
38 */  Example given below,
39 */
40 */  $inopts iadded=10, icfz=1, dltmin=-50.0, rosenm=1.5 $
41 */
42 */  icfz is default to 0 and dltmin is default to 0.0.
43 */  rosenm is defaulted to 1.0
44 */
45 */  If icfz=1, then the cfzmul array must be input following the
46 */ rod multiplier input.  Example given below.
47 */
48 */ input for the uncertainty mods
49 */
50 */ rhgap
51 */ r 4 1.0 r 1 0.5 r 5 1.0 r 1 1.5 r 5 1.0 e
52 */ * rcondf
53 */ r 5 1.0 r 1 0.5 r 5 1.0 r 1 1.5 r 4 1.0 e
54 */ * rcondc
55 */ r 6 1.0 r 1 0.5 r 5 1.0 r 1 1.5 r 3 1.0 e
56 */ * rcapf
57 */ r 7 1.0 r 1 0.5 r 5 1.0 r 1 1.5 r 2 1.0 e
58 */ * rcapc
```

```
59 */ r 8 1.0 r 1 0.5 r 5 1.0 r 1 1.5 r 1 1.0 e
60 */ * rhtc
61 */ r 9 1.0 r 1 0.9 r 5 1.0 r 1 1.1        e
62 */ * rhtcdr
63 */ r 9 1.0 r 1 0.9 r 5 1.0 r 1 1.1        e
64 */ * rhtcfr
65 */ r 9 1.0 r 1 0.9 r 5 1.0 r 1 1.1        e
66 */
67 */ cfzmul input
68 */
69 */ * cfzmul level 1
70 */ r 8 1.0 f 0. e
71 */ *cfzmul level 2
72 */ r 4 1.2 r 4 0.8 f 0. e
73 */ *cfzmul level 3
74 */ r 8 1.0 f 0. e
75 */ *cfzmul level 4
76 */ r 8 1.0 f 0. e
77 */ *cfzmul level 5
78 */ r 8 1.0 f 0. e
79 */ *cfzmul level 6
80 */ r 8 1.0 f 0. e
81 */ *cfzmul level 7
82 */ r 8 1.0 f 0. e
83 */ *cfzmul level 8
84 */ r 8 1.0 f 0. e
85 */ *cfzmul level 9
86 */ r 8 1.0 f 0. e
87 */ *cfzmul level 10
88 */ r 8 1.0 f 0. e
89 */ *cfzmul level 11
90 */ r 8 1.0 f 0. e
91 */ *cfzmul level 12
92 */ r 8 1.0 f 0. e
93 */ *cfzmul level 13
94 */ r 8 1.0 f 0. e
95 */ *cfzmul level 14
96 */ r 8 1.0 f 0. e
97 */ *cfzmul level 15
98 */ r 8 1.0 f 0. e
99 */
100 */
101 */ There are NMROD values input for each available rod heat transfer
102 */ multiplier.  The first array input after the iorder array is the
103 */ hgap multiplier.  If you have 4 average rods, then the first four
104 */ values input apply to the average rods and therefore should
105 */ be equal to 1.0.  There is no input error checking on this so
106 */ be careful or you'll really screw your deck up.  For this example
107 */ the next twelve inputs for rhgap will apply to the additional
108 */ calculational rods.  The next array input is the for the fuel
109 */ conductivity multiplier.  Next is the clad conductivity.
110 */ Next is the fuel heat capacity.  Next is the clad heat
111 */ capacity.  Next is the ratio for the heat transfer coefficient.
112 */ Next is the ratio for the heat transfer coefficient applied only
113 */ to the vapor film boiling htc for post-chf heat transfer.
114 */ Last is the ratio for the heat transfer coefficient applied only
115 */ to the Forsland-Rohsenow film boiling htc for post-chf heat transfer.
116 */
```

```
117 */  Beware of the following effects.
118 */
119 */     The application of the multiplier to the post-chf vapor heat
120 */     coefficient will result in this multiplier being applied to the
121 */     maximum of Dougall-Rohsenow or natural convection.  It should be
122 */     applied to Dougall-Rohsenow most of the time, but for very low
123 */     flow conditions, it will be applied to the natural convection
124 */     correlation also.
125 */
126 */     The application of the Forsland-Rohsenow post-chf multiplier
127 */     will produce a net effect of this multiplier times the general
128 */     heat transfer multiplier imput by the user.  This is done to
129 */     allow use of a multiplier on Bromley while zeroing out Forsland
130 */     Rohsenow if it were desired.
131 */
132 */  Beware of the following feedbacks.
133 */     The multiplier is applied to the TRAC calculated result
134 */     after TRAC calculates it.  However, feedback from other
135 */     calculated results can result in a different value than expected.
136 */     For example, given everything else the same a rod
137 */     with an rhgap =0.5 and a rod with an rhgap =1.0, will not have
138 */     an hgap that is a factor 2 lower.  As the hgap is reduced, then
139 */     fuel tends to get hotter.  Hotter fuel results in
140 */     hotter gap gas and a smaller hot gap, so the calculated TRAC
141 */     hgap, before the 0.5 is applied is higher, than the rod with
142 */     an hgap of 1.0.
143 */     Under these conditions, the hgap with rhgap=1.0,
144 */     might be 4000.0, while the hgap with rhgap=0.5 might be 2800.0.
145 */
146 */  The cfzmul array is of fixed dimension.  Current coding is
147 */ nnr=3,nnt=4,nnz=15.  If the vessel size that you're running is
148 */ smaller or equal to these dimensions, then no problem.  You just
149 */ input the cfzmuls the way you want them for the vessel of your
150 */ choice.
151 */
152 */  Warning Warning
153 */
154 */ cfzmul is a multiplier on the interfacial shear in the vessel,
155 */ therefore a cfzmul of 1.0 results in no effect, while a cfzmul
156 */ of 0.0 turns the interfacial shear off.
157 */
158 */ Also, note that cfzmul(i,j,k) is applied to all three directions
159 */ for cell ijk.
160 */
161 */ Input for cfzmul is by levels starting with level one and going
162 */ to level nnz, which is currently hardwired at 15.  nnz levels of
163 */ input must be input, even if you have a shorter vessel.
164 */ The cfzmul input for a given level, uses the load format, therefore
165 */ nnr*nnt numbers are expected for each level, with all of the thetas
166 */ in ring 1 filled first, then the thetas in ring 2, etc.
167 */
168 */  To change the hardwired size of the cfzmul array, the dimensions
169 */ in the cfzmod comdeck must be changed and the values for nnr,nnt,and
170 */ nnz, which are set in the blkdat routine must be changed and made
171 */ consistent.  If the size of your vessel is too large in any one
172 */ dimension r, theta, or z, then an error message is printed in the
173 */ rvssl or revssl routine.
174 */
```

```
175 */
176 *c core1,corec1,mfrod,core3,corec3,frod,input,htvssl
177 *c tf3de,revssl,rvssl,htcor,blkdat
178 *i core1.17                core1
179 *ca rodmod
180       common/pchfm/ frmult
181 *d core1.54                core1
182      4nmat,ia(lmatb),ia(lptbln),a(lprptb),rcondf(ncr),rcondc(ncr),
183      5rcapf(ncr),rcapc(ncr),nmrodf)
184 *i core1.107               core1
185       frmult=1.0
186       if(nmrodf.eq.1) frmult = rhtcfr(ncr)
187 *i htfxrn2.5               core1
188       if(nmrodf.eq.1) then
189         if(a(lihtf+k2).ne.4.0) then
190             a(lhrlv+k5) = a(lhrlv+k5)*rhtc(ncr)
191           else
192             a(lhrlv+k5) = a(lhrlv+k5)*rhtcdr(ncr)
193         endif
194         a(lhrll+k5) = a(lhrll+k5)*rhtc(ncr)
195         frmult = 1.0
196       endif
197 *i edcore.146              core1
198       frmult=1.0
199       if(nmrodf.eq.1) frmult = rhtcfr(ncr)
200 *i htfxrn2.10              core1
201       if(nmrodf.eq.1) then
202         if(a(lihtf+k2).ne.4.0) then
203             a(lhrfv+k2) = a(lhrfv+k2)*rhtc(ncr)
204           else
205             a(lhrfv+k2) = a(lhrfv+k2)*rhtcdr(ncr)
206         endif
207         a(lhrfl+k2) = a(lhrfl+k2)*rhtc(ncr)
208         frmult = 1.0
209       endif
210 *d corec1.115              corec1
211       rcondf=1.0
212       rcondc=1.0
213       rcapf=1.0
214       rcapc=1.0
215       nmrdf=0
216       call mfrod (a(lburn),a(lcnd),a(lcpnd),
217 *d corec1.119              corec1
218      4nmat,ia(lmatb),ia(lptbln),a(lprptb),rcondf,rcondc,rcapf,
219      5rcapc,nmrdf)
220 *d mfrod.4                 mfrod
221      2  cndr,cpdr,rndr,nmat,matb,lnprp,prptb,rcondf,rcondc,rcapf,
222      3  rcapc,nmrodf)
223 *i mfrod.82                mfrod
224       if(nmrodf.eq.1) then
225         cnd(i,j) = rcondf*cnd(i,j)
226         cpnd(i,j) = rcapf*cpnd(i,j)
227       endif
228 *i mfrod.85                mfrod
229       if(nmrodf.eq.1) then
230         cndr(intr,j)   =   rcondf*cndr(intr,j)
231         cpdr(intr,j)   =   rcapf*cpdr(intr,j)
232       endif
```

```
233 *i mfrod.94                mfrod
234       if(nmrodf.eq.1) then
235         cnd(i,j) = rcondc*cnd(i,j)
236         cpnd(i,j) = rcapc*cpnd(i,j)
237       endif
238 *i mfrod.97                mfrod
239       if(nmrodf.eq.1) then
240         cndr(intr,j) = rcondc*cndr(intr,j)
241         cpdr(intr,j) = rcapc*cpdr(intr,j)
242       endif
243 *i core3.13                core3
244 *ca rodmod
245 *d core3.50,core3.53              core3
246      9a(lrnd+org),a(lrpkf+n2),a(lrpowf+org),a(l2),powavg,
247      aa(ltlr+org+1),a(ltvr+org+1),a(lhrll+org),a(lhrlv+org),
248      bia(lidht+org),a(lcndr+org),a(lcpdr+org),a(lrndr+org),
249      cta,tb,fucrac,a(lnrdx+n1),difmin,amh2,jflg,rhgap(ncr),nmrodf)
250 *i corec3.97               corec3
251       rhgap=1.0
252       nmrdf=0
253 *d corec3.109              corec3
254      *  a(lnrdx),difmin,amh2,jflg,rhgap,nmrdf)
255 *d frod.8                  frod
256      6rnrdx,difmin,amh2,jflg,rhgap,nmrodf)
257 *i frod.167                frod
258       if(nmrodf.eq.1) hgap(1)=rhgap*hgap(1)
259 *i input.32                input
260 *ca rodmod
261 *ca cfzmod
262 *d kapll.3                 input
263       call readi(5hiiiii,numtcr,ieos,inopt,nmat,nmrod)
264 *i input.271               input
265       if(nmrod.ne.0) then
266         if(nmrod.le.16) then
267           nmrodf=1
268           call load(rhgap,rhgap,nmrod,1)
269           call load(rcondf,rcondf,nmrod,1)
270           call load(rcondc,rcondc,nmrod,1)
271           call load(rcapf,rcapf,nmrod,1)
272           call load(rcapc,rcapc,nmrod,1)
273           call load(rhtc,rhtc,nmrod,1)
274           call load(rhtcdr,rhtcdr,nmrod,1)
275           call load(rhtcfr,rhtcfr,nmrod,1)
276           write(iout,4110)nmrod
277           write(imout,4110)nmrod
278           write(itty,4110)nmrod
279           do 4109 k=1,nmrod
280           write(iout,4111)k,rhgap(k),rcondf(k),rcondc(k),rcapf(k),
281      &    rcapc(k),rhtc(k),rhtcdr(k),rhtcfr(k)
282           write(imout,4111)k,rhgap(k),rcondf(k),rcondc(k),rcapf(k),
283      &    rcapc(k),rhtc(k),rhtcdr(k),rhtcfr(k)
284           write(itty,4111)k,rhgap(k),rcondf(k),rcondc(k),rcapf(k),
285      &    rcapc(k),rhtc(k),rhtcdr(k),rhtcfr(k)
286  4109     continue
287         else
288           jflag=1
289           call error(1,26h*input* nmrod is too large,3)
290         endif
```

```
291        else
292          nmrodf=0
293          do 5100 k=1,nmrod
294          rhgap(k)=1.0
295          rcondf(k)=1.0
296          rcapf(k)=1.0
297          rcapc(k)=1.0
298          rhtc(k)=1.0
299          rhtcdr(k)=1.0
300          rhtcfr(k)=1.0
301          rcondc(k)=1.0
302  5100    continue
303        endif
304  4110 format(' NMROD = ',i3,' was input and the following arrays '
305      & 'were found.'
306      &,/,2x,1hI,2x,5hRHGAP,5x,6hRCONDF,4x,6hRCONDC,5x,5hRCAPF,
307      &5x,5hRCAPC,6x,4hRHTC,4x,6hRHTCDR,4x,6hRHTCFR)
308  4111 format(i3,8f10.3)
309        if(icfz.eq.1) then
310          nclx=nnr*nnt
311          do 4115 k=1,nnz
312            call load(cfzmul(1,1,k),cfzmul(1,1,k),nclx,1)
313            write(iout,4113) k
314            write(itty,4113) k
315  4113      format(' level',i3,' input for cfzmul ')
316            write(iout,4114)((cfzmul(j,i,k),j=1,nnt),i=1,nnr)
317            write(itty,4114)((cfzmul(j,i,k),j=1,nnt),i=1,nnr)
318  4114      format(1p6e13.4)
319  4115    continue
320        else
321          do 5103 k=1,nnz
322            do 5102 j=1,nnt
323              do 5101 i=1,nnr
324                cfzmul(i,j,k)=1.0
325  5101        continue
326  5102      continue
327  5103    continue
328        endif
329 *d htvssl.44,htvssl.46          htvssl
330        rcondf=1.0
331        rcondc=1.0
332        rcapf=1.0
333        rcapc=1.0
334        nmrdf=0
335        call mfrod(burn,cnhs(1,i),cphs(1,i),emhs(1,i),fpuo2,ftd,idim,
336       *  maths(1,i),ione,ione,nodhs,int,hst(1,i),rohs(1,i),tmcl,tmfl,
337       *  idhs,cnhsn(1,i),cphsn(1,i),rohsn(1,i),nmat,matb,lnprp,prptb,
338       & rcondf,rcondc,rcapf,rcapc,nmrdf)
339 *d vmextr6.3              input
340       1                   ,iexvss,icfz,dltmin,rosenm
341 *i movtrc.82              tf3de
342 *ca cfzmod
343 *d tf3de.602              tf3de
344        se5=rovk*cjg*se5c*rosenm
345 *i tf3de.1318             tf3de
346        if(icfz.eq.1) then
347          cfti=cfti*cfzmul(it,ir,iz)
348          cfri=cfri*cfzmul(it,ir,iz)
```

```
349          if(xccfl.eq.0.0) cfzi=cfzi*cfzmul(it,ir,iz)
350        endif
351 *i ccfl1.160              tf3de
352        if(icfz.eq.1) cfzi = cfzi*cfzmul(it,ir,iz)
353 *i initcr1.7              revssl
354 *ca cfzmod
355 *i cap13f.4               revssl
356        if(icfz.eq.1) then
357          if(nrsx.gt.nnr) then
358            jflag=1
359            call error(1,34h*rvssl* icfz=1 & nrsx is too large,4)
360          else
361            if(ntsx.gt.nnt) then
362              jflag=1
363              call error(1,34h*rvssl* icfz=1 & ntsx is too large,4)
364            else
365              if(nasx.gt.nnz) then
366                jflag=1
367                call error(1,34h*rvssl* icfz=1 & nasx is too large,4)
368              endif
369            endif
370          endif
371        endif
372 *i vltjrn.254             rvssl
373 *ca cfzmod
374 *i inlab1.543             rvssl
375        if(icfz.eq.1) then
376          if(nrsx.gt.nnr) then
377            jflag=1
378            call error(1,34h*rvssl* icfz=1 & nrsx is too large,4)
379          else
380            if(ntsx.gt.nnt) then
381              jflag=1
382              call error(1,34h*rvssl* icfz=1 & ntsx is too large,4)
383            else
384              if(nasx.gt.nnz) then
385                jflag=1
386                call error(1,34h*rvssl* icfz=1 & nasx is too large,4)
387              endif
388            endif
389          endif
390        endif
391 *i htcor.100              htcor
392 *ca cfzmod
393 *i upfrch.1               htcor
394        tmin = tmin + dltmin
395 *i upfrch.4               htcor
396        tmin = tmin +dltmin
397 *i hlfilm.50              hlfilm
398        common/pchfm/ frmult
399 *i hlfilm.53              hlfilm
400        data frmult/1.0/
401 *d hlfilm.81              hlfilm
402        brac=frmult*gc*rol*rov*hfgp*cv**3/(delt*visv*delta)
403 *i blkdat.69              blkdat
404 *ca cfzmod
405        data icfz/0/,dltmin/0.0/,nnz/15/,nnr/3/,nnt/4/,rosenm/1.0/
406 *af,,twostep
```

```
*cd cfzmod
      common /cfzmod/cfzmul(4,3,15),icfz,dltmin,rosenm,nnz,nnt,nnr
*cd rodmod
      common /rodmod/rhgap(16),rcondf(16),rcondc(16),rcapf(16),rcapc(16)
     &               ,rhtc(16),rhtcdr(16),rhtcfr(16),nmrodf
*
```

APPENDIX K

SENSITIVITY OF LBLOCA PEAK CLADDING TEMPERATURE TO STEAM BINDING

APPENDIX K

SENSITIVITY OF LBLOCA PEAK CLADDING TEMPERATURE TO STEAM BINDING

This appendix documents the sensitivity of peak cladding temperature to the rate of liquid carried to the steam generators (steam binding). Additional experimental results (for another facility) and ranging information are provided in Appendix P.

MPR ASSOCIATES, INC.

December 16, 1988

Dr. N. Zuber
Division of Reactor Safety Research
U. S. Nuclear Regulatory Commission
Washington, D. C. 20555

Subject: Evaluation of Sensitivity of Reflood Peak Clad Temperature to Liquid Carryover (Steam Binding)

Dear Dr. Zuber:

Per your request, we have prepared a brief paper describing our calculations of peak clad temperature sensitivity to liquid carryover (steam binding). The calculations include an approximate hand calculation technique and explicit evaluation of parametric TRAC analyses from the CSAU program. Results from the two methods agree closely.

A copy of our paper is enclosed. Please call me if you have any questions or comments.

Sincerely,

Paul S. Damerell

Paul S. Damerell

Enclosure

cc: G. Rhee
L. Shotkin
D. Bessette
NRC-RES
B. Meehan, NRC-Contracts
G. Wilson, INEL
B. Boyack, LANL

1050 CONNECTICUT AVENUE, N.W. WASHINGTON, D.C. 20036 202-659-2320

SENSITIVITY OF LOCA PEAK CLAD TEMPERATURE TO CHANGE IN WATER CARRYOVER TO STEAM GENERATORS (STEAM BINDING)

PURPOSE

This paper describes calculations which were performed to determine the sensitivity of LOCA peak clad temperature to a change in the amount of water carried over to the steam generators (steam binding). Specifically, calculations were performed using two methods:

1. An approximate hand-calculation method.

2. Explicit evaluation of CSAU TRAC results.

The results are presented below, followed by a detailed description of the calculations.

RESULTS AND CONCLUSION

The two methods used to calculate the sensitivity of PCT to increases in water carryover give similar results. The sensitivity is:

Method	Sensitivity Coefficient $\frac{d(PCT)}{(d\dot{M}_L/\dot{M}_L) \times 100}$ (deg. F change in PCT per percent change in liquid carryover)
Hand calculation	1.58
TRAC results from CSAU Program	1.31

The value from the hand calculation (1.58°F/%) agrees closely with the value determined from explicit evaluation of the CSAU parametric TRAC runs (1.31°F/%). This is a reasonable indicator of the overall PCT sensitivity to this phenomenon.

DESCRIPTION OF CALCULATIONS

1. Approximate Hand Calculation

In this calculation we assume a nominal case where water carryover to the steam generators in the steam flow is occurring. An increase in liquid flow (which will increase SG steam production) is treated as a corresponding decrease in core steam production, i.e.,

$$\frac{d(\dot{Q}_{core})}{Q_{core}} = -\frac{d(\dot{M}_L)}{\dot{M}_S} \qquad [1]$$

Equation [1] indicates that an increase in liquid carryover will reduce core heat transfer; physically this happens by the increased steam binding depressing the core collapsed level (increasing core void fraction) and reducing the heat transfer coefficients. Hence, the core must heat to higher temperatures to get full decay heat removal [that is, at temperature turnaround, local heat removal = decay heat generation, by definition]. Hence,

$$\frac{d(\Delta T_{core})}{\Delta T_{core}} - \frac{d(\dot{M}_L)}{\dot{M}_S} \qquad [2]$$

Where ΔT_{core} is a characteristic temperature difference for the core which represents the driving force for heat transfer.

$$\Delta T_{core} \sim (T_{clad} - T_{sat}) \text{ and}$$

$$\Delta T_{core} \sim (PCT - T_{sat}) \text{ for the peak rod} \qquad [3]$$

From the above, we note that

$$d(PCT) = d(\Delta T_{core}) \qquad [4]$$

Hence from Equations [2] and [4] the following is obtained:

$$d(PCT) = \Delta T_{core} \frac{d(\dot{M}_L)}{\dot{M}_S} = \Delta T_{core} \frac{d(\dot{M}_L)}{\dot{M}_L \left(\frac{X}{1-X}\right)} \qquad [5]$$

where X is quality of the flow into the steam generator.

Equation [5] can be rewritten as

$$\frac{d(PCT)}{d(\dot{M}_L)/\dot{M}_L} = \Delta T_{core} \left(\frac{1-X}{X}\right) \qquad [6]$$

To express Equation [6] per percent of liquid carryover

$$\frac{d(PCT)}{(d(\dot{M}_L)/\dot{M}_L) \times 100} = \frac{\Delta T_{core}}{100} \frac{1-X}{X} \qquad [7]$$

Equation [7] gives the sensitivity of peak clad temperature to a change in liquid carryover, expressed as degrees per percent change in liquid carryover. The expression is now evaluated for typical LOCA conditions. A nominal value of ΔT_{core} is determined from typical tests and TRAC analyses. The TRAC "Minimum Safeguards" Best-estimate Analysis (Reference 1) indicates calculated peak clad temperatures during reflood of 854K (1077°F). Typical CCTF tests show peak clad temperatures ranging from 650K (710°F) to 1150K (1610°F); however, the high values are characteristic of "licensing" rather than best-estimate values. In fact, the 650K value was for the CCTF best-estimate test. For this analysis, a PCT of 1000°F (about 800K) is used. T_{sat} is approximated as the saturation temperature of 50 psia = 281°F.

A nominal value of X is approximated from the UPTF best-estimate coupling test. In this test the average liquid carryover rate to the four steam generator simulators was about 20 kg/sec over a period of 125 sec (e.g., see Reference 2). The steam flow during this test averaged about 90 kg/sec.

$$X = \frac{90}{90 + 120} = 0.82$$

Hence

$$\frac{d(PCT)}{(d(\dot{M}_L)/\dot{M}_L) \times 100} = \frac{1000-281}{100} \quad \frac{(1-.82)}{0.82} = 1.58°F/\%$$

2. <u>Use of TRAC Results From CSAU Program</u>

In the CSAU Program, two comparable TRAC LOCA analyses were made: a nominal case and a modified case where entrainment and interfacial shear coefficients were increased based on separate SCTF evaluations. The modified case is considered to be more realistic and is treated here as the "base case". Figure 1 shows the difference in PCT (at the second reflood peak) between the two cases is 106°F.

Figures 2 and 3 show the integrated steam and liquid mass flowing to the steam generators in the loops, for both TRAC runs (Reference 3). To compare the liquid mass carryover, a suitable time period needs to be selected. Based on Figure 1, a time period of 50-125 seconds is appropriate for the second reflood peak.

$$\frac{d(\dot{M}_L)}{\dot{M}_L} = \frac{\int_{50}^{125} \dot{M}_{L,1} - \int_{50}^{125} \dot{M}_{L,2}}{\int_{50}^{125} \dot{M}_{L,2}} = \frac{385 - 2050}{2050} = -0.81$$

$(d(\dot{M}_L)/\dot{M}_L) \times 100 = -81$ i.e., the liquid flow decreased by 81%

$$\frac{d(PCT)}{(d(\dot{M}_L)/\dot{M}_L) \times 100} = \frac{-106°F}{-81\%} = 1.31°F/\%$$

REFERENCES

1. LA-CP-87-61, "TRAC-PF1/MOD1 Analysis of a Minimum-Safeguards Large-Break LOCA in a US/Japanese PWR with Four Loops and 15 x 15 Fuel."

2. Rhee, G., P. Damerell and J. Simons, "Use of 2D/3D Data to Scale Up Liquid Carryover/De-entrainment (Steam Binding) Phenomena to a PWR," 16th Water Reactor Safety Information Meeting, Gaithersburg, MD, October 24-27, 1988.

3. The plots in Figures 2 and 3 were provided by INEL.

4. Boyack, B. "Use of 2D/3D Data for Peak Cladding Temperature Uncertainty Studies," 16th Water Reactor Safety Information Meeting, Gaithersburg, MD, October 24-27, 1988.

NOMENCLATURE

$\dot{M}_L$	Liquid Flow Rate Into Steam Generators
$\dot{M}_{L,1}$, $\dot{M}_{L,2}$	Liquid Flow Rate Into Steam Generators in Two TRAC Analyses
$\dot{M}_S$	Steam Flow Rate Into Steam Generators
PCT	Peak Clad Temperature
Q_{core}	Core Heat Release Rate
T_{clad}	Clad Temperature
T_{sat}	Saturation Temperature
ΔT_{core}	Characteristic Temperature Difference in Core (See Equation [3]
X	Quality of Flow Into Steam Generators

MPR ASSOCIATES
F-73-26-1755
12/14/88

CSAU Demonstration Plant
Peak Cladding Temperature

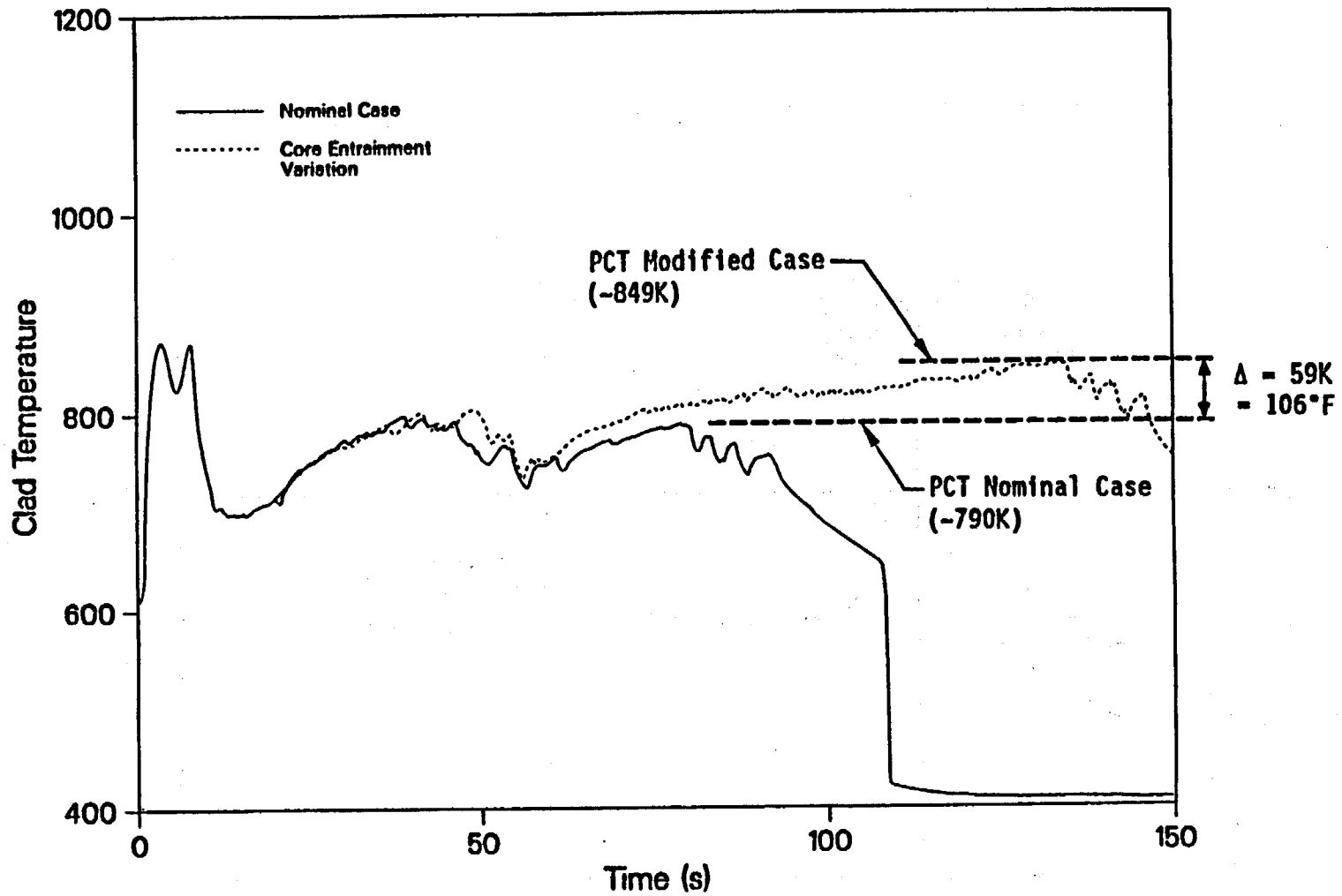

COMPARISON OF PEAK CLAD TEMPERATURE
FOR TWO TRAC PWR LOCA ANALYSES
(FROM REFERENCE 4)

FIGURE 1

MPR ASSOCIATES
F-73-26-1756
12/14/88

Note: Higher Steam Flow in Nominal Case Reflects the More Rapid Core Cooling Shown in Figure 1.

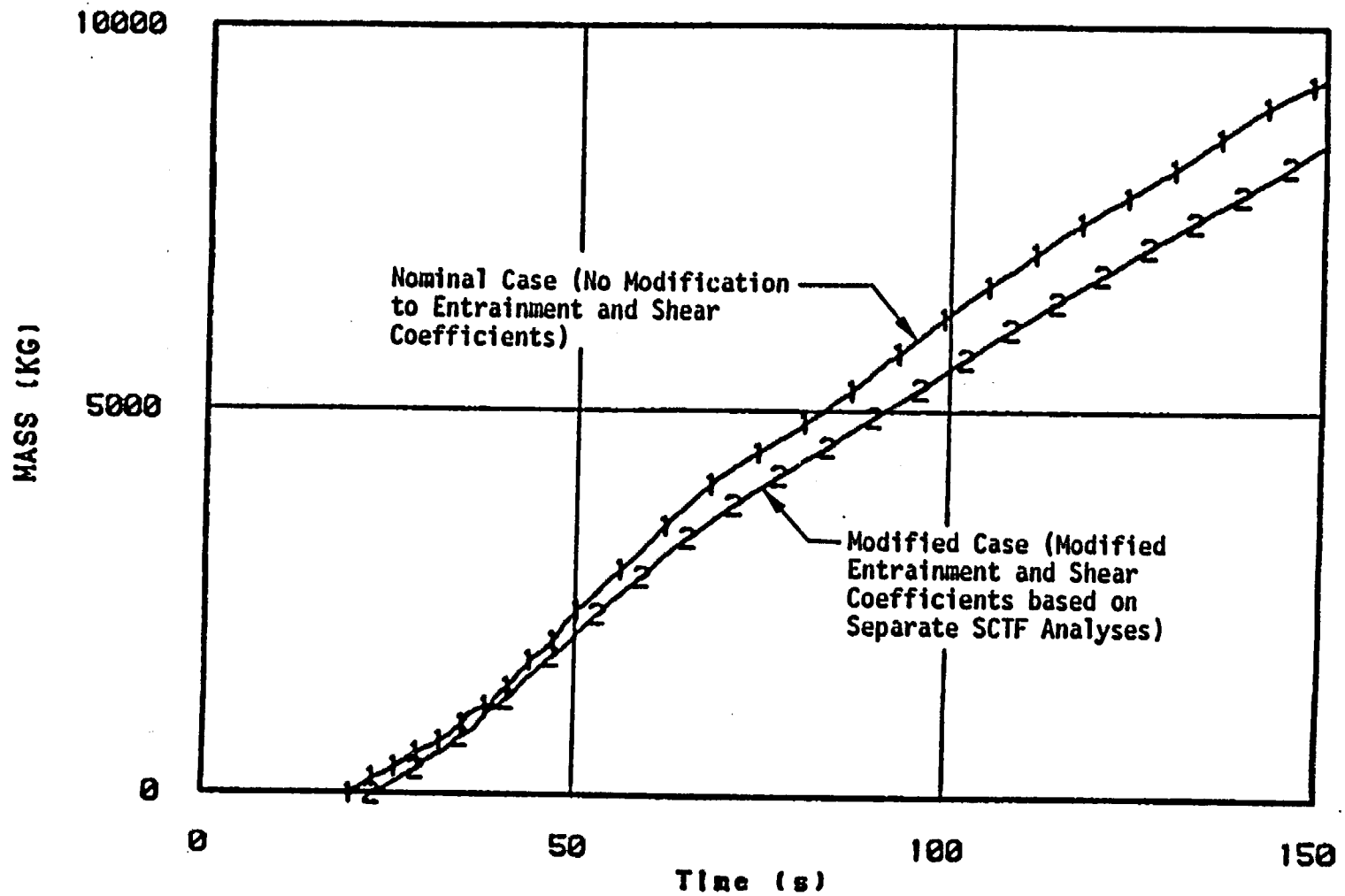

COMPARISON OF INTEGRAL STEAM MASS
INTO STEAM GENERATOR TUBES (FOUR LOOPS)
FOR TWO TRAC PWR LOCA ANALYSES (PROVIDED BY INEL)
FIGURE 2

MPR ASSOCIATES
F-73-26-1757
12/14/88

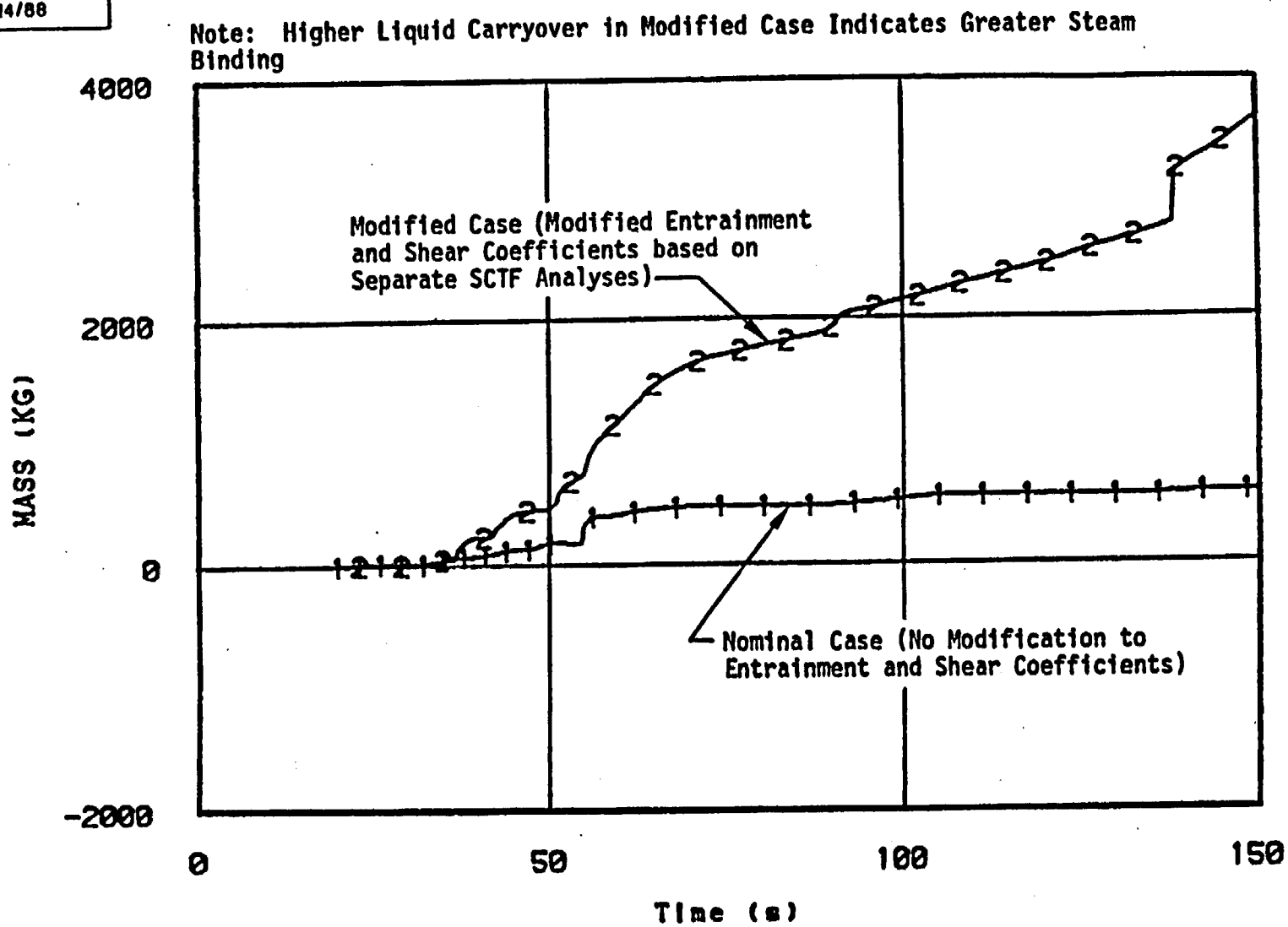

COMPARISON OF INTEGRAL LIQUID MASS INTO STEAM GENERATOR TUBES (FOUR LOOPS) FOR TWO TRAC PWR ANALYSES (PROVIDED BY INEL)

FIGURE 3

APPENDIX L

UNCERTAINTY IN MODELING AND SCALING OF CRITICAL FLOW IN TRAC-PF1/MOD1

APPENDIX L

UNCERTAINTY IN MODELING AND SCALING OF CRITICAL FLOW IN TRAC-PF1/MOD1

Additional details of the break scaling and uncertainty studies given in Part B, Section 3, are documented in this appendix.

UNCERTAINTY IN MODELLING AND SCALING OF PUMP HEAD AND TORQUE IN TRAC-PF1/MOD1

Upendra S. Rohatgi, Wen-Shi Yu, and Wolfgang Wulff
Brookhaven National Laboratory
Department of Nuclear Energy
Upton, New York 11973

The USNRC has established a Code Scalability, Applicability and Uncertainty (CSAU) evaluation methodology to quantify the uncertainty of safety parameters by best estimate code predictions. Codes evaluated according to CSAU can then be applied to evaluate the Emergency Core Cooling System (ECCS). The TRAC-PF1/MOD1 version was selected as the first code to undergo the CSAU analysis for LBLOCA applications. It was established as part of this methodology that the pump model is among the top ranked models in the code affecting the peak clad temperature (PCT) prediction for LBLOCA.

A pump model bias, representing systematic modeling uncertainties, was developed from Westinghouse (1/3 scale) data. The data used represent the largest available test pump relevant to Westinghouse PWRs. It was also shown through the analysis of CE and CREARE pump data that larger pumps degrade less, and that pumps degrade less at higher pressures. Since the model developed here is based on the 1/3 scale pump and on low pressure data, the calculated pump model bias is conservative and will overpredict the degradation when applied to PWRs.

1. INTRODUCTION

1.1 The Need for Uncertainty Estimates

It has been recognized after a decade of research in nuclear reactor thermohydraulics that the Appendix K, 10CFR50 acceptance criteria for the Emergency Core Cooling Systems (ECCS) are too conservative and need to be revised, to permit the use of best-estimate computer codes. The proposed Appendix K revision requires that best-estimate code calculations be accompanied by auditable estimates of the uncertainties associated with the code results.

The Code Scalability, Applicability and Uncertainty (CSAU) evaluation methodology [1] has been developed by the USNRC to determine (i) whether or not a candidate best-estimate code has the capability to simulate a particular transient, (ii) whether or not the code has the capability to model and scale up from facility subscale to Nuclear Power Plant (NPP) full scale condition, the processes occurring during that transient, and (iii) the uncertainty with which the code predicts parameters important to safety. The work reported here is a part of the uncertainty estimations required for Large Break Loss of Coolant Accident (LBLOCA) calculations, carried out with TRAC-PF1/MOD1, Version 14.3 [2] for a generic four-loop Westinghouse plant.

It has been determined in CSAU Step No. 3 (see main report, Section 2.1.3), the identification and ranking of phenomena, that the two-phase flow performance of the Reactor Coolant Pump affects strongly the peak clad temperature during the reflood phase. The uncertainty in the code prediction of Reactor Coolant Pump performance is therefore a major contributor to the overall uncertainty in predicting peak clad temperature.

1.2 Purpose of Uncertainty Estimation

The objective of estimating the uncertainty in pump performance predictions by computer code is to obtain the range and probability distributions of the modeling parameters in the pump model of the code, and to use these statistical measures in the calculation of the probability distribution of the peak clad temperature uncertainty. If systematic errors in the pump model dominate the stochastic uncertainty, then it is necessary instead to estimate the associated systematic bias and its standard deviation. It will be shown in Section 2 below that it is necessary for TRAC-PF1/MOD1 to determine, instead of statistical uncertainty probability distributions, the systematic bias and its standard deviation for the pump.

Bias and standard deviation are to be obtained by comparing code calculations with separate effects tests, and by extrapolating appropriately the bias and standard deviation from small-scale to full-scale NPP conditions, if small-scale test facilities are involved. The extrapolation is to be carried out with respect to those scaling groups which characterize the pump performance.

Since the pump performance is defined in TRAC as input data by the tabulated homologous curves for pump head and pump torque, it is the specific purpose of the work presented here to provide:

(i) best-estimate tabulations of homologous curves for pump head and pump torque, for single-phase and for two-phase flow operations, and

(ii) the uncertainty or bias associated with the above homologous curves.

2. UNCERTAINTY IN PUMP MODELS

During a hypothetical large break LOCA in a PWR, the reactor coolant pump plays an important role in determining the timing of restoring the core inlet flow after core flow reversal at the time of the pipe rupture. The flow into the downcomer and finally at the core inlet is a result of the competing influences of the vessel side cold leg break flow and intact loop cold leg flows into the downcomer due to the pumps in these intact loops. The core inlet flow is restored when the broken cold leg flow decreases below the total flow in the intact loops. In the case of a pump trip, the pump will coast down, but it has enough kinetic energy that it continues to pump the fluid, although at a decreasing rate. During the early part of the transient (up to the first peak) the intact loop pump flows are almost single-phase flows, and there will be at first no appreciable degradation in the pump performance. The situation changes as the transient proceeds; the primary system will have more vapor

leading to two-phase flow through the pump and a corresponding performance degradation.

2.1 Available Pump Models

The single-phase performance curves for the pump head and the torque for full-size pumps or equivalent (same specific speed) small-scale pumps, are known with good accuracy (within 2%). Also for pumps of the same specific speed, the effect of the size is negligible and the single-phase curves from smaller-size pumps could be used for larger-size pumps. The dominant source of pump modeling uncertainty is the description of two-phase flow pump degradation.

There are two pump models published [3, 4] which are superior to the TRAC pump model because they account for the effects from important parameters (e.g., pressure) which are ignored in TRAC. These models could in principle serve to develop the homologous curves and the correlation for pump degradation and thereby substitute for separate-effects test data on pumps.

However, the first model [EPRI, 3] employs constitutive relationships for stationary pipes outside their range of validity, namely for rotating impeller ducts. The EPRI model has been assessed only for small-scale pumps and reveals a large uncertainty for void fractions below $\alpha = 0.5$. Also, utilization of the EPRI model requires access to proprietary pump specifications which are available only to pump vendors. Therefore, the EPRI model could not be used for the development of homologous curves, nor of pump degradation data, nor of uncertainties in TRAC pump modeling.

The second model [KWU, 4] also could not be used here because the relationships between the pump scaling groups were developed from small-scale pump data and not validated in the scaling group range appropriate for NPP Reactor Coolant Pumps.

Experimental data were used therefore instead of the above models to develop pump characteristics for TRAC input and to estimate their uncertainties. Table 2.1 shows the available small-scale test data.

2.1.2 Pump Model in TRAC

TRAC-PF1/MOD1 has a pump model [2] which is based on the model developed by Idaho National Engineering Laboratory (INEL) from the Semi-Scale test data. The model is intended to apply to any other pump for which single phase homologous curves, two-phase fully degraded homologous curves and degradation multipliers as a function of void fraction (α) are available for the head and torque. The head across the pump is computed as follows:

$$H_{2\phi} = H_{1\phi} + M(\alpha)\,(H_{DEGRAD} - H_{1\phi}) \qquad (2.1)$$

where $H_{2\phi}$, $H_{1\phi}$, H_{DEGRAD}, $M(\alpha)$ are two phase head, single phase head, fully degraded head and degradation multiplier, respectively. $H_{1\phi}$, H_{DEGRAD} and $M(\alpha)$ have to be supplied to TRAC through input. The $M(\alpha)$ function serves to interpolate between the single-phase head curve and the fully degraded, or lowest two-phase, head curve. The static pressure rise across the pump can be computed from the two-phase pump head, $H_{2\phi}$, and the inlet

Table 2.1 Rated Pump Parameters and Operating Conditions at Full-Scale and Test Conditions

Parameter	Westinghouse PWR	PWR Primary Coolant Pump (Bingham-Williamette)	PWR Primary Coolant Pump (Byron-Jackson)	Westinghouse Pump	B&W Pump	C-E Pump	Creare Pumps	KWU Pump
Scale	1/1	1/1	1/1	1/3	1/3 of Bingham-Williamette Pump	1/5 of Byron Jackson Pump	1/20 of Byron-Jackson Pump	1/5, RS111
Rated Volumetric Flow Rate (gpm)	94,600	104,200	87,000	6210	11,200	3500	181 (219)	3148
Rated Total Head (ft)	290	397	252	64.4	390	252	252	293.7
Rated Speed (rpm)	1190	1190	900	1500	3580	4500	18,000	8480
Specific Speed rpm $(gpm)^{0.5}/(ft)^{0.75}$	5200	4319	4200	5190	4317	4200	4200	6700
Fluid*	S/W	S/W	S/W	A/W & S/W	A/W	S/W	A/W and S/W	S/W
Pressure (psia)	15-2250	15-2250	15-2250	15-420	20-120	15-1250	A/W at 90 S/W at 400	435-1305

* A/W is air/water mixture
S/W is steam/water mixture

density, ρ_{in}, as follows:

$$\Delta P = H_{2\emptyset}\rho_{in}. \tag{2.2}$$

The head curves $H_{1\emptyset}$ and H_{DEGRAD}, denoted below by H, are homologous curves with the following homologous variables:

$$(H/H_{ref})/(Q/Q_{ref})^2 \text{ vs. } (\Omega/\Omega_{ref})/(Q/Q_{ref}), \quad (\Omega/\Omega_{ref})/(Q/Q_{ref}) \leq 1.0,$$

$$(H/H_{ref})/(\Omega/\Omega_{ref})^2 \text{ vs. } (Q/Q_{ref})/(\Omega/\Omega_{ref}), \quad (Q/Q_{ref})/(\Omega/\Omega_{ref}) \leq 1.0,$$

where Q and Ω represent volumetric flow rate and pump angular speed, respectively. The subscript "ref" denotes normal, full speed and nominal flow conditions.

A similar description is used for predicting the hydraulic torque for the pump:

$$T_{2\emptyset} = T_{1\emptyset} + N(\alpha)\,(T_{DEGRAD} - T_{1\emptyset}) \tag{2.3}$$

where $T_{2\emptyset}$, $T_{1\emptyset}$, T_{DEGRAD} and $N(\alpha)$ are two-phase, single-phase, two-phase fully degraded torques and torque degradation multiplier, respectively. $T_{1\emptyset}$ and T_{DEGRAD} are supplied through input tables or homologous curves. The homologous curves for torque are of the following form:

$$\beta = T/T_{ref}$$

$$\beta/(Q/Q_{ref}) \text{ vs. } (\Omega/\Omega_{ref})/(Q/Q_{ref}), \quad \text{for } (\Omega/\Omega_{ref})/(Q/Q_{ref}) < 1.0,$$

$$\beta/(\Omega/\Omega_{ref}) \text{ vs. } (Q/Q_{ref})/(\Omega/\Omega_{ref}), \quad \text{for } (Q/Q_{ref})/(\Omega/\Omega_{ref}) \leq 1.0.$$

The single-phase torque estimated from the homologous curves is corrected for the density if that is different from the rated density:

$$T = T_{ref}\,(\rho/\rho_{ref})\,(\beta).$$

The torque obtained from the homologous curves is used to compute the pump speed under transient conditions.

The TRAC-PF1/MOD1 pump model is very simple and requires most of the information through input data. However, this model does not allow for the effect of many important parameters. In general, the pump head for two phase flow is a function of the following variables:

$$H_{2\emptyset} = H_{2\emptyset}\,(Q/Q_{ref}, \Omega/\Omega_{ref}, \alpha, P, N_s, \text{Geom})$$

where P, and N_s are pressure and pump specific speed, the other variables are as defined before.

Figure 2.1 shows homologous head curves as functions of void fraction for

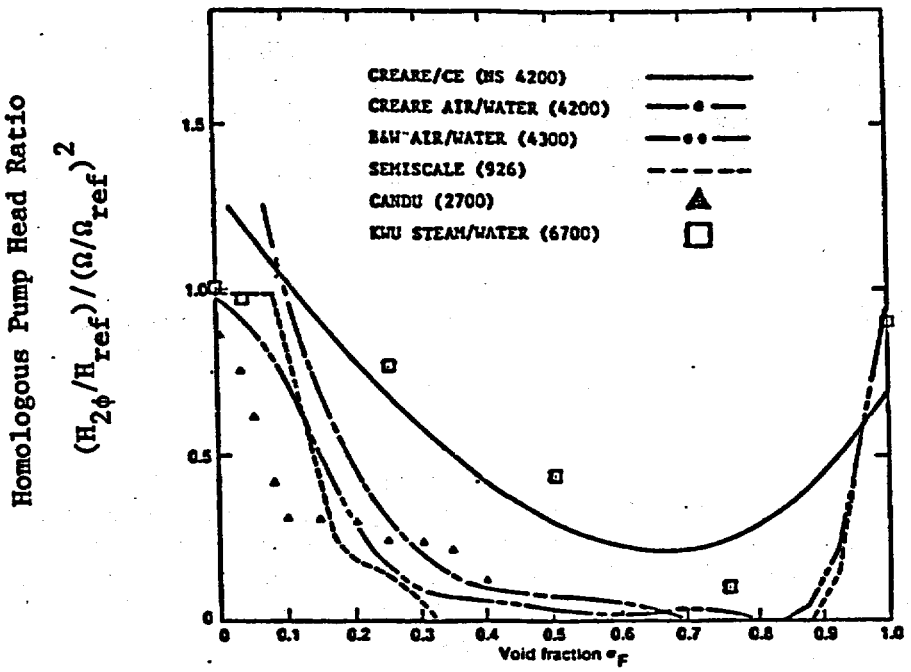

Figure 2.1 Comparison of Two-Phase Head for Various Pumps at Their Design Conditions, from Ref. [3]

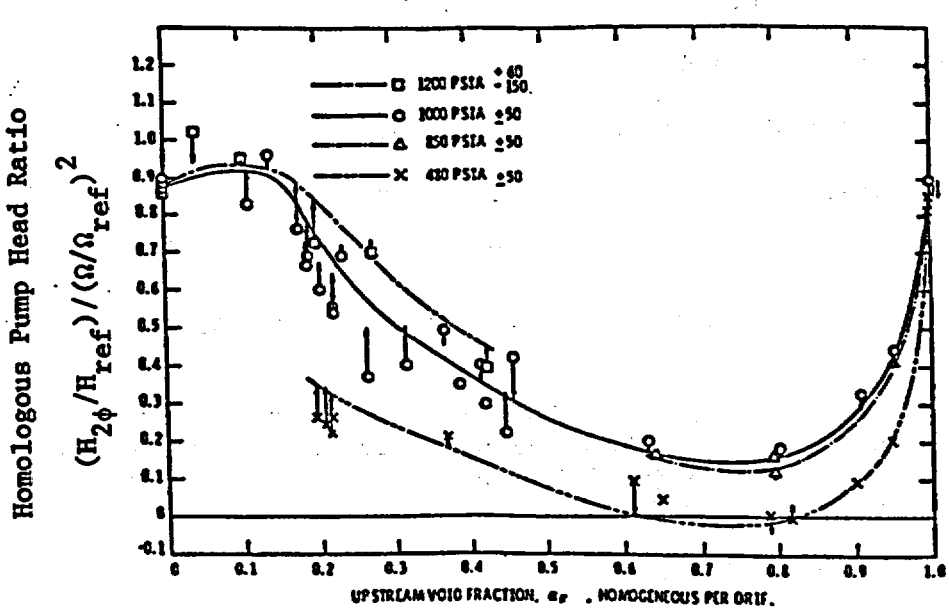

Figure 2.2 Effect of System Pressure on Two-Phase Flow Performance of CE Pump, from Ref. [3]

five pumps of different specific speeds and sizes at the rated condition of flow and speed. It can be seen from this figure that there is a significant effect of pump design on pump degradation. The KWU pump, which has the highest specific speed and is closest to the axial pump design of reactor pumps, undergoes the least degradation. However, the uncertainty from the specific speed and geometry effects can be eliminated if the data are available for the same specific speed N_s as that of the Reactor Coolant Pump:

$$H_{2\emptyset} = H_{2\emptyset}\,(Q/Q_{ref},\ \Omega/\Omega_{ref},\ \alpha,\ P)$$

The TRAC-PF1/MOD1 pump model does not account for pressure effects. Figure 2.2 shows the effect of pressure on degradation for the CE pump [3]. It is clear from this figure that degradation increases with decreasing pressure.

The TRAC-PF1/MOD1 model as described earlier interpolates between the single phase head curve and the corresponding fully degraded head curve through a degradation multiplier which is only a function of void fraction. The omission of pressure and possibly of specific speed and geometry from the model and possibly from the input data specification will be reflected in the correspondingly large pump model uncertainty.

3. DETERMINATION OF HOMOLOGOUS PUMP CURVES

The following six parameters were prepared as homologous curves from proprietary Westinghouse data for the 1/3-size test pump, having the same specific speed of $N_s = 5{,}200\ [gpm^2/ft^3]^{1/4}$ as the Westinghouse NPP Reactor Coolant Pump, but operating at 420 psia:

Single-phase pump head	$H_{1\emptyset}$,
Single-phase pump torque	$T_{1\emptyset}$,
Fully degraded pump head	H_{DEGRAD},
Fully degraded pump torque	T_{DEGRAD},
Pump head interpolant	$M(\alpha)$, and
Pump torque interpolant	$N(\alpha)$.

Since the homologous curves were prepared from proprietary data, they cannot be reproduced here.

The homologous curves for the above six parameters were entered in tabular form as input in TRAC-PF1/MOD1 and used for the reference calculations. See Section 4 below for the justification of using the low-pressure, small-scale data as reference input data.

4. UNCERTAINTY IN TRAC PUMP MODELING

The uncertainties in the pump model of TRAC-PF1/MOD1 arise from the fact

that:

(a) Two-phase pump performance is stochastic; precise measurements and predictions are difficult when two-phase flow conditions exist.

(b) There are no full-scale pump data available for reactor pressure conditions on H_D, T_D, M and N, and TRAC is unable to account through mechanistic modeling for pump size, or specific speed, or pressure.

(c) The model does not account for the effects of pressure (phasic densities), which are recognized as being important [2].

4.1 Modeling Uncertainty Under Conditions of Separate Effects Test

The pump head and torque degradations, $M(\alpha)$ and $N(\alpha)$, were evaluated from over 400 test data, taken from the 1/3-size Westinghouse Test Pump. The evaluation was performed by solving Eqs. (2.1) and (2.3) for $M(\alpha)$ and $N(\alpha)$, respectively, and by using the vendor-supplied single-phase pump characteristics $H_{1\emptyset}$ and $H_{2\emptyset}$, and the measured H_{DEGRAD} and T_{DEGRAD} data in the range of void fraction α from zero to one.

All but two of the $M(\alpha)$ and $N(\alpha)$ data were each enclosed, in the range $0 \leq \alpha \leq 1$, by an upper and lower degradation curve. The difference between the upper and lower degradation curve, taken at selected α-values, was divided by $\sqrt{12}$ to yield the standard sample deviations $s_M(\alpha)$ and $s_N(\alpha)$ by conservatively assuming (see below) that the distribution of experimental data points is uniform between the upper and lower degradation curves and that 95% of all the data lie between the two curves, i.e., between plus or minus two standard sample deviations, s. The results are shown in Table 4.1 below.

Table 4.1 Pump Modeling Uncertainty in TRAC-PF1-MOD1

Void Fraction α	Sample Standard Deviation for Pump Head s_M	Sample Standard Deviation for Pump Torque s_N
0	0.00	0.00
0.01	0.105	———
0.05	0.00	———
0.09	———	0.00
0.10	0.042	———
0.17	0.111	———
0.20	0.111	———
0.21	———	0.139
0.30	0.129	———
0.50	0.193	———
0.57	———	0.139
0.63	———	0.300
0.69	———	0.460
0.70	0.70	———
0.80	0.319	0.468
0.90	0.306	0.414
0.98	0.153	0.212
1.00	0.00	0.00

Since it was impossible to determine reliably probability distributions for s_M and s_N, as the deviation of measured data from the calculated mean value, a uniform distribution was adopted, because the uniform distribution reflects the maximum possible uncertainty about the distribution and it produces the most pessimistic (conservative) estimation of peak clad temperature.

4.2 Uncertainty from Geometric Scale Distortions

The homologous curves developed from the Westinghouse pump data are for the correct specific speed, but need a correction for the size effect, before they can represent the full size pump. In order to estimate the size effect, the data from CE (1/5 scale) [3] and CREARE (1/20 scale) [5] pumps $(Q/Q_{ref})/(\Omega/\Omega_{ref})$ were analyzed in the range of $0.0 \leq (Q/Q_{ref})/(\Omega/\Omega_{ref}) \leq 2.0$. Here Q and Ω designate volumetric flow rate and rotational pump speed, respectively. Subscript "ref" denotes the normal operating conditions (design conditions). In order to minimize the uncertainty in determining the size effect, the data were grouped in the increment of 0.25 for $(Q/Q_{ref})/(\Omega/\Omega_{ref})$. For each of these groups, least-square fit curves for $(H/H_{ref})/(\Omega/\Omega_{ref})^2$ or $(H/H_R)/(Q/Q_R)^2$ were obtained as a function of void fraction, for both the CE and CREARE pumps, as shown in Figures 4.1 through 4.4. RMS in these figures denotes the root-mean square of the differences between data and the best-fit curve. The number of data points used for each curve fit are given in the figures. The conclusion from these numbers is that the size effect is smallest near the design conditions $((Q/Q_{ref}/(\Omega/\Omega_{ref}) \approx 1.0)$, and that the larger pump degrades less than the small pump. The difference between the curves would be less if CREARE data were available at the same higher pressure as CE data.

The CE and CREARE pump data were further analyzed by obtaining mean degradation functions which are shown in Figure 4.5. The CREARE data are available only for void fractions less than 0.5. This figure reconfirms our earlier conclusion that large-size pumps degrade less than small-size pumps.

This can be explained by the observation that as the pump size increases, the dimensions of two-phase flow structure becomes smaller relative to the pump channel dimensions, and the flow becomes more homogeneous. It was therefore concluded, that extrapolation of pump degradation data with respect to geometric scale would only decrease degradation and associated uncertainties.

Since there are insufficient data to estimate this decrease of uncertainty, however, the full range of uncertainty as obtained from the 1/3-scale Westinghouse pump, and listed in Table 4.1 above, was used to analyze PCT uncertainty. A reduction in the uncertainty of predicting pump degradation requires more pump experiments, taken from larger pumps than 1/3 of full-size.

4.3 Uncertainty from Pressure Scale Distortion

Figure 2.2 shows that pumps operating at high pressures degrade less during two-phase flow operation than pumps operating at low pressure. This is expected, because the differences in phasic densities diminishes with increasing pressure. Consequently, the two-phase pump flow approaches homogeneous flow conditions as the pressure increases.

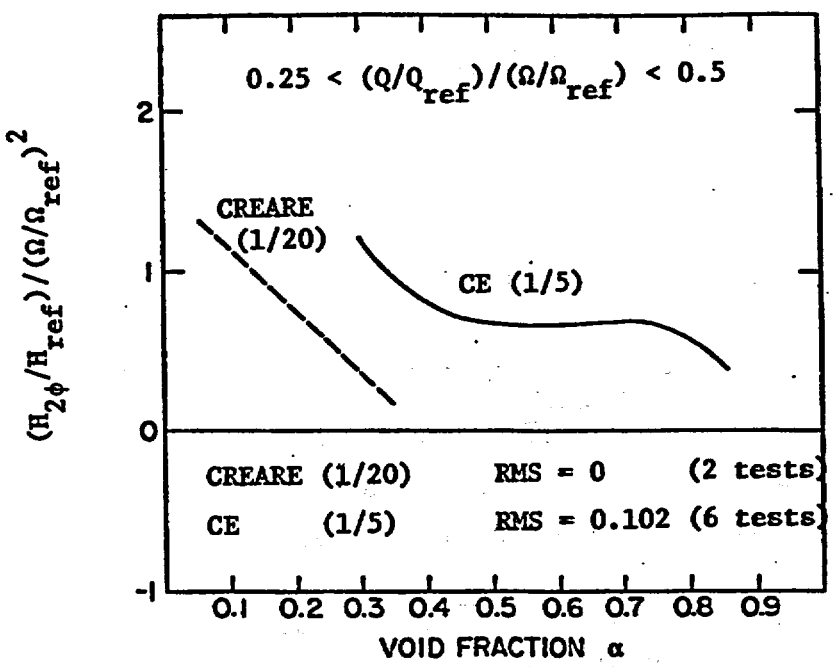

Figure 4.1 Comparison of CE and CREARE Pump Performance for $0.25 < (Q/Q_{ref})/(N/N_{ref}) < 0.5$

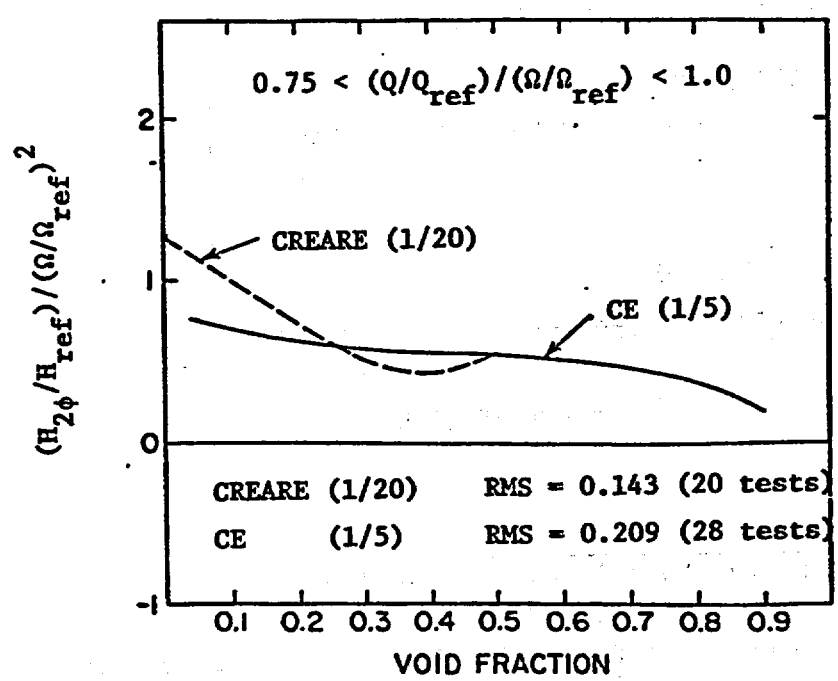

Figure 4.2 Comparison of CE and CREARE Pump Performance for $0.75 < (Q/Q_{ref})/(\Omega/\Omega_{ref}) < 1.0$

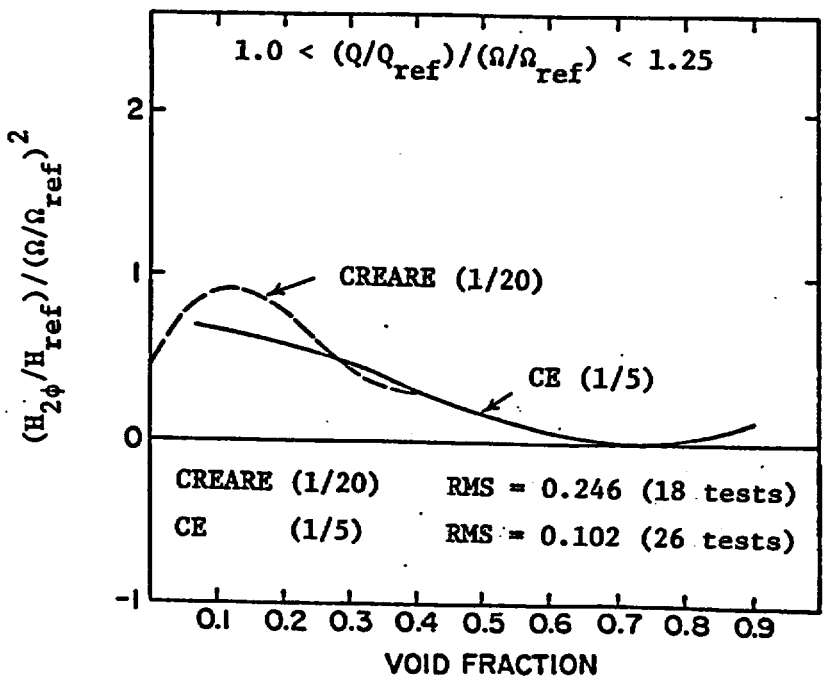

Figure 4.3 Comparison of CE and CREARE Pump Performance for $1.0 < (Q/Q_{ref})/(\Omega/\Omega_{ref}) < 1.25$

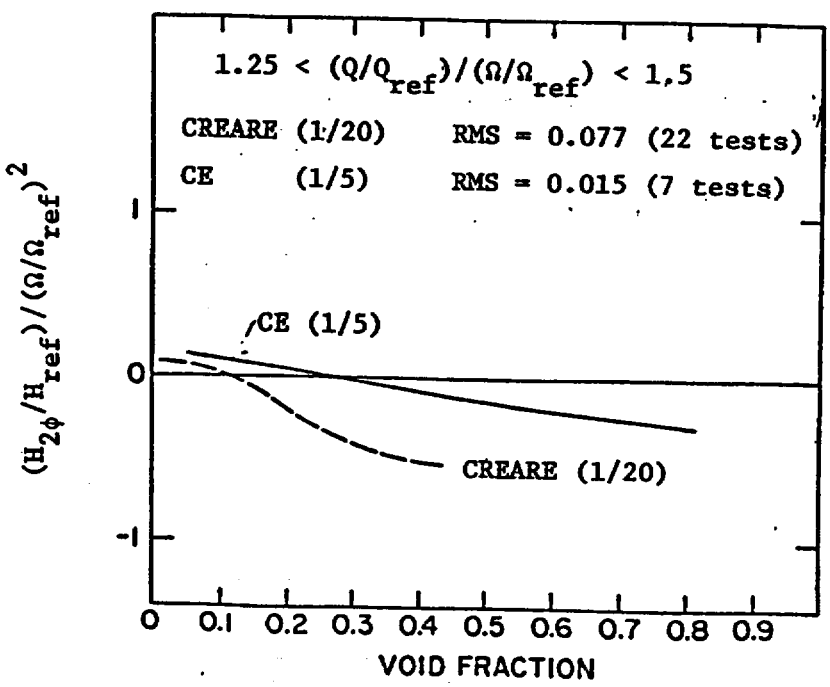

Figure 4.4 Comparison of CE and CREARE Pump Performance for $1.25 < (Q/Q_{ref})/(\Omega/\Omega_{ref}) < 1.5$

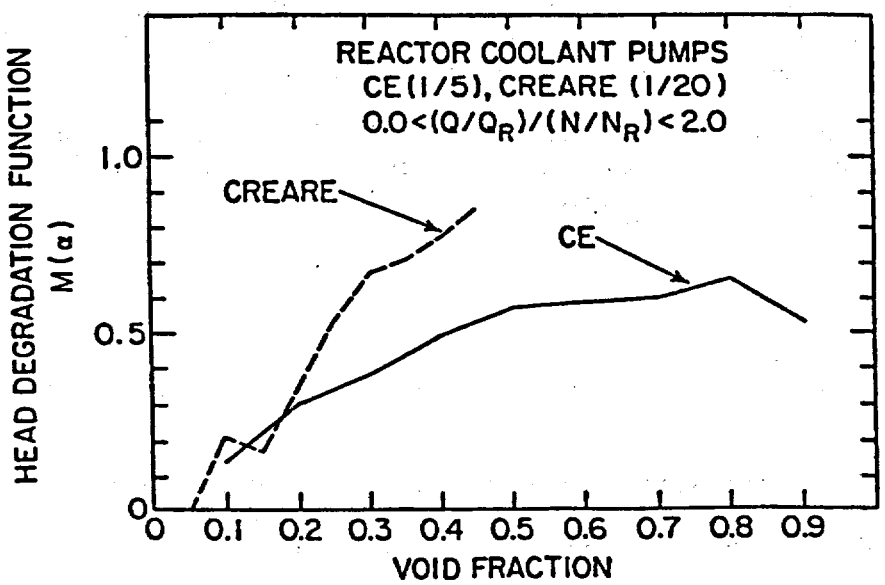

Figure 4.5 Comparison of Head Degradation Functions Developed from CREARE and CE Pump Data, Showing a Decrease in Pump Degradation with Increasing Pump Size

It is, however, not possible to quantify how much less a full-scale Reactor Coolant Pump would degrade than the 1/3-size Westinghouse test pump, because the data available for assessing pressure effects on pump degradation were obtained from pumps of different design and different specific speeds. Therefore, the full degradation of the 1/3-size test pump and the uncertainties as listed in Table 4.1 are used for estimating peak clad temperature uncertainty.

4.4 Total Pump Modeling Uncertainty

The pump modeling uncertainty is completely represented by the uncertainties s_M and s_N for pump head and torque degradations, respectively. The uncertainty ranges are twice the values listed in Table 4.1. Twice the values given in Table 4.1 are added and subtracted from the (proprietary) $M(\alpha)$ and $N(\alpha)$ multipliers in Eqs. (2.1) and (2.3), which are then evaluated to give upper and lower bounds* for $H_{2\emptyset}$ and $T_{2\emptyset}$, respectively.

For the reasons given in Sections 4.2 and 4.3 above, the uncertainties are then considered reasonable but conservative (pessimistic) uncertainty estimates for modeling the full-scale NPP Reactor Coolant Pump at all pressures occurring during an LBLOCA.

5. CONCLUSIONS

Pump head and torque correlations needed for TRAC-PF1/MOD1 have been developed.

Pump modeling uncertainties are derived as the uncertainties in predicting pump degradation during two-phase flow conditions. Degradation uncertainties are derived for pump head and torque, from the 1/3-size Westinghouse test pump.

It is shown that pump degradation and its uncertainties decrease with increasing pressure and increasing pump size. Therefore, the pump performance characteristics ($H_{2\emptyset}$ and $T_{2\emptyset}$) and the uncertainties (s_M and s_N), as derived from low-pressure tests on the 1/3-size test pump are reasonable and conservative for the purpose of estimating the uncertainty of peak clad temperature predictions.

A more realistic pump model is needed than the current TRAC pump model, to properly account for pressure, flow rate, pump speed and the pump size. The inability to account for these parameters is the largest contributor to the TRAC model uncertainty. There are data available for full-scale CANDU pumps and smaller scale KWU pumps (1/5 scale) which should be utilized. Furthermore, the EPRI model [6] or KWU semi-empirical [4] model should be utilized. The current TRAC model also does not account for the enthalpy rise of the fluid in the energy equation and it is assumed that homogenous two-phase flow discharges from the pump. These two model weaknesses should also be resolved.

*Intermediate values are also computed for generating the response surface.

6. ACKNOWLEDGEMENTS

The authors greatly appreciate the fine typing of Mrs. Linda Hanlon.

7. REFERENCES

1. Compendium of ECCS Research for Realistic LOCA Analysis, NUREG-1230, Chapter 4, April 1987.

2. Liles, D. R., et al., "TRAC-PF1/MOD1: An Advanced Best Estimate Computer Program for Pressurized Water Reactor Thermal-Hydraulics," NUREG/CR-3858, April 1987.

3. Kennedy, W. C., et al., "Pump Two-Phase Performance Irogram," EPRI Reports, NP-1556 (Vol. 1-8), September 1980.

4. Seeberger, G. J. and Schneider, K., "Development of a Two-Phase Pump Model for the Main Coolant Pumps in Pressurized Water Reactors," Foreign Document I.D. R 917/85/003, NRC Translation 1821, May 1986.

5. Swift, W. L., "Model Pump Performance Program - Data Report," EPRI NP-2379, May 1982.

6. Furaya, O. and Maekawa, S., "An Analytical Method for Prediction of Pump Performance Operating in Condensable Two-Phase Flows," Proc. of 1987 ASME/JSME Thermal Engineering Joint Conference, Hawaii, March 1987.

APPENDIX M

UNCERTAINTY IN MODELING AND SCALING OF PUMP HEAD AND TORQUE

APPENDIX M

UNCERTAINTY IN MODELING AND SCALING OF PUMP HEAD AND TORQUE

Additional details of the pump uncertainty and scaling study given in Part B, Section 3, are documented in this appendix.

UNCERTAINTY IN MODELLING AND SCALING OF CRITICAL FLOW IN TRAC-PF1/MOD1

Upendra S. Rohatgi, Wen-Shi Yu, and Wolfgang Wulff
Brookhaven National Laboratory
Department of Nuclear Energy
Upton, New York 11973

The USNRC has established a Code Scalability, Applicability and Uncertainty (CSAU) evaluation methodology to quantify the uncertainty of safety parameters by best estimate code predictions. Codes evaluated according to CSAU can then be applied to evaluate the Emergency Core Cooling System (ECCS). The TRAC-PF1/MOD1 version was selected as the first code to undergo the CSAU analysis for LBLOCA applications. It was established as part of this methodology that the break flow model is among the top ranked models in the code affecting the peak clad temperature (PCT) prediction for LBLOCA.

The break flow model bias or discrepancy and the uncertainty of the bias were determined by comparing TRAC-PF1/MOD1 results with experimental results from 12 Marviken tests. It was observed that TRAC-PF1/MOD1 consistently underpredicts the break flow rate and that the prediction improves with increasing pipe length (larger L/D). This is true for both subcooled and two-phase critical flows.

1. INTRODUCTION

1.1 The Need for Uncertainty Estimates

It has been recognized after a decade of research in nuclear reactor thermohydraulics that the Appendix K, 10CFR50 acceptance criteria for the Emergency Core Cooling Systems (ECCS) are too conservative and need to be revised, to permit the use of best-estimate computer codes. The proposed Appendix K revision requires that best-estimate code calculations be accompanied by auditable estimates of the uncertainties associated with the code results.

The Code Scalability, Applicability and Uncertainty (CSAU) evaluation methodology [1] has been developed by the USNRC to determine (i) whether or not a candidate best-estimate code has the capability to simulate a particular transient, (ii) whether or not the code has the capability to model and scale up from facility subscale to Nuclear Power Plant (NPP) full scale condition, the processes occurring during that transient, and (iii) the uncertainty with which the code predicts parameters important to safety. The work reported here is a part of the uncertainty estimations required for Large Break Loss of Coolant Accident (LBLOCA) calculations, carried with TRAC-PF1/MOD1, Version 14.3 for a generic four-loop Westinghouse plant.

It has been determined in CSAU Step No. 3 (see main report, Section 2.1.3), the identification and ranking of phenomena, that the critical break flow affects strongly the peak clad temperature during the reflood phase. The uncertainty in the code prediction of critical break flow is therefore a major contributor to the overall uncertainty in predicting peak clad tempera-

ture.

1.2 Purpose of Uncertainty Estimation

The objective of estimating the uncertainty in break flow predictions by computer code is to obtain the range and probability distributions of the modeling parameters in the critical break flow model of the code, and to use these statistical measures in the calculation of the probability distribution of the peak clad temperature uncertainty. If systematic errors in the break flow model dominate the stochastic uncertainty, then it is necessary instead to estimate the associated systematic bias and its standard deviation. It will be shown in Section 2 below that it is necessary for TRAC-PF1/MOD1 to determine systematic bias and its standard deviation for the break flow.

Bias and standard deviation are to be obtained by comparing code calculations with separate effects tests, and by extrapolating appropriately the bias and standard deviation from small-scale to full-scale NPP conditions, if small-scale separate effects test facilities are involved. The extrapolation is to be carried out with respect to those scaling groups which characterize the dominant phenomena of critical break flow.

Since the TRAC code has a built-in bias compensation for critical break flow in the form of two input break flow multipliers, one for subcooled critical and the other for two-phase critical flow, the break flow modeling bias is to be evaluated to provide the best estimates for the break flow multipliers. The standard deviation of the break flow bias or multiplier represents then the uncertainty associated with estimating the multiplier and with the break flow model deficiencies.

2. UNCERTAINTY IN CRITICAL FLOW MODEL

The coolant inventory in the reactor system is controlled by the break flow rate. However, a more significant role of the break flow rate is its influence on the distribution of the liquid inventory during the blowdown phase. The fuel rod clad starts to heat up at the time of break as the flow stagnates in the core. However, around 2.3 seconds after break initiation, the break flow decreases below the flow through the pumps in the intact loops, after the break flow changes from subcooled to two-phase critical flow. This results in the restoration of some liquid flow into the core, in core-wide rewet, and in the occurrence of the first peak of the clad temperature in the blowdown phase.

2.1 The Critical Flow Model in TRAC-PF1

TRAC-PF1/MOD1 has three models for critical flow. One is for subcooled liquid, the second is for two-phase flow conditions and the third one is for single-phase vapor. This paper deals with the first and second models, because the third model is irrelevant for peak clad temperature predictions.

2.1.1 Subcooled Critical Flow is computed in TRAC from a modified Bernoulli equation, as described in Appendix D on Page 530 of Reference [2]. This TRAC code document gives in Eq. (D-9) the critical velocity for subcooled liquid, calculated for the break plane location, as the velocity V_e:

$$V_e = \text{Max}\left\{a_{HE}, \sqrt{V_c^2 + 2\,(p_c - p_e)/\rho_m}\right\}, \tag{2.1}$$

where a_{HE} is the sound speed of homogeneous two-phase mixtures, V_c and p_c are the velocity and pressure at the nearest upstream computational cell center, while p_e and ρ_m are the break plane pressure and the mixture density at a location not specified in the TRAC documentation. A number of questionable explanations are given to justify Eq. (2.1). They can be found in Section II-B of Appendix D, in Reference [2]. Particularly, the second argument of the maximizing function in Eq. (2.1) produces a velocity which is neither related to the pressure wave propagation velocity, nor does it satisfy a mass flux maximizing condition. Therefore, it is not clear why Eq. (2.1) should always produce a critical mass flow rate.

Equation (2.1) applies in TRAC, whenever the void fraction α_c at the upstream cell center nearest to the break satisfies $\alpha_c < 0.01$. The break plane pressure p_e is computed in TRAC on the basis of the nonequilibrium flashing model by Jones [3] (who used Alamgir and Lienhard's earlier work). The pressure p_e computed from Eq. (D-10) of Reference [2] according to:

$$p_e = p_s - \text{Max}\left\{0, \Delta p\right\}. \tag{2.2}$$

Here p_s is the saturation pressure (at unspecified location), and:

$$\Delta p = 0.258 \frac{\sigma^{1.5}\left(\frac{T_\ell}{T_{crit}}\right)^{13.76}}{1 - \frac{\rho_g}{\rho_\ell}} \sqrt{\left[1 + 13.25\left(\frac{-Dp/Dt}{1.01325\text{x}10^{11}}\right)\right]^{0.8}/(kT_{crit})}$$

$$- 0.070\left(\frac{A_e}{A_c}\right)^2 \rho_\ell V_e^2, \tag{2.3}$$

where σ, k, T and ρ designate surface tension, Boltzmann constant, temperature and density, respectively, all quantities being expressed in S.I. units. Subscripts g, ℓ and crit designate gas, liquid and thermodynamic critical, while subscripts e and c are, as before, designating break plane and upstream cell center locations. The locations associated with subscripts g and ℓ are also not specified in Reference [2].

Notice that Eq. (2.3) contains the limiting critical velocity V_e, that substitution of Eq. (2.3) first into Eq. (2.2) and then into Eq. (2.1) renders Eq. (2.1) implicit in the velocity V_e. The TRAC code document [2] fails to indicate the method by which V_e is computed from Eqs. (2.1, 2 and 3), with T_ℓ, ρ_ℓ and p_s all dependent on V_e.

Notice also that Reference [2] fails to specify the method for computing the substantial derivative Dp/Dt. The RELAP5 code documentation shows the same model for critical flow of subcooled liquid* [4, p. 79] as TRAC and

*Aside from a factor of 2 discrepancy in the last term of Eq. (2.3).

specifies:

$$Dp/Dt = (\rho_\ell V_e^3/A_e)(dA/dx)_e \ , \tag{2.4}$$

where $(dA/dx)_e$ is the variation of cross sectional area with respect to axial distance at the break. Obviously, Eq. (2.4) fails to produce nonequilibrium pressure undershoot for breaks in straight pipes.

Finally, it must be pointed out that Reference [2] fails to indicate how V_e, as computed from Eq. (2.1), limits the mass flux as computed from the field equations in TRAC.

2.1.2 Two-Phase Critical Flow is computed in TRAC from the condition that the maximum value of the real part of the characteristic roots λ_i, associated with the field equations:

$$\underset{\approx}{A}\partial \underset{\sim}{U}/\partial t + \underset{\approx}{B}\partial \underset{\sim}{U}/\partial x = \underset{\sim}{C} \tag{2.5}$$

is zero [2, p. 528]. The field equations are the mass balances of an inert gas and the two-phase mixture, the phasic momentum balances and the mixture entropy balance for isentropic flow. $\underset{\approx}{A}$ and $\underset{\approx}{B}$ in Eq. (2.5) are 5x5 matrices and the state variable vector $\underset{\sim}{U}$ has the components of inert gas pressure p, vapor pressure p_v, void fraction α and phasic velocities v_ℓ and v_g. The source vector $\underset{\sim}{C}$ is unimportant for all but the entropy equation. In TRAC it is completely ignored.

The characteristic roots λ_i are computed numerically from the characteristic equation:

$$\det\left[\underset{\approx}{A}\lambda + \underset{\approx}{B}\right] = 0. \tag{2.6}$$

The numerical scheme [2, p. 530] involves also the maximization of the mass flux at the location of the break plane. Thus, the two-phase critical flow model in TRAC contains two independent choking criteria, but not the standard compatibility criteria of quasi-steady critical flow (see Reocreux, NUREG-tr-0002, Vol. 1, p. 75).

The above two-phase flow choking criterion is imposed in TRAC for $\alpha_c > 0.1$ at the nearest upstream cell center. In the range of $0.01 \leq \alpha_c \leq 0.1$, a linear interpolation with respect to α_c is used between the critical flows calculated from Eq. (2.1) and from Eq. (2.6).

2.2 Bias vs. Uncertainty Estimate for Break Flow

It has been shown in Section 2.1 above, that the two critical break flow models relevant to LBLOCA analysis are not consistent with physics. Therefore, it is not possible to compute the break flow uncertainty from the uncertainties of the parameters appearing in Eqs. 2.1 and 2.6. Instead, the systematic modeling error in Eqs. 2.1 and 2.6, and in their implementations in TRAC-PF1/MOD4, is determined as a bias and its standard deviation. The bias is used in the code as the input multiplier for critical break flow.

The break flow modeling bias is defined as the ratio:

$$R_m = \frac{(W_c)_m}{(W_c)_p} \tag{2.7}$$

of critical break mass flow rate W_c as measured (subscript m) over the critical mass flow rate as predicted by the code (subscript p). The measured critical mass flow rate, $(W_c)_m$, is obtained from Separate Effects Tests (SET), namely from the Marviken test facility, the largest test facility available, having also the smallest scale distortion available. The code predictions are obtained from TRAC-PF1/MOD1 calculations, performed for the Marviken test conditions.

The bias R_m accounts for all modeling uncertainties, both for systematic errors and for stochastic uncertainties in all modeling parameters and in experimental data, but only to the extent that they are associated with the critical flow prediction and its assessment.

3. SEPARATE EFFECTS TEST DATA

The bias R_m as defined by Eq. (2.7) and its standard deviation S_R were determined from the 12 Marviken tests [5 to 15] listed in the first column of Table 3.1 below. The Marviken test facility provides the smallest available geometrical scale distortion.

Table 3.1 Marviken Test Matrix for Determination of Bias in Critical Break Flow Predictions

Test Number	Nozzle Exit Diameter (ft)	Nozzle Length to Diameter Ratio	Nozzle Entrance Conditions	
			Subcooling Temp (°F)	Static Pressure psia
12	0.984	3.0	54	----
13	0.656	3.0	54	----
15	1.64	3.6	54	----
16	1.64	3.6	54	----
17	0.984	3.7	54	----
18	0.984	3.7	54	----
19	0.984	3.7	9	----
20	1.64	1.5	9	----
21	1.64	1.5	54	----
22	1.64	1.5	90	----
24	1.64	0.32	54	----
25	0.984	1.7	9	----

The tests cover the ranges of geometric and operational parameters as follows:

	MARVIKEN	NPP
Pipe Diameter (ft)	0.656-1.64	1.97
Length/Diameter	0.3-3.0	~8
Upstream Subcooling Temperature (°F)	0-90	0-110
Upstream Static Pressure (bar)	40-50	3-155

Abdollahian et al. [16] have concluded that pipe diameters D > 1 ft and L/D > 1.5, the subcooled critical flow does not depend on diameter D or length L of the broken pipe. For smaller pipe diameters, D < 1 ft, however, the critical flow varies with L/D. The ratio L/D for a power plant depends upon the postulated break location, but is most likely greater than 1.5, in which case the subcooled critical flow is expected to be independent of L/D. Two-phase critical flow is nearly in thermal equilibrium and therefore not strongly dependent upon L/D. However, the data evaluation shown below in Chapter 4 show a trend of $R_{\dot{m}}$ with L/D. Therefore, L/D dependence of L/D is accounted for in the bias estimation.

Marviken tests are blowdown experiments started at pressures of approximately 800 psia. These tests do not cover the NPP pressure range above 800 psia, up to 2,250 psia. The pressure upstream of the break location is about one second long above 1200 psia and between 1200 and 725 psia for the subsequent four seconds, for a total of 1/3 to 1/4 of the entire blowdown period. Therefore, the pressure dependence of the bias $R_{\dot{m}}$ must be accounted for.

Figure 3.1 below shows the discharge pipe of the Marviken Test Facility. Pressure and temperature measurements at locations 004M109 and 004M405, respectively, all 5.608 m below the vessel exit, were used to impose entrance conditions on the TRAC code calculations. The mass flow rate $(W_c)_m$ in Eq. (2.7) was obtained from pitot tube measurements in Ring II, 3.470 m below the vessel exit.

The Marviken vessel (not shown, see [5 to 16]) was filled with water, heated and thereby pressurized to approximately 50 bar, with saturation temperature reached at the liquid-vapor interface in the vessel. Rupture of the diaphragm at the nozzle exit started the test. Data recordings at one minute intervals were used to evaluate $R_{\dot{m}}$ in Eq. (2.7).

4. TRAC -PF1 CALCULATIONS AND BIAS EVALUATIONS

TRAC calculations are needed to obtain $(W_c)_p$ in Eq. (2.7). The calculations were performed with the nodalization scheme as shown in Figure 3.2 and with the dimensions given in Table 3.2. The number of cells in the nozzle section must be the same as for the break nodalization of NPP calculations, namely 2. As seen in Table 3.2, five of the twelve calculations satisfy this nodalization rule; the others do not because the calculations had been completed before the rule was established. The nodalization effect on the results, $R_{\dot{m}}$ (L/D), however is small.

Note: All dimensions are in millimeters
at room temperature.

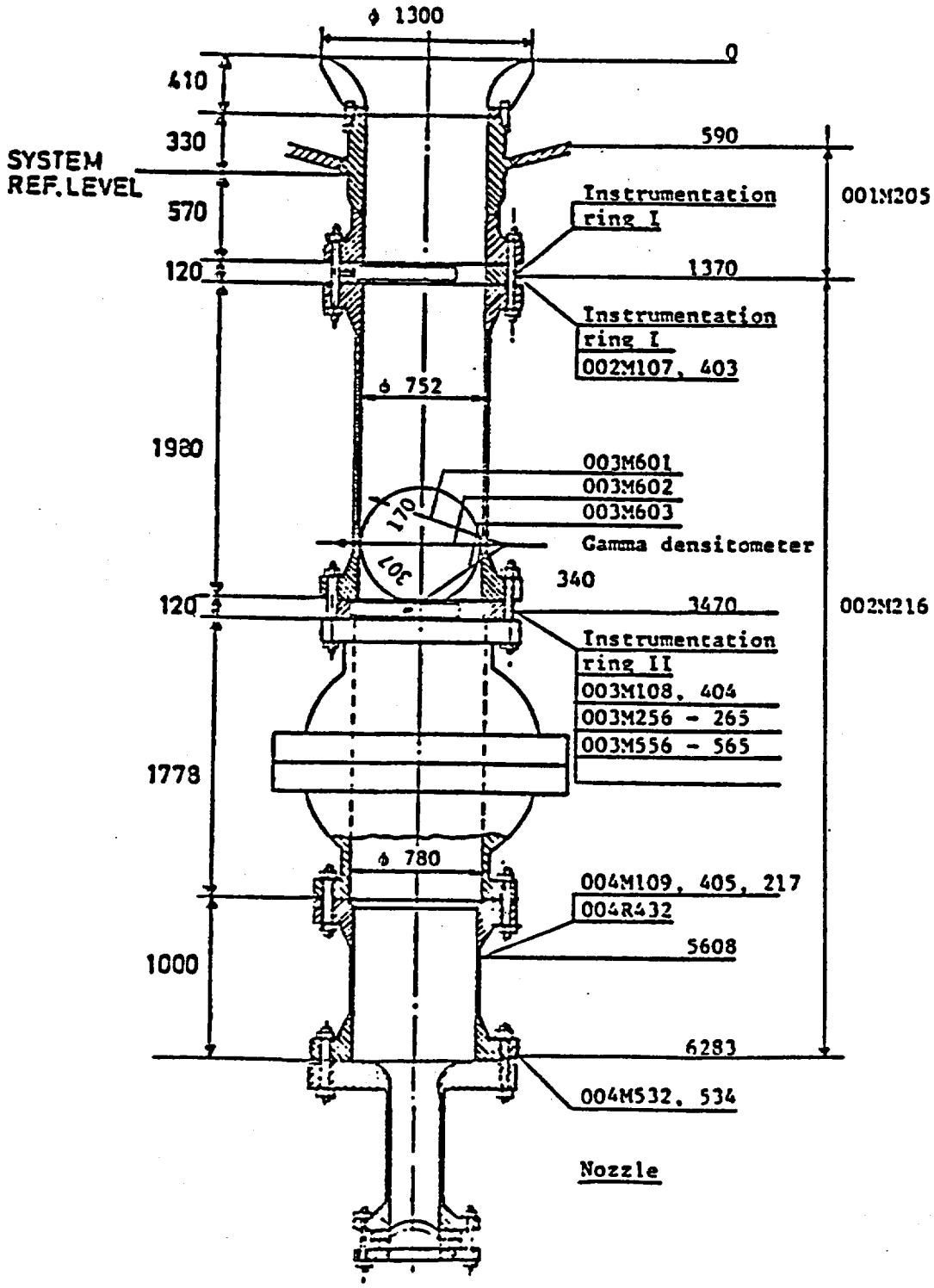

Figure 3.1 Marviken Discharge Pipe. Shown are the Test Section with Nozzle and Location of Instruments

Table 3.2 Nodalization (Refer to Figure 3.2)

Test Number	Diameter (ft)	Cell Size in Discharge Pipe DX_1, (ft)	Cell Size in Converging Section DX_2 (ft)	No. of Cells in Straight Section	Cell Size in Straight Section (ft)
12	.98	1.15	0.49	3	0.97
13	.66	1.15	0.33	2	0.97
15	1.64	1.15	0.75	3	1.90
16	1.64	1.15	0.75	3	1.90
17	.98	1.15	0.49	3	1.22
18	.98	1.15	0.49	3	1.22
19	.98	1.15	1.15	3	1.22
20	.98	1.15	0.75	2	1.20
21	1.64	1.15	0.75	2	1.20
22	1.64	1.15	0.75	2	1.20
24	1.64	1.15	0.75	1	0.52
25	.98	1.15	0.49	2	0.84

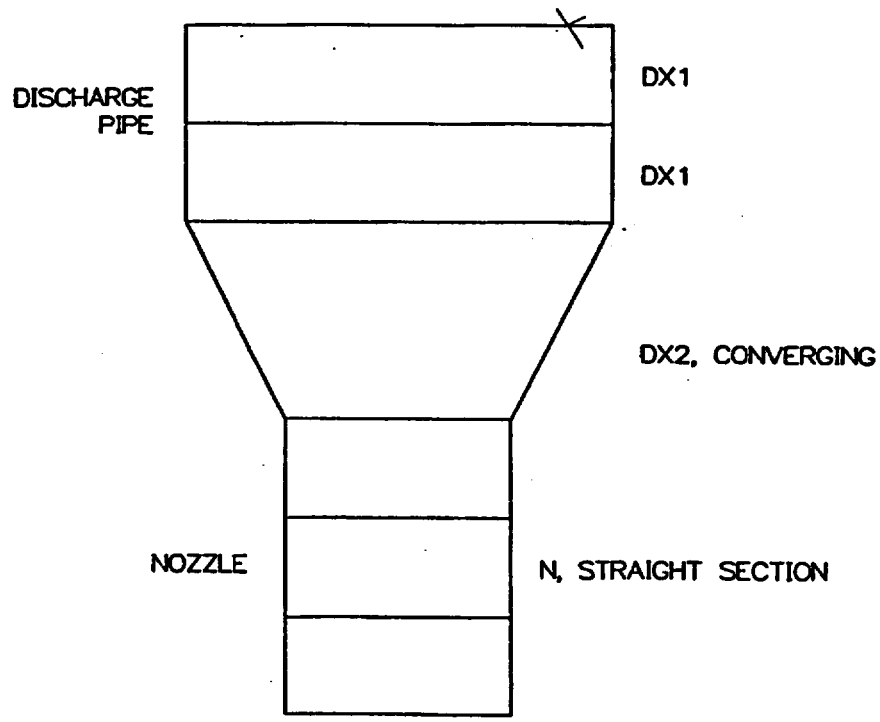

Figure 3.2 Nodalization for Scheme Marviken Tests

Pressure and temperature, both obtained as functions of time from sensors 004M109 and 00M405 shown in Figure 3.1 were imposed as boundary conditions, along with $\alpha = 0$ at the nozzle entrance, and with choking conditions at the nozzle exit. The constraint $\alpha = 0$ means that only a short time span after break initiation could be used for the bias determination. The relaxation of the constraint $\alpha = 0$ would have required the inclusion into the computer simulation of the test section up to the location of the gamma densitometer, which might have compromised the isolation of break flow bias estimation from other modeling uncertainties. Thus, data from Marviken tests and from TRAC calculations were compared only during the time when TRAC predicted $\alpha = 0$ at the nozzle entrance.

Each one of the 12 Marviken tests listed in Tables 3.1 and 3.2 have been simulated with TRAC-PF1/MOD1, Version 14.3. From each transient calculation were selected all the results, at intervals of one second, for which the nozzle entrance void fraction was computed to be zero, and compared with Marviken test results. The test results were sorted into data for subcooled critical flow and two-phase critical flow regimes, according to whether the TRAC code-computed void fraction α_c in the cell upstream of the break is less than 0.01 or greater than 0.10, respectively.

The arithmetic mean $\overline{R_{\dot{m}}}$ of the critical mass flow ratios $R_{\dot{m}}$ according to Eq. (2.7) and their standard deviation S_R were then computed, one for each flow regime and for each test. The results are listed in the last four columns of Table 3.3. The individual critical mass flow rates, as measured in the Marviken tests, are plotted versus computed critical mass flow rates in the scatter diagram of Figure 3.3. The results show that TRAC underpredicts critical flow. Therefore, the critical flow calculations in TRAC cause the peak clad temperature predictions to be too low.

The third column in Table 3.3 shows the mean pressure, averaged over the time (≈ 2-10 sec. depending on subcooling) that the data were compared. The pressure oscillated because of acoustic effects, but remained in the mean fairly constant because of the large vapor volume in the Marviken pressure vessel, acting to maintain constant pressure. The results shown in the last four columns of Table 3.3 must be extrapolated from (≈ 700 psia) to the pressure of 2,250 psia, for the reasons given in Section 3 above.

TRAC calculations performed for the LBLOCA in LOFT [18] show, that the bias $R_{\dot{m}}$ decreases with increasing pressure. This is explained by pointing out that the phasic density difference and the enthalpy of evaporation decrease with increasing pressure, causing the flow to approach homogeneous equilibrium flow for increasing pressure. Thus, the critical flow velocity approaches a_{HE} in Eq. (2.1), and the bias $R_{\dot{m}}$ approaches unity. Since it was not possible to determine how far $R_{\dot{m}}$ approaches unity and since it is not possible in TRAC to accommodate a pressure-dependent $\overline{R_{\dot{m}}}$, the pessimistic, low-pressure value of $R_{\dot{m}}$ and S_R as obtained from Marviken test data were used for the peak clad temperature uncertainty analysis.

The mean bias values $\overline{R_{\dot{m}}}$ and their standard deviation s_R were curve-fitted with respect to the geometric scaling group (L/D). Linear, logarithmic and exponential curve fits were developed and exponential curve fit produced the largest value for the coefficient of determination and thusly the best fit. The results are for:

Subcooled Choking Flow

$$(\overline{R_{\dot{m}}})_{sc} = 0.696 \exp\left(0.649 \left(\frac{L}{D}\right)^{-0.168}\right) \tag{4.1}$$

$$(S_R)_{sc} = 0.9 \exp\left(-1.737 \left(\frac{L}{D}\right)^{0.227}\right) \tag{4.2}$$

Two-phase Choking Flow

$$(\overline{R_{\dot{m}}})_{2-\phi} = 0.778 \exp\left(0.679 \left(\frac{L}{D}\right)^{-0.25}\right) \tag{4.3}$$

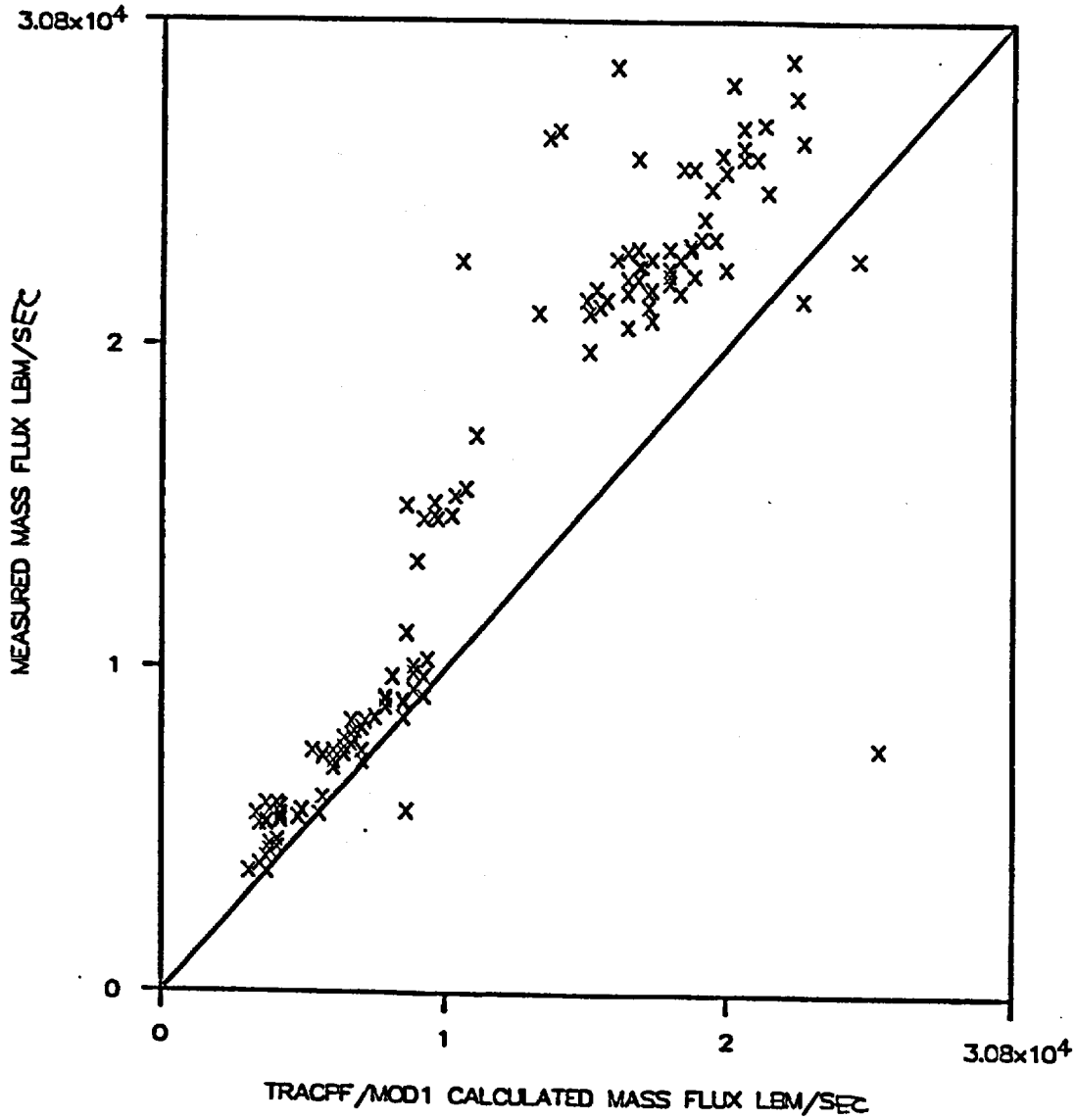

Figure 3.3 Comparisons of the Marviken Data with TRACPF1/MOD1 Results for Critical Break Flow

Table 3.3 Bias Estimates Comparison of Marviken Test Results with TRAC Calculations

Test No.	L/D	Pressure p (psia)	Nozzle Diam. D (ft)	Subcooling Temp. ΔT (F)	Subcooled Two-Phase Flow Regimes			
					$\overline{R}_m$	S_R	$\overline{R}_m$	S_R
12	3.0	755	0.98	54	1.115	0.024		
13	3.0	740	0.66	54			1.112	0.068
15	3.6	633	1.64	54	1.219	0.118		
16	3.6	621	1.64	54	1.258	0.084		
17	3.7	691	0.98	54	1.146	0.056		
18	3.7	716	0.98	54	1.157	0.030		
19	3.7	718	0.98	9	1.11	0.109	1.309	0.088
20	1.5	682	1.64	9			1.54	0.107
21	1.5	621	1.64	54	1.364	0.097		
22	1.5	599	1.64	90	1.35	0.186		
24	0.32	594	1.64	54	1.533	0.246	1.92	0.59
25	1.7	693	0.98	9	1.18	1.485	0.125	

$$(S_R)_{2-\phi} = 2.027 \exp\left(-2.16 \left(\frac{L}{D}\right)^{0.25}\right) \quad (4.4)$$

The two bias values, $(\overline{R_m})_{sc}$ and $(\overline{R_m})_{2-\phi}$, constitute the systematic modeling errors in Eqs. (2.1) and (2.6). they are computed from Eqs. (4.1) and (4.3) for the postulated break location and used as the two break flow multipliers in TRAC, which are required input parameters. The standard deviations $(S_R)_{sc}$ and $(S_R)_{2-\phi}$ account for all the uncertainties other than geometric scale. They are used to determine the range of $\overline{R_m}$ -uncertainty in the statistical analysis of Peak Clad temperature uncertainty.

4. CONCLUSIONS

TRAC-PF1/MOD1 underpredicts the critical break flow rate. The underprediction of break flow rate causes the peak clad temperature to be too low.

The standard deviation, which accounts for all but the geometric parameter uncertainties, varies from 0.02 to 0.59 in the L/D range between 0.33 and 3.70, while the mean bias varies between 1.10 and 1.92, as the code underpredicts the flow rate between 10 and 92 percent.

5. ACKNOWLEDGEMENTS

The authors greatly appreciate the fine typing of Mrs. Linda Hanlon.

6. REFERENCES

1. Compendium of ECCS Research for Realistic LOCA Analysis, NUREG-1230, Chapter 4, April 1987.

2. Liles, D. R., et al., "TRAC-PF1/MOD1: An Advanced Best Estimate Computer Program for Pressurized Water Reactor Thermal-Hydraulics," NUREG/CR-3858, April 1987.

3. Jones, Jr., O. C., "Flashing Inception in Flowing Liquids," Brookhaven National Laboratory Report, BNL-NUREG-51221, 1980.

4. Ranson, V. H., "RELAP5/MOD 1 Manual, Volume 1: System Models and Numerical Methods," NUREG/CR-1826 (1981).

5. "The Marviken Full Scale Critical Flow Tests, Results from Test 12," MXC-212, September 1979, Joint Reactor Safety Experiments in the Marviken Power Station, Sweden.

6. "The Marviken Full Scale Critical Flow Tests, Results from Test 13," MXC-213, September 1979, Joint Reactor Safety Experiments in the Marviken Power Station, Sweden.

7. "The Marviken Full Scale Critical Flow Tests, Results from Test 15," MXC-215, September 1979, Joint Reactor Safety Experiments in the Marviken Power Station, Sweden.

8. "The Marviken Full Scale Critical Flow Tests, Results from Test 16," MXC-216, September 1979, Joint Reactor Safety Experiments in the Marviken Power Station, Sweden.

9. "The Marviken Full Scale Critical Flow Tests, Results from Test 17," MXC-217, September 1979, Joint Reactor Safety Experiments in the Marviken Power Station, Sweden.

10. "The Marviken Full Scale Critical Flow Tests, Results from Test 18," MXC-218, September 1979, Joint Reactor Safety Experiments in the Marviken Power Station, Sweden.

11. "The Marviken Full Scale Critical Flow Tests, Results from Test 19," MXC-219, September 1979, Joint Reactor Safety Experiments in the Marviken Power Station, Sweden.

12. "The Marviken Full Scale Critical Flow Tests, Results from Test 20," MXC-220, September 1979, Joint Reactor Safety Experiments in the Marviken Power Station, Sweden.

13. "The Marviken Full Scale Critical Flow Tests, Results from Test 21," MXC-221, September 1979, Joint Reactor Safety Experiments in the Marviken Power Station, Sweden.

14. "The Marviken Full Scale Critical Flow Tests, Results from Test 22," MXC-222, September 1979, Joint Reactor Safety Experiments in the Marviken Power Station, Sweden.

15. "The Marviken Full Scale Critical Flow Tests, Results from Test 24," MXC-224, September 1979, Joint Reactor Safety Experiments in the Marviken Power Station, Sweden.

16. "The Marviken Full Scale Critical Flow Tests, Results from Test 25," MXC-225, September 1979, Joint Reactor Safety Experiments in the Marviken Power Station, Sweden.

17. Abdollahian, D., "Critical Flow Data Review and Analysis," EPRI Report, NP-2192, January 1982.

18. Coddington, P., "OECO-LOFT LP-LB-1 Comparison Report," Winfrith Atomic Energy Establishment, AEEW-R2478, Draft Report, March 1989.

APPENDIX N

UNCERTAINTY IN TRAC-PF1/MOD1 MINIMUM FILM BOILING TEMPERATURE

APPENDIX N

UNCERTAINTY IN TRAC-PF1/MOD1 MINIMUM FILM BOILING TEMPERATURE

This appendix documents comparison of the TRAC-PF1/MOD1 T_{min} model with data and provides recommendations for ranging in the CSAU procedure.

UNCERTAINTY IN TRAC-PF1/MOD1 MINIMUM FILM BOILING TEMPERATURE

Rex W. Shumway

November 1987

UNCERTAINTY IN THE TRAC-PF1/MOD1 MINIMUM FILM BOILING TEMPERATURE

The following discussion addresses the CSAU uncertainty in the minimum film boiling temperature (TMIN) used by the TRAC-PF1/MOD1 code and its relation to the value of the film boiling heat transfer coefficient.

Transition of a hot surface from film boiling to nucleate boiling is governed by many factors. Consequently there are many correlations that specify the temperature below which return to nucleate boiling is allowed. TRAC-PF1 uses a modification of the homogeneous nucleation temperature (THN), suggested by Bjornard and Griffith (Reference 1). The correlation is:

$$TMIN = THN + (THN - Tliq)*Beta \qquad \text{Eq. 1}$$

where:

$$Beta = sqrt((k\ rho\ c)_{liq} / (k\ rho\ c)_{wall})$$

The Beta term was derived by Carslaw and Jaeger (Reference 2) when describing the interface temperature between two semi-infinite slabs.

Figure 1 shows rod quench temperature data, from Reference 3, ranging from about 600 K to 900 K. Table 1 gives the legend information for Figure 1. The two "8's" in the figure are the upper and lower bounds of the Lehigh University data. The INEL THTF (sometimes referred to as LTSF) data is similar to the Lehigh data and was not included. The "A's" at the left side of Figure 1 are the upper and lower bound of the FLECHT and Semiscale data. Although there are data from Zircaloy surfaces from LOFT and FLECHT, there are potential problems with the LOFT data because of external thermocouples and with FLECHT because of possible clad swelling.

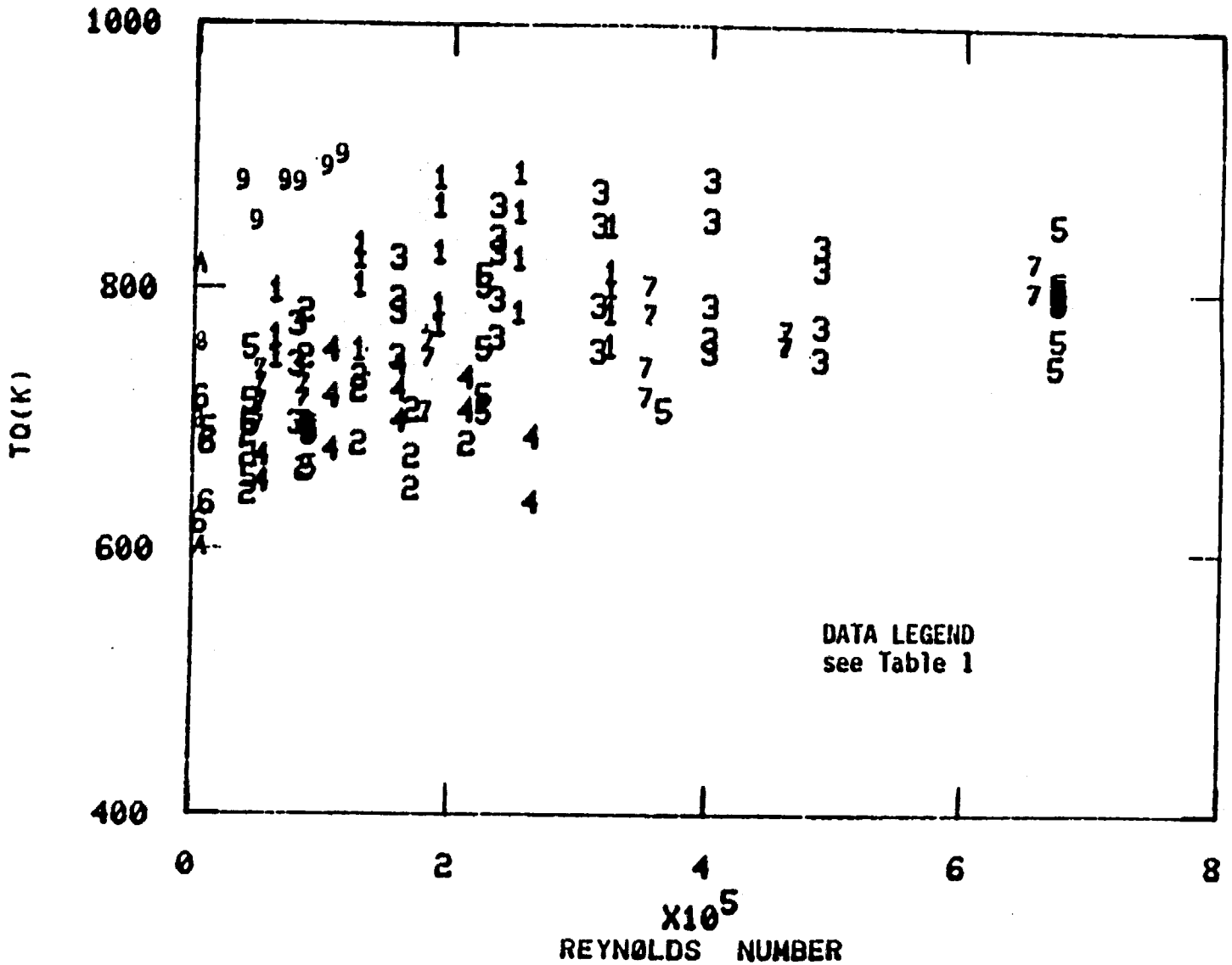

Figure 1. TMIN versus Reynolds Number.

TABLE 1. LEGEND FOR FIGURE 1

	Name	P(MPa)	D_h(m)	G(kg/s-m**2)	Geometry	Material
1.	Becker	3.	0.01	500.	Tube	SS
2.	Becker	3.	0.0149	500.	Tube	SS
3.	Becker	7.	0.01	500.	Tube	SS
4.	Becker	7.	0.0149	500.	Tube	SS
5.	Janssen	7.	0.0125	68.	Tube	SS
6.	Janssen	0.7	0.0125	68.	Tube	SS
7.	Bennett	6.9	0.0126	400.	Tube	SS
8.	Lehigh-U	0.38	0.0154	15.	Tube	SS
9.	ORNL	4.-9.	0.0121	200-800	Rods	SS
10.	Semiscale	0.413	0.0136	13-42	Rods	SS
11.	FLECHT	0.276	0.0120	20-140	Rods	SS
12.	Dhir	0.1	0.08	20-290	Rods	SS-Zr

The Bjornard-Griffith correlation (Equation 1) gives results which are lower than most of the data. One deficiency of most correlations is that they do not consider the effect of the fluid void fraction or flow rate. TRAC-BF1 uses a correlation developed by Shumway (Reference 3), which includes void and flow effects.

The correlation used by the TRAC-P code has pressure dependence but no Reynolds number dependence so the data was re-plotted in Figure 2 with pressure as the abscissa. Also only the upper and lower TMIN values were chosen from the low flow data and the Dhir data was added at the left of Figure 2. Data from small scale "clean" surfaces was not used because it would tilt the total data base to the low side. The TMIN lower bound is the one that will yield the highest peak clad temperature in TRAC calculations. If the TMIN lower bound were lowered even further because of considering clean or polished surface data, it could very adversely affect future TRAC-P calculations of PCT (at least at high values of mass flux; low mass flux values would only be slightly influenced as will be shown later).

I recommend the TRAC-PF1 (Bjorard-Griffith) equation plus 200 K as an upper bound as shown in Figure 2. Only the ORNL data on the right and some Dhir data on the left exceed this value. Although a higher value could be justified, this value is already high enough to cause early quenching in the large break calculations I am aware of. I recommend the homogeneous nucleation temperature (THN) as the TMIN uncertainty lower bound since it is along the lower bound of the stainless-steel data, and therefore conservative. Zircaloy rods quench at a higher temperature than stainless-steel rods because of the Beta effect. Some lower bound data is low only because there was insufficient water present in the experiment earlier in time when the wall temperature was higher.

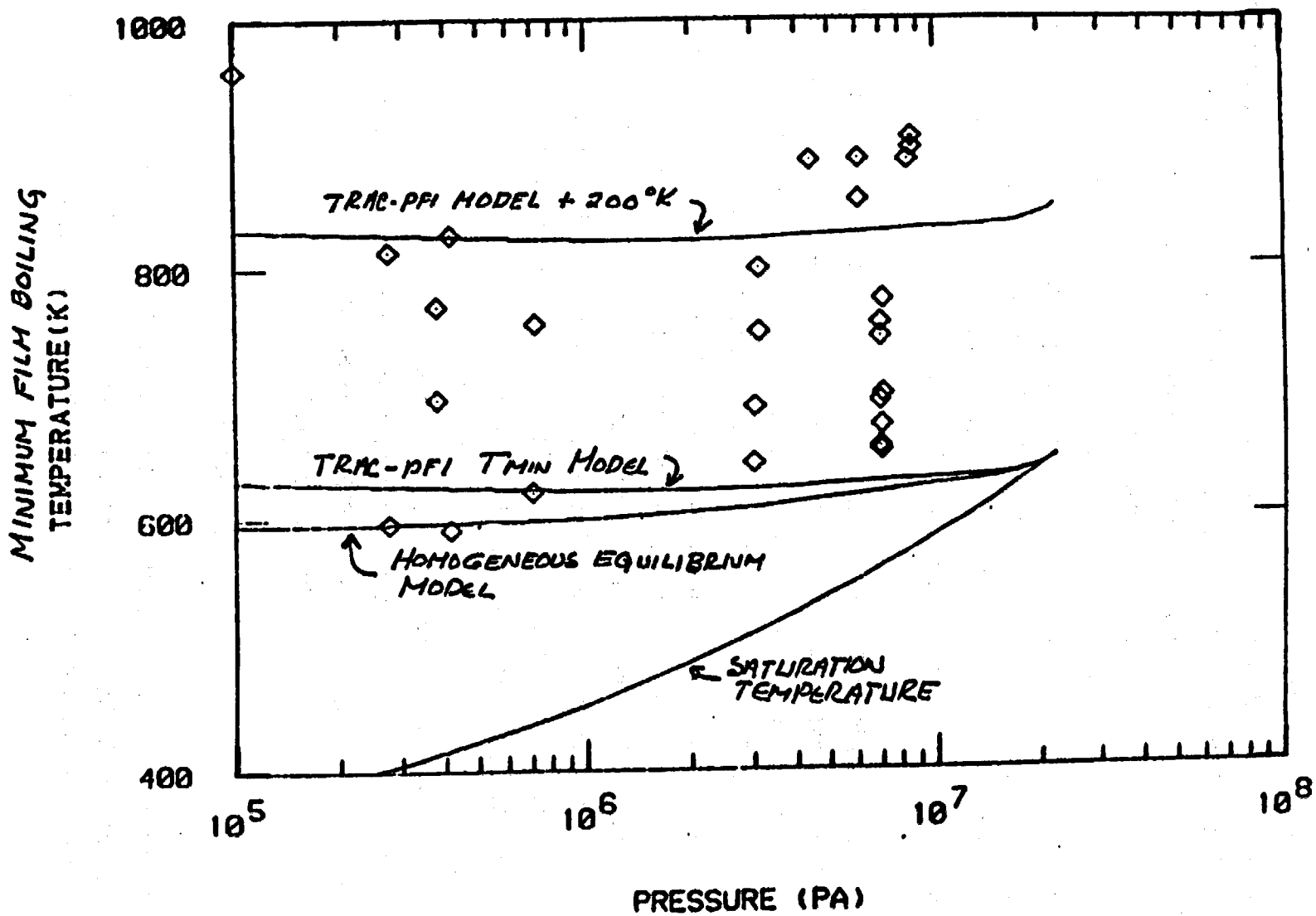

Figure 2. TRAC-PF1 TMIN uncertainty.

To show the effect of the above recommended TMIN bounds on the TRAC-PF1 heat flux, a calculation was performed by driving the TRAC heat transfer subroutines with boundary conditions specified below. The initial wall temperature was initiated at Tsat plus 500 K and reduced in small increments for Nominal conditions, Best case conditions and Worst case conditions. Nominal conditions resulted from using TRAC-PF1 subroutines with no modifications (TMIN = Eq. 1). Best case conditions show the result of having a 40% increase in film boiling heat transfer coefficients and Equation 1 plus 200 K for TMIN. The Worst case assumes a 40% reduction in the heat transfer coefficient and TMIN=THN. The coupled effect of changing TMIN and the heat transfer coefficient is shown in Figure 3. Table 2 gives the boundary conditions for the calculation shown in Figure 3.

Notice, from Figure 3, that if TMIN were much lower than THN it would go below the critical heat flux temperature (TCHF). Therefore, for low mass flux cases, values of TMIN much lower than THN would be ignored because they would be below TCHF. Since the Biasi CHF value decreases with increasing mass flux, a smaller TMIN lower bound would have an effect at larger mass flux values. The way Biasi is programmed in the TRAC-PF1 code the maximum CHF occurs at G=200 kg/s-m^2 and is a constant for lower values of G. However, this brings up the fact that Biasi CHF value may be too large. The predicted value of TCHF more than 150 K larger than TSAT is suspicious. Professor Becker (Reference 4) reports that Biasi gives values that are larger than the experimental values in rod bundles. He is uncertain what correlation to recommend for low pressure cases such as the one used to generate Figure 3. CHF errors have a negligible influence on the rod temperature rise during reflood but CHF errors be addressed because they can have a significant effect on the blowdown PCT.

CONCLUSION

The lower bound on the CSAU TRAC-PF1 minimum film boiling temperature should be set to the homogeneous nucleation temperature (THN). The upper bound should be about 200 K larger than the value the code currently calculates.

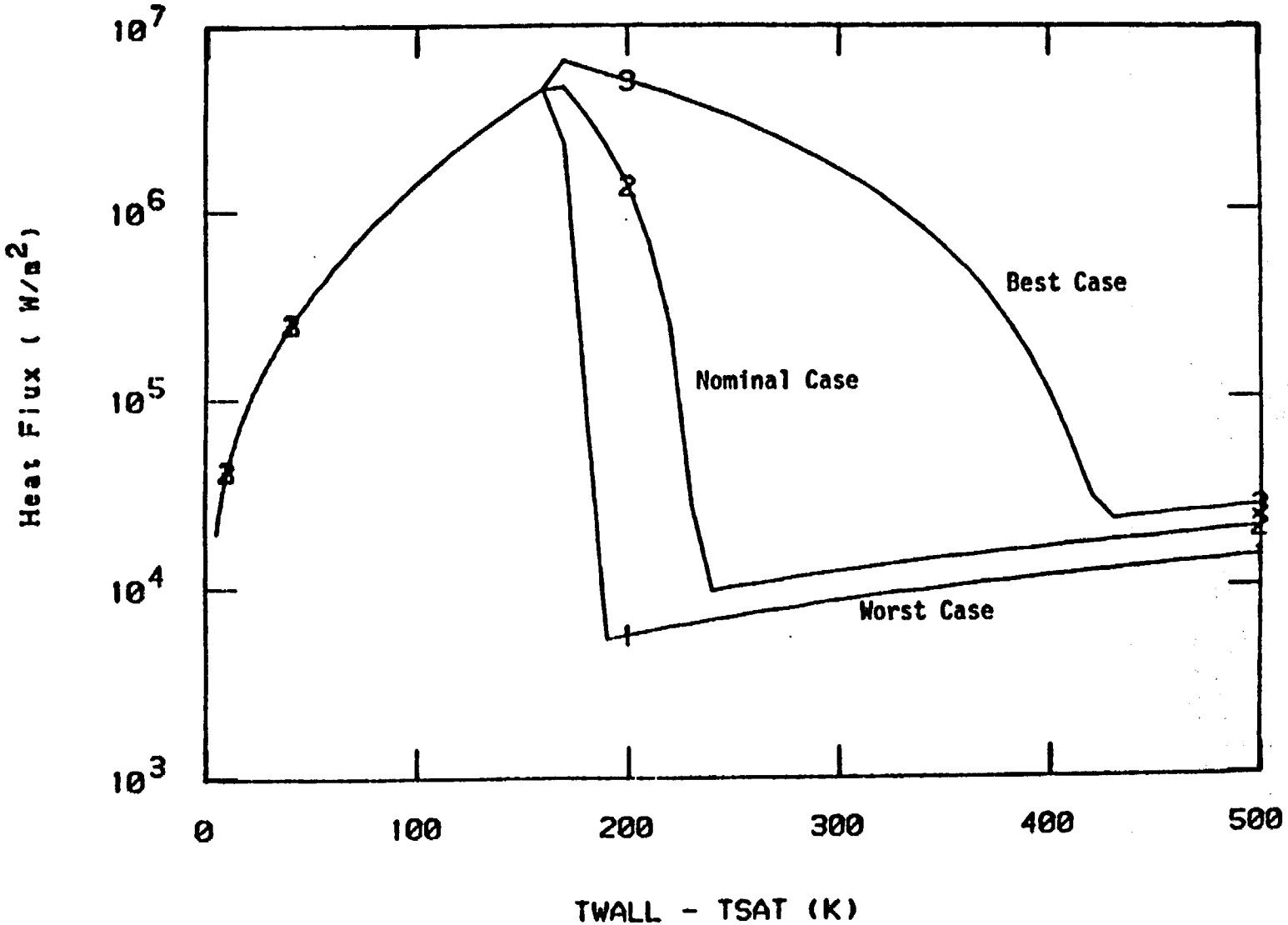

Figure 3. TRAC-PF1 surface heat flux for low flow, low pressure.

TABLE 2. BOUNDARY CONDITIONS FOR FIGURE 3

Pressure	0.37 MPa.
Mass flux	100. kg/s-m**2
Void Fraction	0.95
Hydraulic diameter	0.015 m
Wall material	Zircaloy

REFERENCES

1. H. S. Carslaw, and J. C. Jaeger, Conduction of Heat in Solids, 2nd Edition, Clarendon Press, Oxford, 1959.

2. T. A. Bjornard and P. Griffith, "PWR Blowdown Heat Transfer," Symposium on the Thermal and Hydraulic Aspects of Nuclear Reactor Safety, Volume 1: Light Water Reactors, ASME Winter-Annual, Atlanta, Georgia, Nov. 27-Dec. 2, 1977, pp. 17-41.

3. R. W. Shumway, "Return to Nucleate Boiling," ANS Proceedings, National Heat Transfer Conference, Denver Colorado, August 4-7, 1985, pp. 372-388.

4. L. Sardh and K. M. Becker, Assessment of CHF Correlations Based on Full-Scale Rod Bundle Experiments, KTH-NEL-36, February 1986.

APPENDIX O

TRAC-PF1/MOD1 POST-CHF HEAT TRANSFER COEFFICIENT VARIATION FOR CSAU

APPENDIX O

TRAC-PF1/MOD1 POST-CHF HEAT TRANSFER COEFFICIENT VARIATION FOR CSAU

An evaluation of the multiplier range to be applied to the code-calculated convective heat transfer coefficient in the CSAU procedure is documented in this appendix.

TRAC-PF1 POST-CHF HEAT TRANSFER COEFFICIENT VARIATION FOR CSAU

by

Rex W. Shumway

INEL

July 7, 1988

TRAC-PF1 Post-CHF Wall Heat Transfer Coefficients

The purpose of this report is to: (1) present a comparison between the TRAC-PF1/MOD1 wall heat flux calculated in the post-CHF Mode 4 heat transfer regime and experimental film boiling results, and (2) determine an overall multiplier for the convective heat transfer coefficient for the CSAU uncertainty evaluation. The wall heat flux (q_{wall}) is evaluated from the following expression:

$$q_{wall} = h_l(T_{wall} - T_{liq}) + h_v(T_{wall} - T_{vap})$$

where:

h_l = liquid heat transfer coefficient
h_v = vapor heat transfer coefficient
T_{wall} = wall surface temperature
T_{liq} = liquid temperature
T_{vap} = vapor temperature

The heat transfer coefficients are large during the nucleate boiling steady state reactor operation but become small when flow conditions are disrupted following an accident. The heat transfer after the coefficients become small is known as the post critical heat flux (CHF) or film boiling regime. The fuel cladding temperature escalates due to the decreased heat transfer and the temperature rise is terminated only when the heat transfer increases or the power reduces.

The calculated film boiling heat flux values are compared to experimental data to help determine the uncertainty range of the heat transfer coefficients during a postulated accident. TRAC-PF1/MOD1[1] wall surface heat transfer coefficients are a strong function of the amount of vapor (void fraction) in the flow channel next to the wall. If the void fraction is 1.0 and the wall temperature is above the vapor saturation temperature, the heat transfer regime is specified as Mode number 6; the steam cooling mode. The liquid heat transfer coefficient is set to zero and the vapor value is set from the Sieder-Tate correlation. Under two-phase flow conditions, however, the logic is not as straight forward. If the void fraction is greater than 0.97 the Mode 6 value is first

calculated then the Mode 4 (two-phase conditions) value is determined and void fraction weighting is used between these to values. Below a void fraction of 0.97, only the Mode 4 value is calculated. The code prints Mode 4 as the mode number even above a void fraction of 0.97 unless the void fraction is 1.0. In Mode 4, the heat flux to vapor is the maximum of a natural convection correlation and the Dougall-Rohsenow correlation. The liquid coefficient is composed of a radiation term, and a dispersed flow Forslund-Rohsenow term, or a Bromley film term. Below a void fraction of 0.5, the Forslund-Rohsenow term is zero and above 0.75 the Bromley term is zero. The upper limit (maximum allowed) of the Forslund-Rohsenow term is the Bromley value. Between a void fraction of 0.5 and 0.75, interpolation of the two terms is used.

The accuracy of the Mode 4 correlations has been checked by comparing it with 760 INEL POST-CHF data[2] points. Rather than doing 760 TRAC calculations, a driver-plotter routine was used which incorporated only the essential TRAC subroutines; i.e., fluid property and wall heat transfer subroutines. To verify that errors were not introduced into the driver, conditions from a TRAC calculation of a large break LOCA were input to the driver and the heat transfer coefficients compared with the TRAC values. Table 1 shows the input conditions and the results.

Table 1 Driver-plotter Results Compared to a TRAC Calculation

	Input							TRAC		Driver error	
Time	P	Void	Tw	Tv	Tl	Vv	Vl	hv	hl	hv	hl
(s)	(MPa)		(K)	(K)	(K)	(m/s)	(m/s)	(w/m2-k)	(w/m2-k)		
1.	11.08	.937	734.	595.	591.	1.1	0.34	939.	841.	0.02	0.03
2.	9.5	.984	831.	625.	580.	2.6	1.6	238.	727.	0.06	0.07
5.	7.28	.929	816.	595.	561.	2.5	1.4	592.	683.	0.07	0.01
12.	3.53	.963	708.	547.	516.	-6.4	-4.6	288.	689.	0.09	0.09
20.	0.42	.999	725.	545.	417.	-16.	-6.4	15.	168.	0.05	0.01

The driver heat transfer coefficients differ from TRAC results by up to 9%. This is considered adequate since TRAC output does not display the exact values used as input to the heat transfer subroutines. The input shown in Table 1 is taken from vessel level 6 cell 4 and rod 9 level 3 of the nominal CSAU NPP calculation. The velocities are those donnered into this cell at the lower axial face for positive flow and at the upper face for negative flow.

Comparisons with Post-CHF Data

The range of the INEL post-chf tube data is shown in Table 2.

Table 2 INEL Post-CHF Test Conditions

Parameter	Range
Pressure	0.28 - 7.1 MPa
Mass Flux	12.1 - 71.5 kg/s-m^2
Heat Flux	3.1 - 179.3 kW/m^2
Wall Superheat	190.8 - 709.9 K
Vapor Superheat	2.5 - 507.5 K
Equilibrium Quality	0.13 - 1.05
Void Fraction (slip=1)	0.91 - 0.999
Void Fraction (slip=2)	0.84 - 0.999
Steam Reynolds (inlet)	2000 - 27000
Water Reynolds (inlet)	400 - 8000

The TRAC-PF1 predicted heat flux was compared with the 760 INEL post-CHF data points. The error was calculated for each point by:

$$\text{error} = (Q_{measured} - Q_{predicted})/Q_{measured}$$

The RMS and average error were calculated by:

$$\text{RMS error} = \sqrt{(\Sigma \text{error}^2)/760}$$

$$\text{Average error} = \Sigma \text{error}/760$$

The measurement error is stated to be less than 8 percent.

RMS and average errors are given on Figures 1-4. The variables in the figures are the phasic slip, used to calculate the void fraction from the measured flow quality, and the multiplier used on the calculated total heat flux or used only on the Forslund-Rohsenow correlation. The results from using an overall multiplier of 0.75 certainly is an improvement relative to the 45 degree line (see Figure 1 versus Figure 2). A multiplier of just under 0.6 would be needed to drive the average completely to zero. However, a multiplier as small as 0.6 would overly penalize PWR reflood cooling. The PWR core void fractions become very high during reflood and the steam convection part does not need to be penalized. Figure 3 proves this point. When the Forslund-Rohsenow liquid term is removed the points lie mainly underneath the 45 degree line.

Phasic slip is another uncertainty in the comparisons. Slip is used to calculate the void fraction from the measured flow quality. When the slip increases the calculated void fraction decreases as shown in Table 1. The errors increase significantly with a slip of two, as shown in Figure 4, because Forslund-Rohsenow becomes more important. A slip of two may be overstating the problem since a study of FLECHT reflood data given in Reference 3 shows slip ratios more like 1.25.

The error has also been plotted against void fraction, mass flux, pressure and heat flux in Figures 5 through 8, respectively, with a slip of 1.0 and a heat transfer multiplier of 1.0. Errors are particularly large at low void fractions which occurred at low heat flux values in the intermediate pressure tests. The three fingers on the left of Figure 8 are the three pressure ranges from Figure 7.

A calculation was performed where just the data above a void fraction of 0.98 was considered. There were 602 data points and the average error was -0.33; a reduction of 58% when the number of points was reduced by only 21%. A major source of the errors is the large values calculated by the Forslund-Rohsenow correlation at the lower void fractions. A calculation was performed where only the Forslund-Rohsenow correlation was reduced to help determine the bias caused by this particular correlation. The magnitude of the multiplier on only the Forslund-Rohsenow correlation necessary to reduce the average error to zero for all 760 points in the INEL data set was 0.265.

For CSAU a multiplier was desired which could be used on the total code convection instead of one specific part. Using an overall multiplier of 0.75 on all the points brings the average error down to -0.34 and the RMS error to 0.75.

Conclusions

A comparison of the TRAC-P calculated post-CHF heat transfer and experimental data was made. From this, a 0.75 overall heat transfer multiplier used in the PWR calculations is not small enough for Mode 4 calculations when the void fractions are below about 0.98. However, in order to not penalize nucleate boiling and very high void convection cooling too much, an overall multiplier of 0.75 is acceptable. Particularly since the calculated reflood void fractions are close to one.

REFERENCES

1. TRAC-PF1/MOD1: An Advanced Best-estimate Computer Program for Pressurizrd Water Reactor Thermal-hydraulic Analysis, LA-10157-ms NUREG/CR-3858.

2. R. C. Gottula, et al., Forced Convection, Nonequilibrium, Post-CHF Heat Transfer Experiment Data and Correlation Comparison Report, NUREG/CR-3193, EGG-2245, March 1985.

3. S. Wong, A Model for Dispersed Flow Heat Transfer in Rod Bundles During Reflood, Carnegie-Mellon University, Thesis, September 28, 1979.

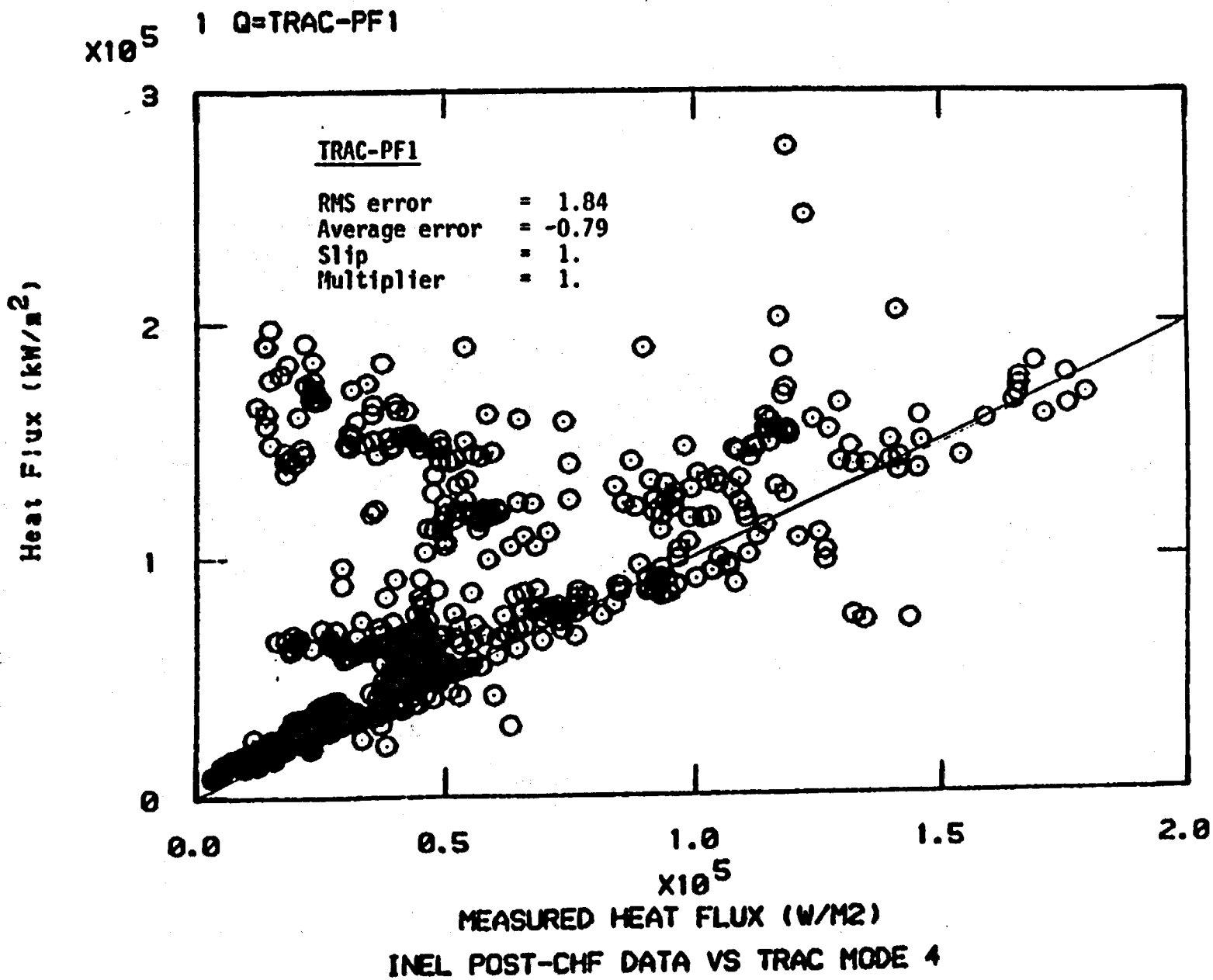

Figure 1. INEL data, multiplier = 1, slip = 1

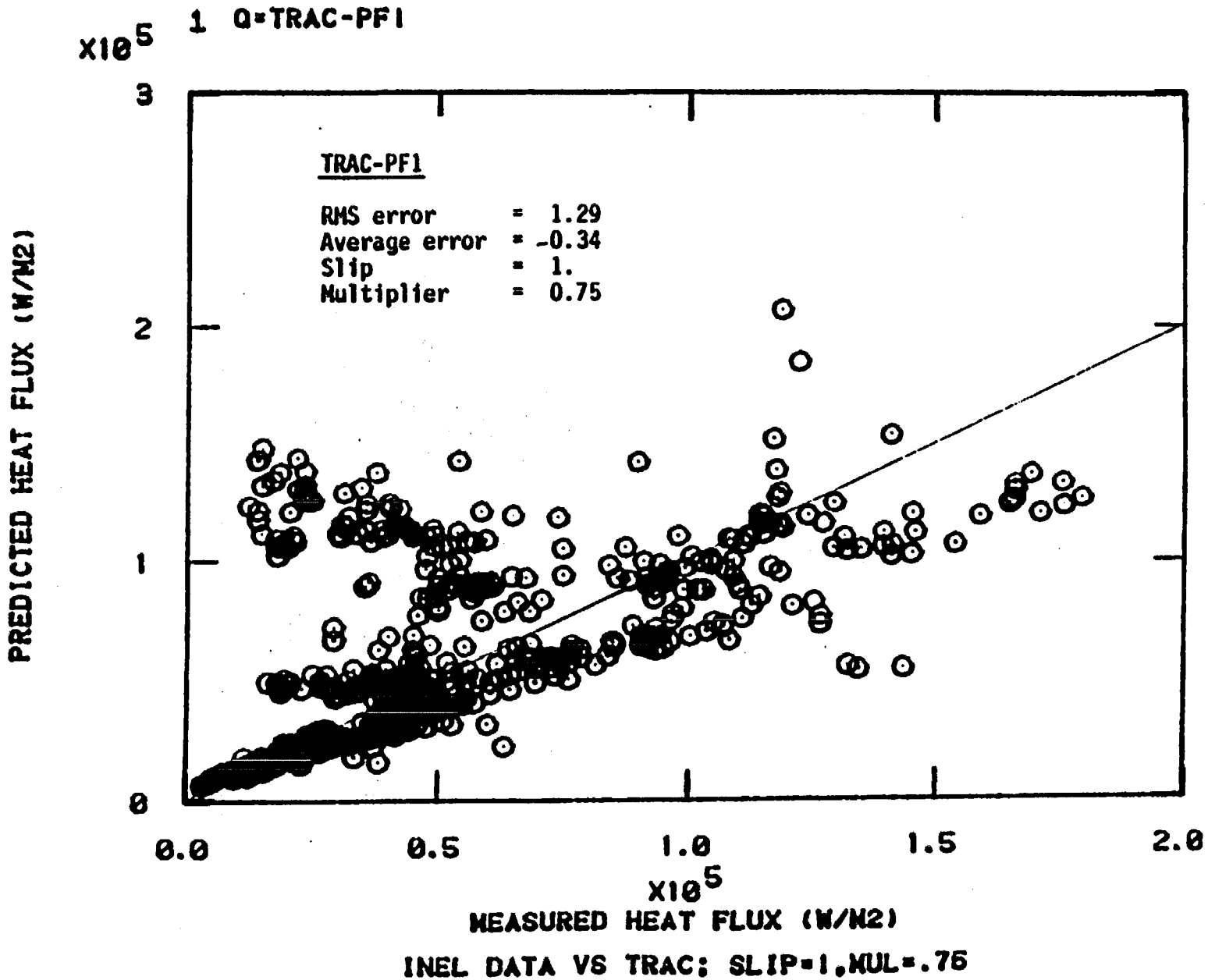

Figure 2. INEL data, slip = 1, multiplier = 0.75

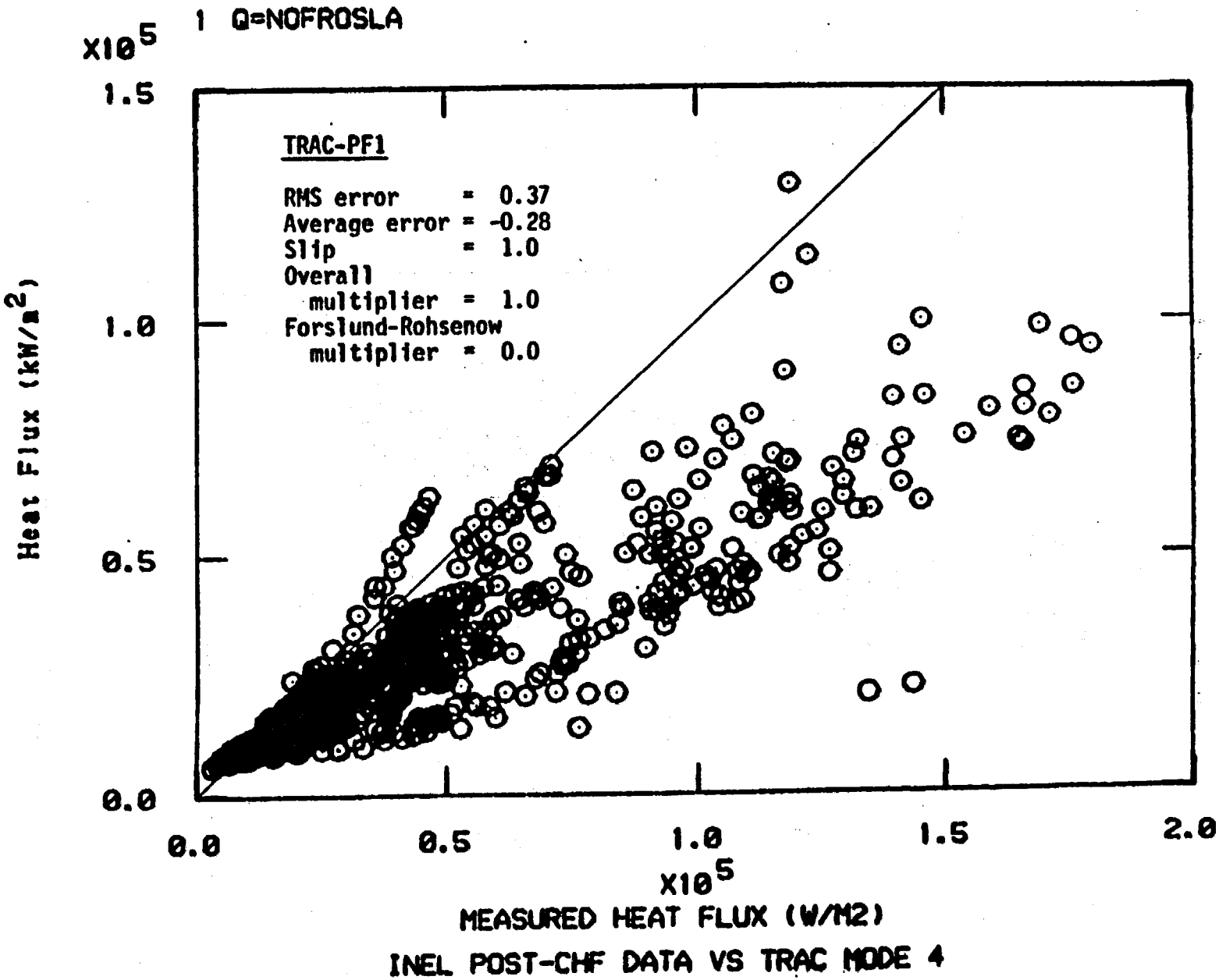

Figure 3. INEL data, slip = 1, no Forslund-Rohsenow

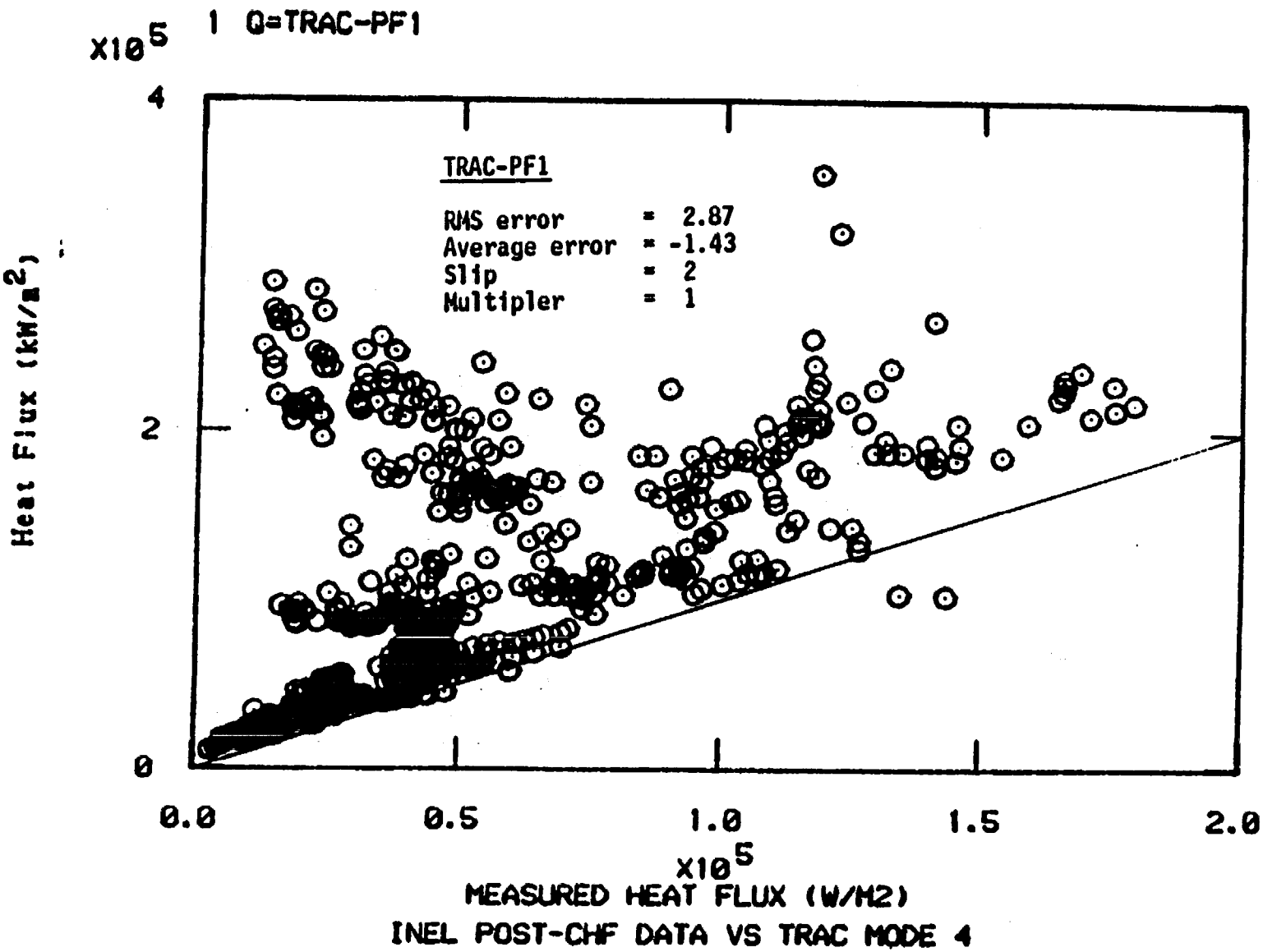

Figure 4. INEL data, slip = 2, multiplier = 1

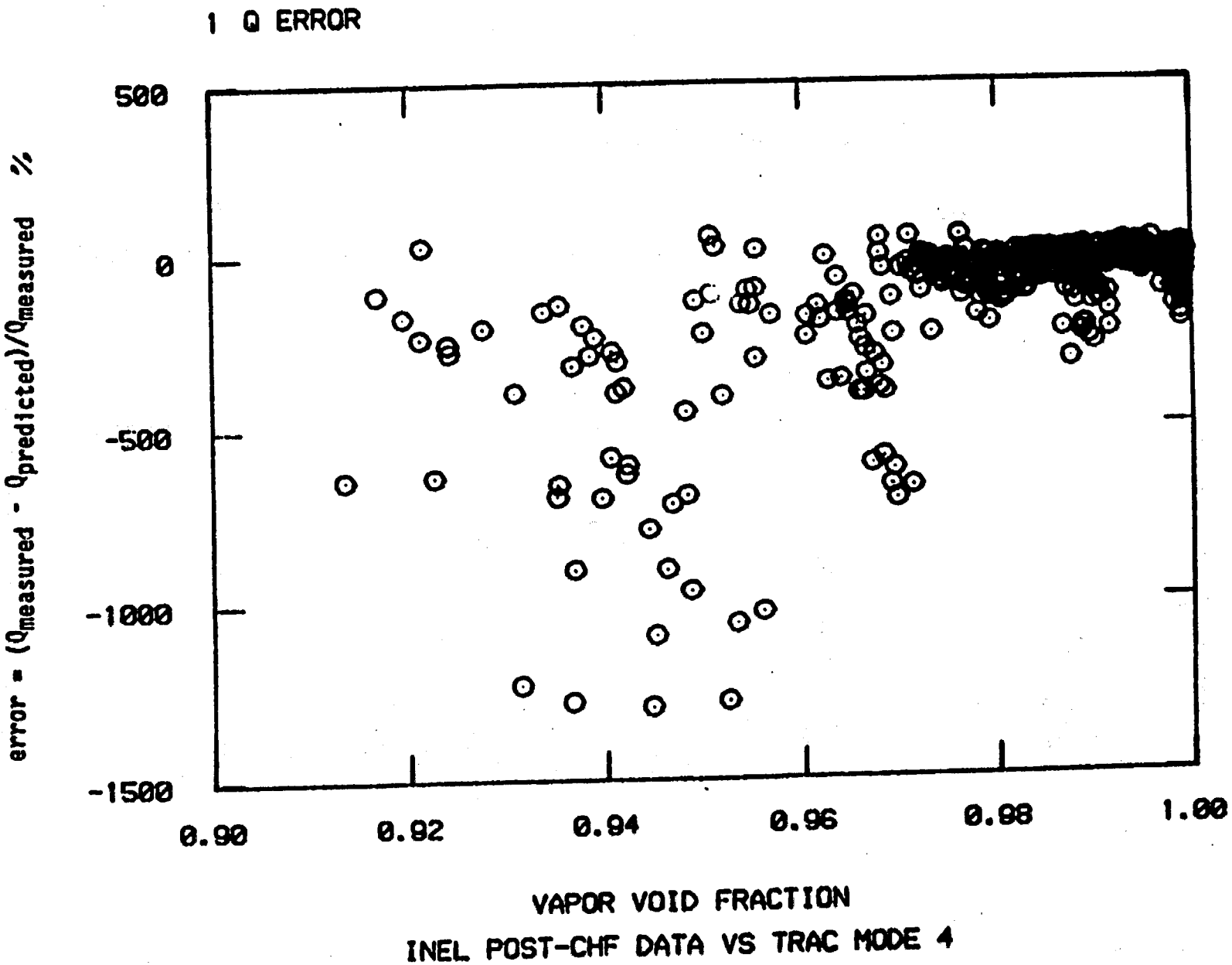

Figure 5. Error vs. void fraction, slip = 1, multiplier = 1

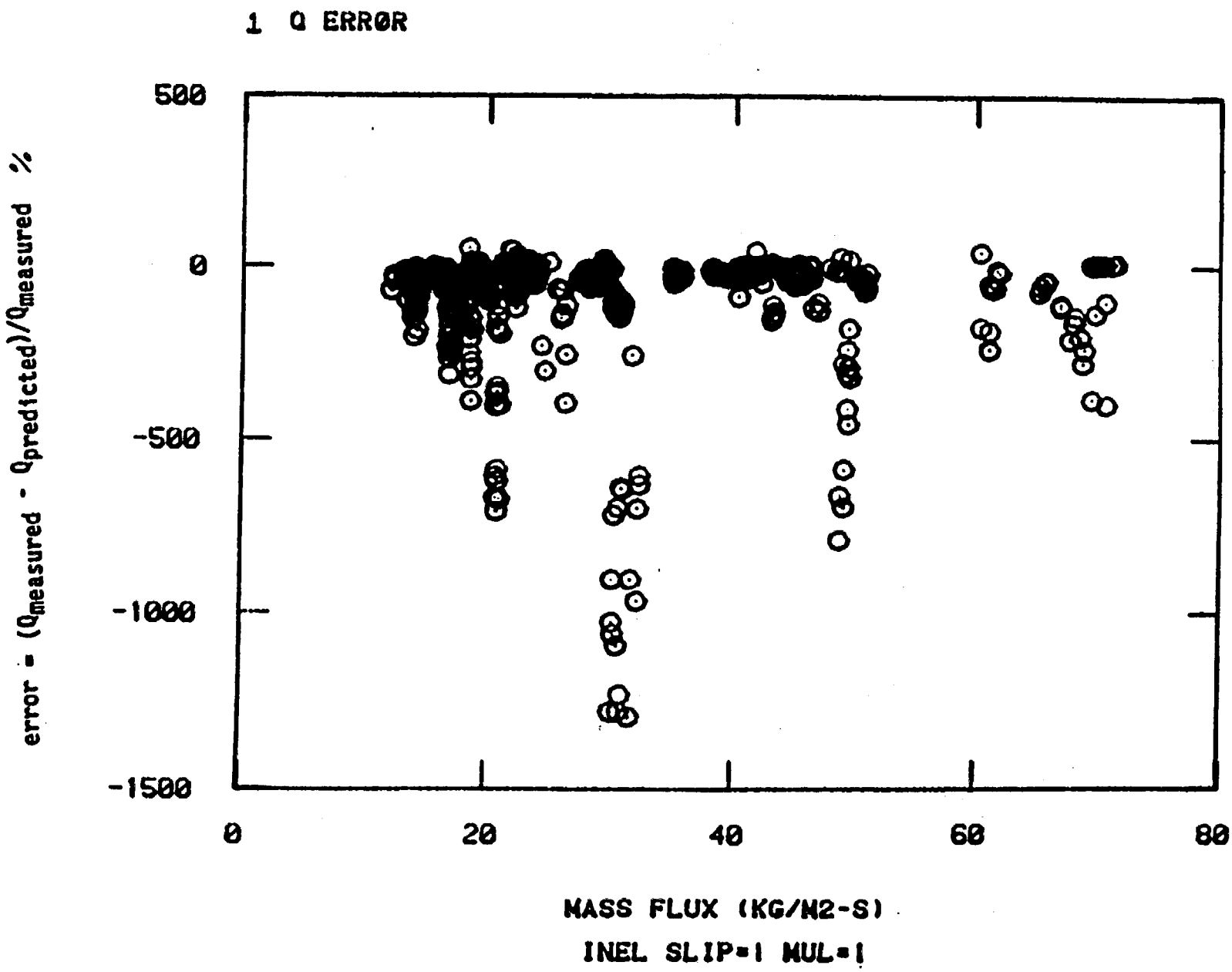

Figure 6. Error vs. mass flux, slip = 1, multiplier = 1

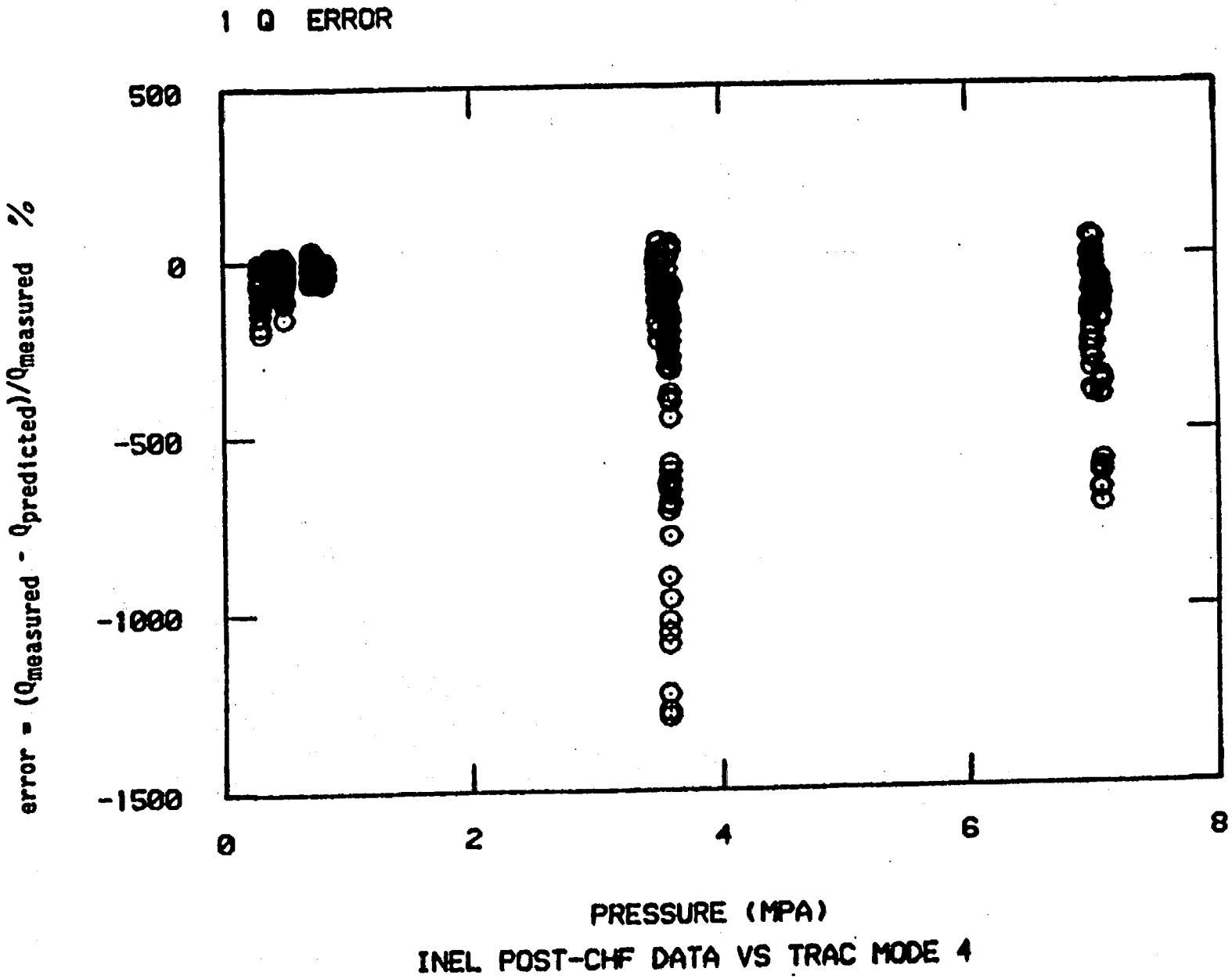

Figure 7. Error vs. pressure,
slip = 1, multiplier = 1

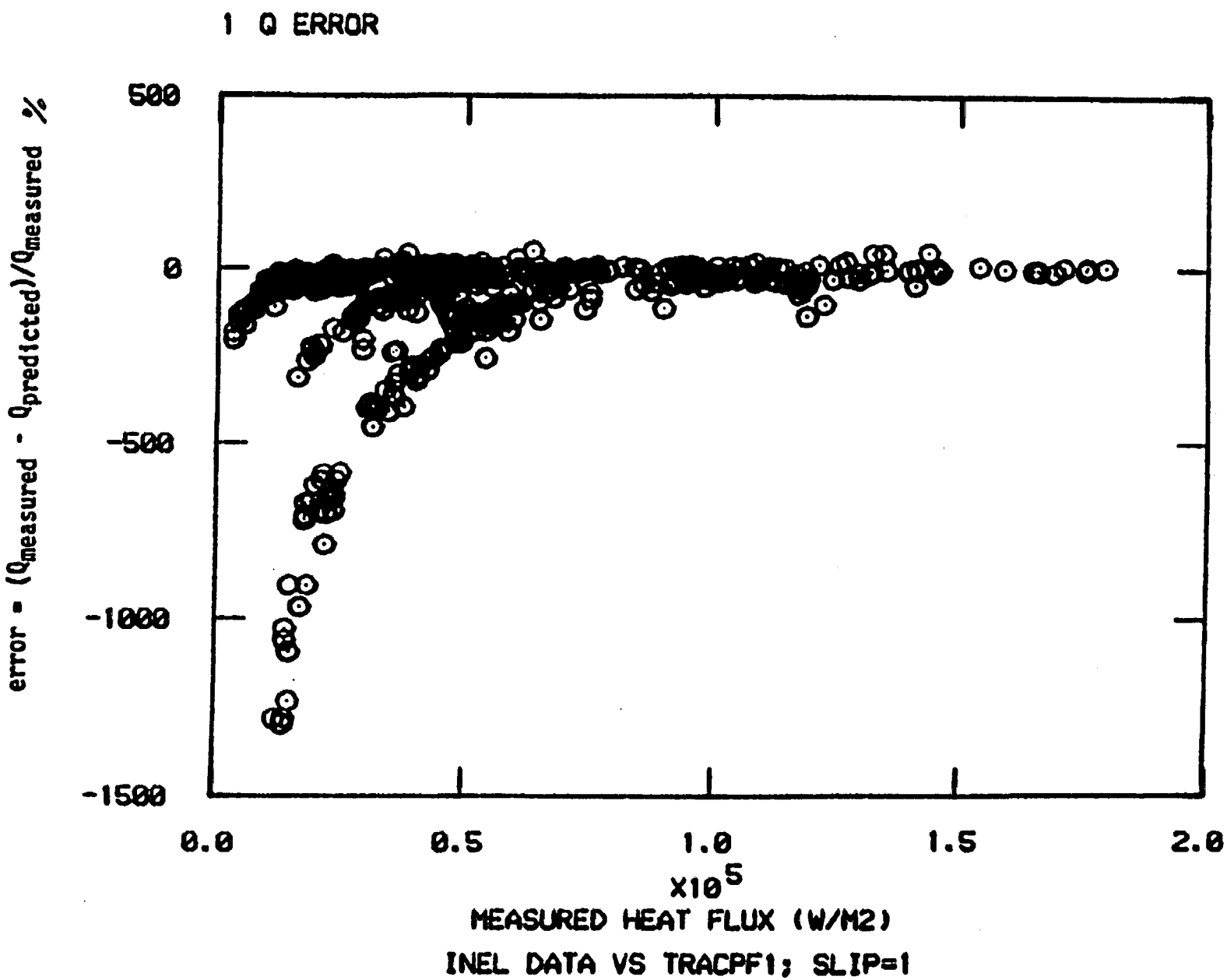

Figure 8. Error vs. heat flux, slip = 1, multiplier = 1

APPENDIX P

PROCEDURE AND RESULTS TO SCALE MULTIPLIERS FOR TRAC-PF1/MOD1 INTERFACE SHARPENER AND CORE INTERPHASE DRAG MODELS TO SUPPORT QUANTIFICATION OF UNCERTAINTY DUE TO STEAM BINDING

APPENDIX P

PROCEDURE AND RESULTS TO SCALE MULTIPLIERS FOR TRAC-PF1/MOD1 INTERFACE SHARPENER AND CORE INTERPHASE DRAG MODELS TO SUPPORT QUANTIFICATION OF UNCERTAINTY DUE TO STEAM BINDING

The information in this appendix is a summary of work performed by Drs. B. Boyack and P. Shire (LANL) to support determination of liquid carried from the core to the steam generators and, thereby, the quantification of uncertainty due to steam binding.

Procedure and Results to Scale Multipliers for TRAC-PF1/MOD1 Interface Sharpener and Core Interphase Drag Models to Support Quantification of Uncertainty Due to Steam Binding

For the reflood peak, steam binding has been identified as an important phenomena by both the experts panel and the PIRT process. Analyses of reflood tests at LANL have shown that the TRAC code does not transfer sufficient liquid from the core to the upper plenum during reflood. Therefore, the code may underpredict steam binding effects. Analyses have shown that (1) sufficient liquid must pass through the pool interface, which is based on an entrainment correlation of Rozen, Golub, and Botiutseva, and (2) the interfacial drag must be sufficient to carry the entrained liquid to the upper plenum and hot legs.

At the request of the TPG, studies were performed by the TRAC code developers and analysts, using SCTF test data, to develop multipliers and code updates for the Rozen correlation and interfacial drag models in the core and upper plenum regions. Parametric studies, using the same axial nodalization as the CSAU NPP runs, were made using SCTF Tests 601 and 602. The variations are shown in the attached schematic, and the results are shown in the attached figure. The result of the study was a proposal to the TPG to use multipliers as follows:

1. For the Rozen correlation, use a multiplier of 20.0.

2. For the core interfacial drag model, use a multiplier of 10.0.

3. For the upper plenum interfacial drag model, use a multiplier. of 1.0

These recommendations were accepted by the TPG and used in the CSAU sensitivity calculations for steam binding.

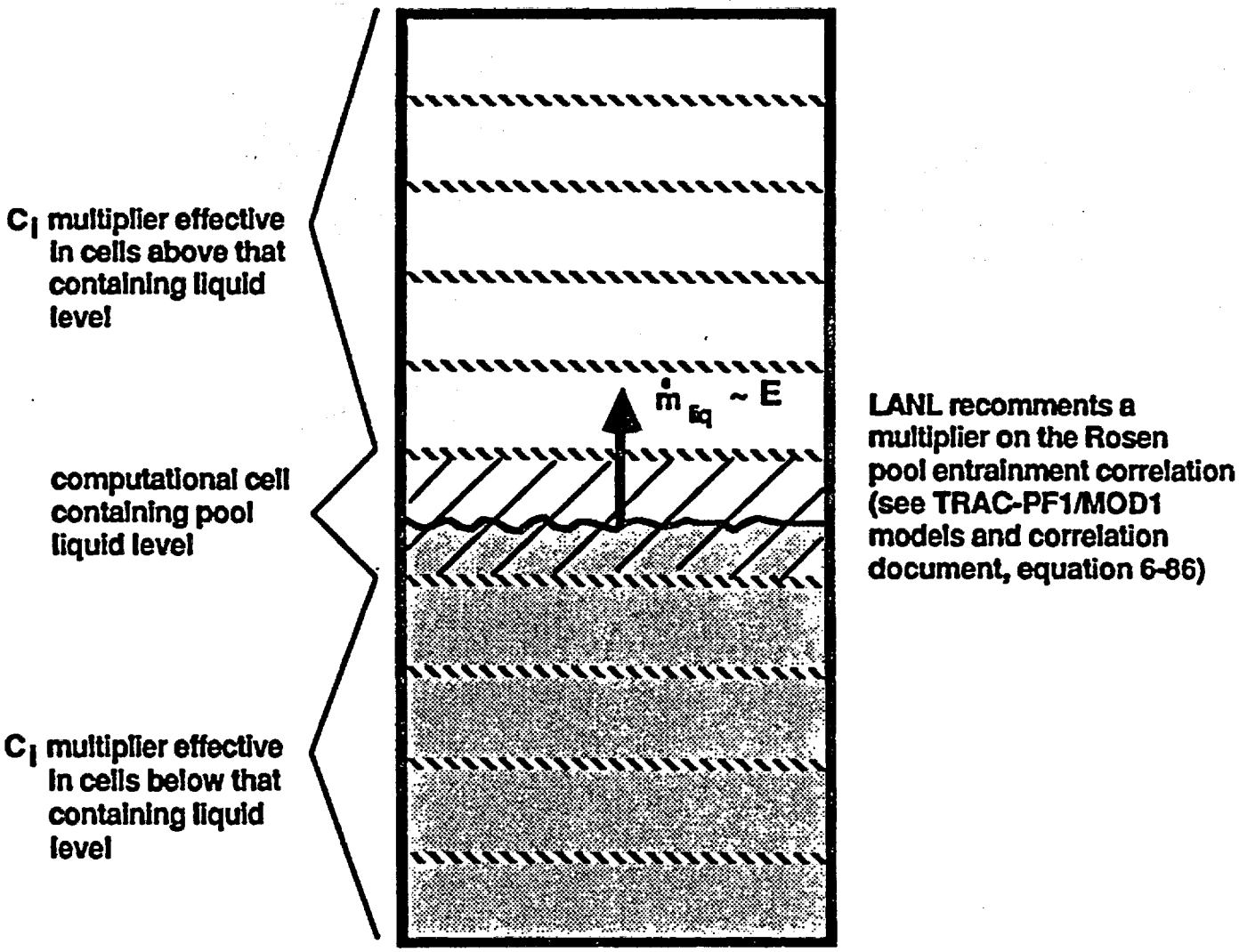

Note: The interface sharpener restricts the amount of liquid leaving the pool or quench front to the value determined from the Rosen pool entrainment correlation.

Fig. 1. Core entrainment and interface sharpener model

PARAMETRIC RUNS

outcome

selected cases for full runs

9

12

13

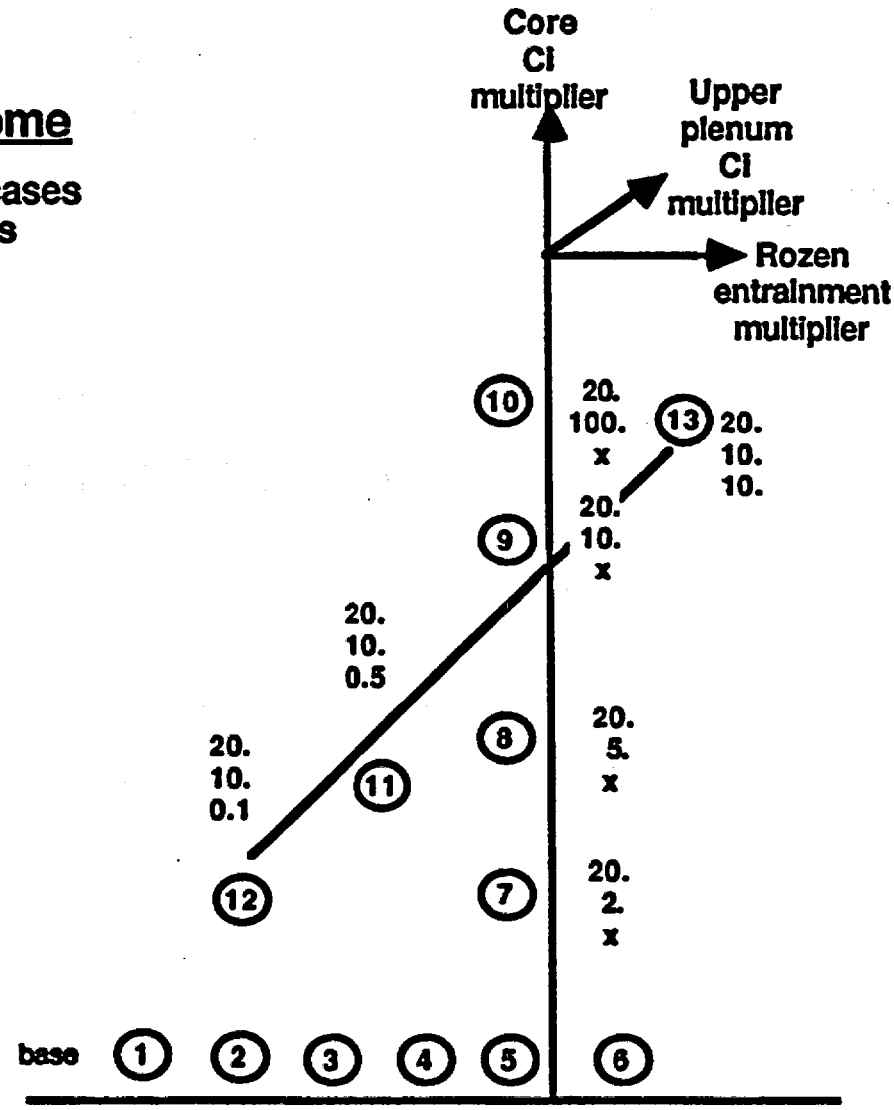

	base	1	2	3	4	5	6
Rosen	x	x	1.01	2.	10.	20.	50.
Core C_l	x	x	x	x	x	x	x
UP C_l	x	10.	x	x	x	x	x

x Denote multiplier = 1.

LOS ALAMOS

4/22/88-3

APPENDIX Q

PHYSICALLY BASED ESTIMATION OF LBLOCA PEAK CLADDING TEMPERATURE

APPENDIX Q

PHYSICALLY BASED ESTIMATION OF LBLOCA PEAK CLADDING TEMPERATURE

This appendix describes a physically based method for estimating the peak cladding temperature during a LBLOCA, testing of the method, and the data base used for the testing.

A PHYSICALLY BASED METHOD OF ESTIMATING PWR LARGE BREAK LOSS OF COOLANT ACCIDENT PCT*

I. Catton (UCLA)
R. B. Duffey and R. A. Shaw (INEL)

and

B. E. Boyack (LANL), P. Griffith (MIT), K. R. Katsma (INEL),
G. S. Lellouche (SLI), S. Levy (SLI), U. S. Rohatgi (BNL),
G. E. Wilson (INEL), W. Wulff (BNL), and N. Zuber (NRC)

1. INTRODUCTION

The NRC effort to quantify the uncertainty in estimates of pressurized water reactor (PWR) large break loss-of-coolant accident (LBLOCA) peak clad temperature (PCT), and to examine the results of TRAC-PF1/MOD1, Version 14.3, simulations, led to a renewed effort to understand the important contributors. It became clear as the Code Scaling, Applicability and Uncertainty (CSAU) effort progressed that there was only a small number of key phenomena and design parameters.[1] Of these design parameters, many do not differ appreciably from plant to plant and, as a result, from test facility to test facility. For example, the fuel is UO_2, the core is approximately 12 feet tall, the core diameter is approximately 12 feet (here local one-dimensional behavior would dominate in any event) and hot leg and cold leg elevations are relatively constant among the PWRs. These observations manifested themselves in the calculated and measured PCTs being functions of a limited set of input parameters with a moderate uncertainty due to the influence of all other factors.

In this paper we develop a method for establishing clad temperature history during a PWR LBLOCA by using physically based arguments andengineering correlations. This simple approach has parallels in the modeling of probabilistic safety assessments.[1] The adequacy of this method is tested by comparison to the large code results. The purpose of this paper is to demonstrate understanding of the physical phenomena and to show consistency with the large code analyses.

2. THEORETICAL BASIS

Simple physical modeling leads to an explicit correlation of the clad temperature history, as follows.

2.1 Blowdown Peak

Immediately following a large break incident, core flow is reduced and liquid is expelled from the core, resulting in a large reduction of fuel-to-coolant heat transfer. The clad temperature then increases rapidly, due primarily to the redistribution of the stored energy in the fuel, and to a lesser degree, to the continued generation of energy in the fuel. Both of these processes can be modeled mathematically as shown below.

If one considers the steady-state condition of the fuel rod, the heat diffusion equation for the fuel can be written as

$$\frac{1}{r}\frac{d}{dr}\left(kr\frac{dT}{dr}\right) = -q_i''' \qquad (1)$$

where q_i''' and k are the volumetric heat generation rate and the fuel thermal conductivity respectively. Assuming effectively constant conductivity, Equation (1) can be integrated to yield the parabolic temperature profile in the fuel, i.e.,

$$T - T_w = \frac{q_i'''}{4k}(R^2 - r^2) \qquad (2)$$

where T_w and R are the fuel surface temperature during normal operation and the pin radius, respectively.

The rod stored energy is, for an axially uniform flux over length L,

$$\int_0^R 2\pi r \rho c L T \, dr \qquad (3)$$

which, after substituting Equation (2), gives

$$\pi R^2 L \rho c \left(T_w + \frac{q_i''' R^2}{8k}\right) \qquad (4)$$

where ρc is the volumetric heat capacity.

The first term of Equation (4) represents a reference temperature and the second the normal stored energy. This second term thus represents the surface temperature rise due to the stored energy redistribution, and can be written

$$\Delta\hat{T}_1 = a_1 q_i' \tag{5}$$

where q_i' is the steady-state linear heat generation rate, and a_1 is a constant. It should be noted here that there was an implicit assumption of thin clad used during the above derivation, the effect of which can be accounted for by a volumetric weighted thermal capacity or by adjustment of the value of a_1.

It was stated above that part of the blowdown clad temperature increase is due to the continued heat generation within the fuel. An energy balance for the time period following the break is given by

$$(\rho c V)_f \frac{dT}{dt} = q'''V - hA\,(T-T_s) \tag{6}$$

where V, A, h, T and T_s are the fuel volume, the fuel surface area, the convective heat transfer coefficient, and the clad and coolant saturation temperatures, respectively.

Soon after expulsion of liquid from the core, the convective heat transfer is sufficiently small that Equation (6) can be approximated by

$$\Delta\hat{T}_2 = \hat{T}_2 - T_i \simeq \frac{1}{\rho c} \int_0^{\hat{t}} q'''\, dt \tag{7}$$

or more compactly,

$$\Delta\hat{T}_2 \propto \frac{K(t)}{\rho c}\, q_i''' \tag{8}$$

where $\hat{T}_2$ is the maximum clad temperature due to decay heating during the time period, $0\text{-}\hat{t}$, and K(t) is the integral of the normalized power decay. The normalized power decrease to decay level during LBLOCA has been simulated in experiments. The temperature increase generally occurred during the same time frame; therefore, K(t) should be relatively constant among the experiments and calculations. With this assumption and a local linear heat generation rate, q_i', we can argue that

$$\Delta\hat{T}_2 = a_2 q_i' \tag{9}$$

where a_2 is a constant.

It has thus been argued that both contributors to the blowdown temperature rise are proportional to the linear heat generation rate. Next we assume that they are additive and, from Equation (5) and Equation (9)

$$\Delta\hat{T} \propto (a_1 q_i' + a_2 q_i') = a q_i' \tag{10}$$

where a, the constant, has been determined from the available experimental data in Figure 1 to be

$$a \approx 60. \tag{11}$$

It should be noted that the data cover a wide range of scaled experiments with both nuclear and electrically heated bundles.

2.2 Blowdown Convective Cooling

The complete specification of the clad temperature history requires estimating the temperature decrease following the blowdown peak. An estimate can be obtained from the heat balance following some simple approximations. The starting point is a heat balance with convective cooling, Equation (6),

$$hA\,(T-T_s) = -(\rho cV)_f \frac{dT}{dt} + q'''V. \tag{12}$$

A solution to Equation (12) is easily found if one uses average values of the convective heat transfer coefficient and saturation temperature, and neglects the decay heat term. Neglecting the decay heat during the blowdown period is justified by comparison of the stored heat with decay heat during the blowdown. The result is

$$\check{T} = (\hat{T}-\bar{T}_s)e^{-\frac{\bar{h}A}{(\rho cV)_f}(\check{t}-\hat{t})} + \bar{T}_s \tag{13}$$

where $\check{T}$, $\bar{T}_s$ and $\bar{h}$ are the temperature at the end of blowdown, the average saturation temperature, and average heat transfer coefficient, respectively, and $\check{t}$ is the time at which the minimum temperature occurs.

The available experimental data from LOFT and Semiscale experiments are shown in Figure 2 in terms of

$$\frac{\hat{T}-\bar{T}_s}{\check{T}-\bar{T}_s} \text{ vs } \frac{\bar{h}A}{(\rho cV)_f}(\check{t}-\hat{t}).$$

It is found that a straight line fit over the range observed is given by

$$\frac{\hat{T}-\bar{T}_s}{\check{T}-\bar{T}_s} = 1.09 + 0.9\, m\tau \qquad (14)$$

$$= r + st, \text{ say,}$$

where $m \equiv (\frac{\bar{h}A}{\rho c V})_f$ and $\tau \equiv (\check{t}-\hat{t})$. The data fit given by Equation (14) is in good agreement with the lead terms of a power series expansion of the expression given by Equation (13). This gives us confidence in the approach taken.

It should be noted that data points indicating rewet were deliberately omitted from this analysis to provide an upper estimate of the clad temperature during this time period.

2.3 Refill Heatup

The heatup of the core during lower plenum refill has been shown to be the refill time, τ_r, times the core heating rate, dT/dt (approximately 5.2°K/s per reference 3), or

$$\Delta T_r = \tau_r \times \frac{dT}{dt} \qquad (15)$$

and the temperature after refill at time t_r is

$$T_r = \Delta T_r + \check{T} \qquad (16)$$

2.4 Reflood Peak

For a period of time after the lower plenum has been filled with water, the rod temperature continues to increase. A transient heat balance during that period [see Equation (6)] is given by

$$(\rho c V)_f \frac{dT}{dt} = q'''V - hA\,(T-T_s). \qquad (17)$$

Because we assume that a uniform temperature exists over the fuel rod cross-section, the time rate of change of the clad temperature is zero at the reflood peak. Letting $\hat{\hat{T}}$ be the reflood peak temperature, Equation (17) at the peak becomes

$$\hat{\hat{T}}-T_s = \frac{q'''R}{\bar{h}} \qquad (18)$$

where $\bar{h} = \frac{1}{t} \int_{t_r}^{\hat{\hat{t}}} h \, dt$ and $\hat{\hat{t}}$ is the time of the reflood peak.

It is known from experimental data that $\bar{h} \propto U_R^n$ where n is an empirically derived constant and U_R is the cold reflood rate defined by

$$U_R \equiv \frac{\text{ECC injection mass flow}}{\text{Core Flow Area x ECC density}} .$$

Furthermore, q''' is relatively constant during this time period, allowing one to approximate the temperature increase as,

$$\Delta\hat{\hat{T}} = \hat{\hat{T}} - T_r \propto \frac{K}{U_R^n} - (T_r - T_s) \qquad (19)$$

where K and n are constants that have been determined from experimental data (see Figure 3) to be

K = 339, n = 1.14; and from a review of LOFT LBLOCA Experiments L2-2 and L2-3, the $(T_r - T_s)$ term was found to be approximately 350 ^oF.

The data cover a wide range of experimental scales, with both nuclear and electrical heaters.

2.5 Peak Clad Temperature

The above analysis enables convenient estimates of clad temperature changes using these simple correlations (Equations 10, 14, 15, and 19). Thus, a universal engineering correlation is possible for the clad temperature history during LBLOCA in U.S. PWRs. Furthermore, it is important to note that the only parameters appearing in the above expressions are the fuel thermal characteristics and geometry. These parameters are reasonably constant for PWRs in the United States.

3. ESTIMATING THE PEAK TEMPERATURE AND UNCERTAINTY

We are now in a position to develop, from the above physical reasoning, a simple engineering method for estimating the clad temperature history and the uncertainty. Given the following three design parameters for a specific PWR:

(1) Peak linear heat generation rate, q', (2) Blowdown cooling time, $T = \check{t}-\hat{t}$, and (3) Core cold reflooding rate, U_R, the peak temperatures can be derived using Figures 1, 2, and 3.

The only parameter not directly defined is τ. It is known that the time to reach the blowdown peak is a few fuel pin thermal time constants,

$$\hat{t} \propto (R^2/\alpha) \qquad (20)$$

where the thermal diffusivity $\alpha = (k/\rho c)_f$, and R is the pin radius.

The time of the minimum temperature, $\check{t}$, is related to the blowdown time, which is easily shown to be

$$\check{t} \propto (M/A_B) \tag{21}$$

where M is the initial liquid mass and A_B is the break area. Thus, one could estimate τ to be

$$\tau \simeq \check{t}-\hat{t} = c_1(\frac{M}{A}) - c_2\,(\frac{R^2}{\alpha}) \tag{22}$$

where c_1 and c_2 are constants of proportionality. Alternatively τ can be derived from a simple blowdown analysis.

To summarize, there are four correlations, based on data and physics that yield the peak clad temperatures. They are as follows:

1. The first temperature peak is due to stored and decay heat less blowdown heat removal due to DNB and post-dryout cooling. It is given by

$$\Delta\hat{T} = \hat{T}-T_i = aq_i' \tag{23}$$

with uncertainty $\hat{\sigma}_{95}$ at the 95th percentile.

2. The temperature decrease during blowdown resulting from forced convective cooling is given by

$$\Delta\check{T} = \hat{T}-\check{T} = (\hat{T}-\bar{T}_s)(1-\frac{1}{r+s\tau}) \tag{24}$$

with uncertainty $\check{\sigma}_{95}$ at the 95th percentile.

3. The temperature rise, ΔT_r, during refill is given by[2]

$$\Delta T_r = \frac{V_{LP}\,\rho}{\dot{m}_{ECC}} \times \frac{dT}{dt} \tag{25}$$

with uncertainty $\sigma_{r,95}$ at the 95th percentile,
where V_{LP} is the lower plenum volume, and $\dot{m}_{ECC}$ is the injection rate.

4. The temperature rise during reflood resulting from decay heating is given by

$$\Delta\hat{\hat{T}} = K/U_R^n \tag{26}$$

with uncertainty $\hat{\hat{\sigma}}_{95}$ at the 95th percentile.

The reflood peak temperature, $\hat{\hat{T}}$, is found by algebraically combining the expressions given by Equations (23) through (26). The result is

$$\hat{\hat{T}}-T_i = aq' - (\hat{T}-\bar{T}_s)(1-\frac{1}{r+s\tau}) + \Delta T_r + \frac{K}{U_R^n} - (T_r - T_s) \quad (27)$$

or, in words,

$$\hat{\hat{T}}-T_i = \text{heating from stored energy} - \text{post peak blowdown cooling} + \text{refill heating} + \text{reflooding heating}$$

with overall uncertainty,

$$\sigma_{95} \simeq (\hat{\sigma}_{95}^2 + \check{\sigma}_{95}^2 + \sigma_{r,95}^2 + \hat{\hat{\sigma}}_{95}^2)^{1/2} \quad (28)$$

Additionally a simple approximate expression can be derived for establishing whether the peak occurs in the blowdown or reflood phases by comparing Equation (10) with Equation (27). It will be found that

$$1 - (\hat{T}-\bar{T}_s)(1-\frac{1}{r+s\tau}) + \frac{\Delta T_r}{aq_i'} + \frac{K}{aq_i' U_R^n} \quad \begin{matrix} >1 & \text{reflood peak} \\ <1 & \text{blowdown peak} \end{matrix} \quad (29)$$

where r = 1.09 and s = 0.9m, [see equation (14)].

4. RESULTS

We will now evaluate each of the terms in Equations 27 and 28 and compare the result obtained by this approach with a TRAC analysis and a pdf estimate of uncertainties. We need best estimate values for the design parameters in Equation (27), which we take as typical PWR estimates.

For a q_i' of 9.5 kw/ft, a τ of approximately 20 seconds, and design cold reflood rate of approximately 4 in./s, the elements of Equations (27) and (28) are the following:

I. $\Delta\hat{T} = 570^0F$, $\hat{\sigma}_{95} = \pm 364$ [Equation (10)]

II. $\Delta\check{T} = 164^0F$, $\check{\sigma}_{95} = +60, -82$

III. $\Delta T_r = 134^0F$, $\sigma_{r,95} = +16, -0$ [Equation (25)]

IV. $\Delta\hat{\hat{T}}_r = 70^0F$, $\hat{\hat{\sigma}}_{95} = +230, -55$

where elements I, II, and IV were derived from Figures 1, 2, and 3 respectively, and element III was based on the results given in Reference 2.

The peak temperatures that result are:

$$\hat{T} = 1150^{o}F, \ \hat{\sigma}_{95} = \pm 364$$

$$\hat{\hat{T}} = 1150 - 164 + 134 + 70 - 350 = 840^{o}F,$$

with an overall $\sigma_{95} = (\hat{\sigma}^2_{95} + \check{\sigma}^2_{95} + \sigma^2_{r,95} + \hat{\hat{\sigma}}^2_{95})^{1/2} \simeq 435^{o}F$ and $377^{o}F$, where $435^{o}F$ was obtained by using the positive values of uncertainty in Equation (28) and $377^{o}F$ resulted from using the negative values, thus resulting in a skewed distribution.

A comparison of the results with nuclear plant calculations for a LBLOCA in a Westinghouse 4-loop PWR using the TRAC/PF1 reactor safety code is presented in the table below.

	Blowdown		Reflood	
		Present Model		Present Model
	TRAC	$\hat{T}$	TRAC*	$\hat{\hat{T}}$
Mean	1162	1150	758- 978	840
95th	1447	1514	1336-1399	1217-1275
w/bias**	1557		1572-1483	

These results confirm the overall similarity of the present predictions, as based on the experimental data, and the reactor analysis results, and are consistent with the distribution functions.[1] It also demonstrates that the overall uncertainty is comparable to that obtained from the available data, and that the experiments were well-founded. Furthermore, it confirms our understanding of the physical processes involved during a LBLOCA.

---

* The TRAC calculations predicted two temperature peaks during reflood and both are shown in this column as opposed to the present model elements which are upper and lower uncertainty bounds.

** The TRAC results were adjusted by a bias due to obvious effects of scale and code deficiencies.

4. CONCLUSIONS

Physical arguments show that a simple method can be utilized to provide an estimate of PCT during PWR LBLOCA. The resulting estimate is based on data and physical reasoning and is consistent with the computer analyses. It was found that the estimated peak clad temperature is a simple linear combination of temperature changes occurring during the various phases of the LBLOCA. The results were derived from elementary correlations based on well founded experimental data. Refinements to these correlations are, of course, possible, and justified when uncertainties need reducing.

5. REFERENCES

1. D. C. Bley, D. R. Buttemer and J. W. Stetkar, "Light Water Reactor Sequence Timing: its Significance to Probabilistic Safety Assessment Modeling", Reliability Engineering and Systems Safety, Vol. 22, Issue 1-4, pp27-60, 1988.

2. U. S. Rohatgi, J. Jo, L. Y. Neymotin, and W. Yu, Bias in Prediction of PCT Due to Uncertainty in ECC Bypass Modeling, NUREG/CR-5254, June 1989.

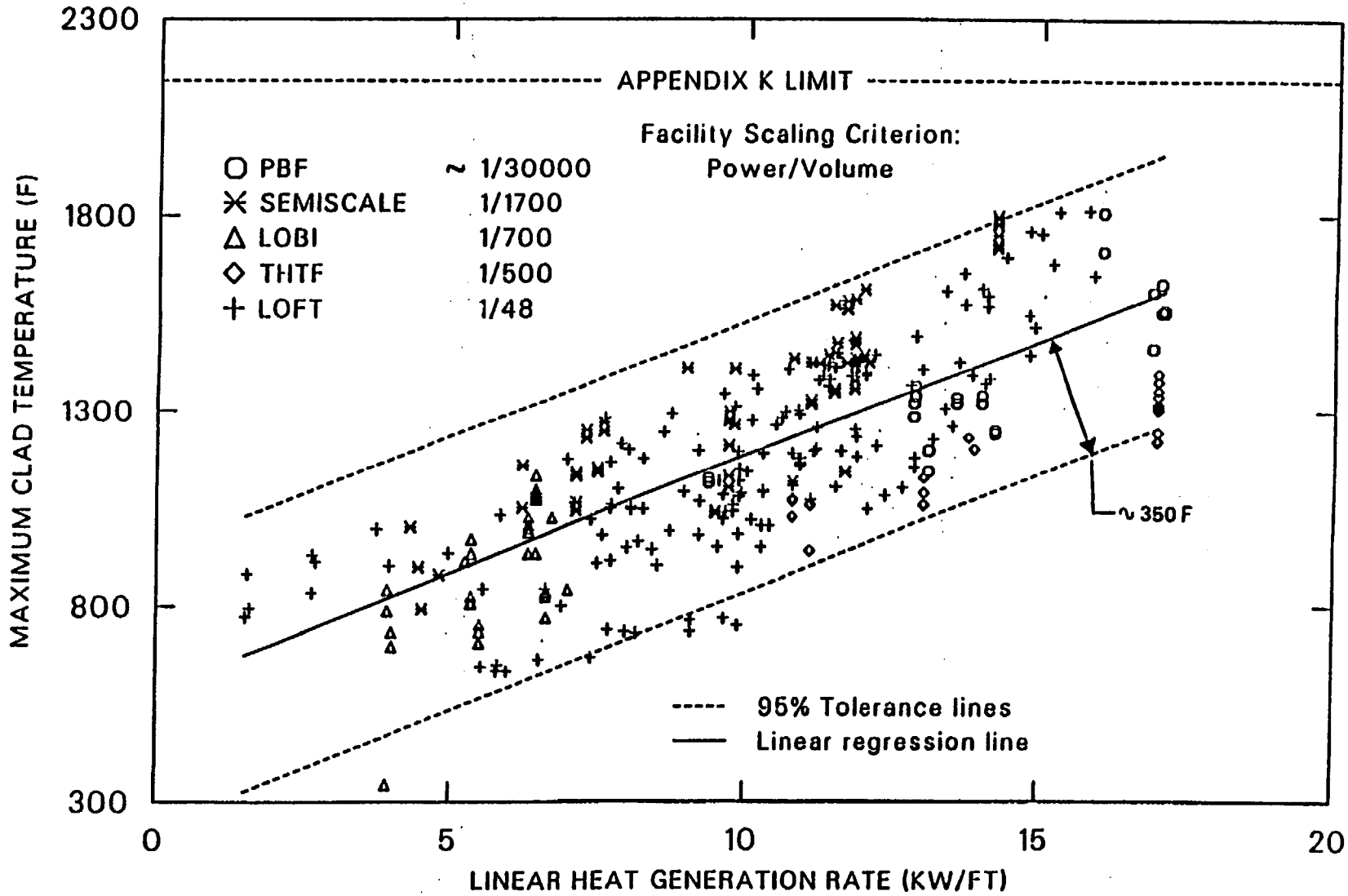

Figure 1. Maximum measured clad temperature from several scaled experimental facilities (301 data points) during blowdown.

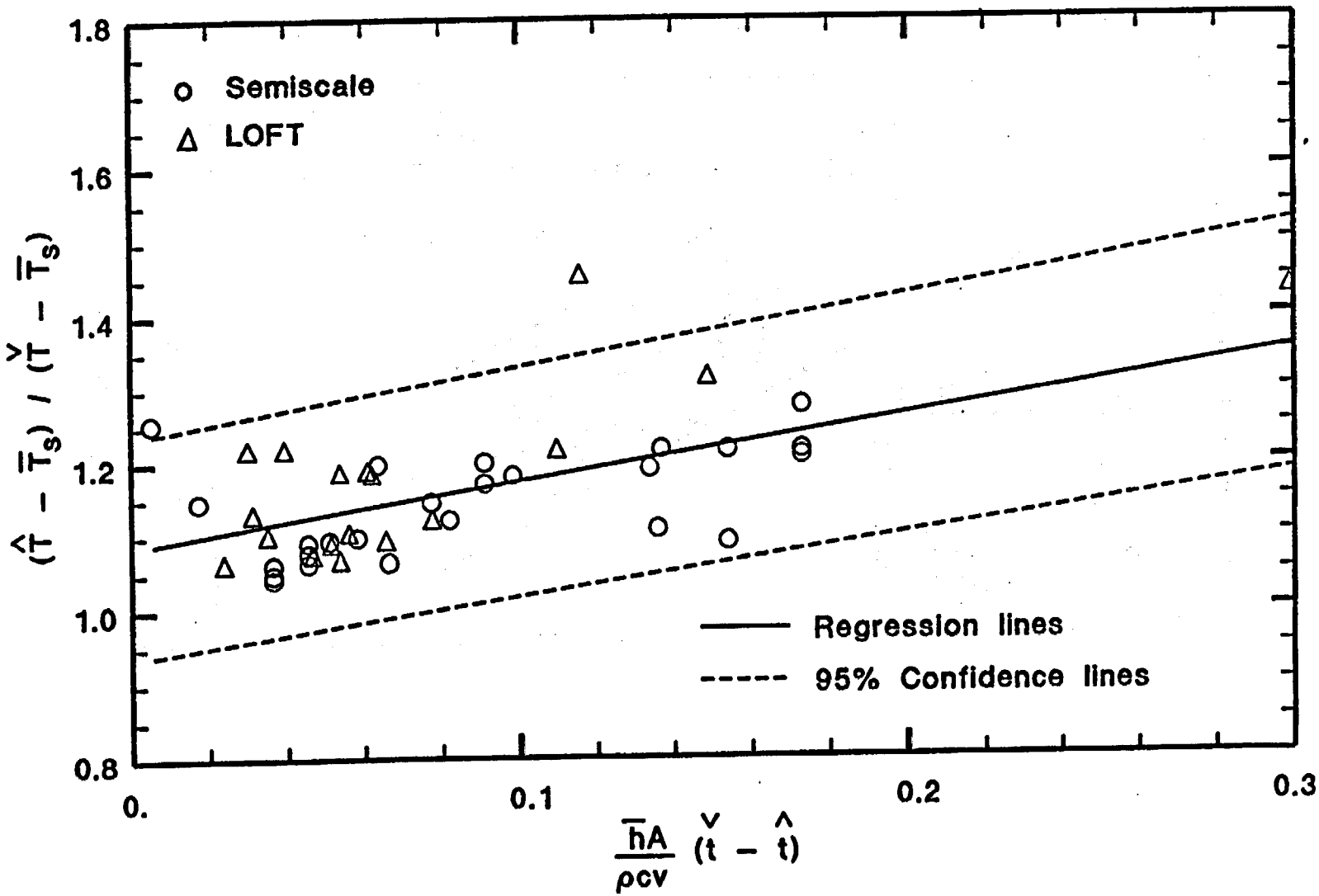

NSL01125

Figure 2. Blowdown convective cooling data (46 points).

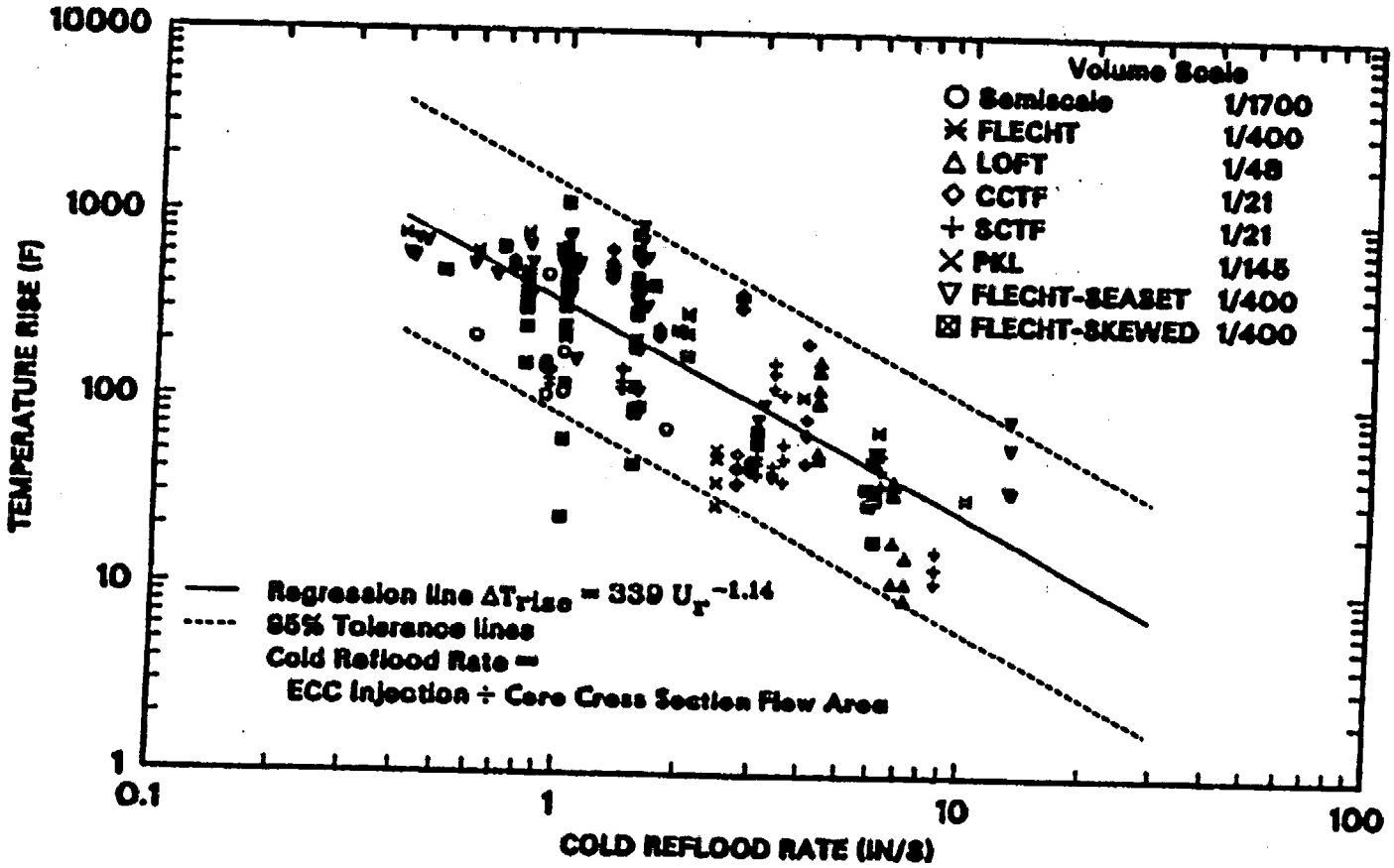

Figure 3. Measured temperature rise data from scaled experimental facilities during reflood (217 points).

APPENDIX R

STATISTICAL METHODOLOGY AND RESULTS

APPENDIX R

STATISTICAL METHODOLOGY AND RESULTS

This appendix, supplied by Dr. G. Lellouche (SLI), provides additional information with respect to the response surface and other statistical methods used in Part B, Section 4.

APPENDIX
STATISTICAL METHODOLOGY AND RESULTS

Although the three sections on Ranging, Establishing the Calculational Matrix, and Response Surface provide everything needed for an engineer to run his own statistical package, it is felt that a more detailed description and detailing of the numerical results might be helpful. The particular code package (RAM-CAM) used was created for internal SLI use and is not documented. The statistical methodology used, however, is quite standard. The regression analysis uses a matrix factorization of the normal equations P matrix known as the singular value decomposition (SVD). This is, we believe, the most reliable method for computing the coefficients for general least squares problems and minimizes the effect of data errors, round off, and linear dependence. The Monte Carlo Analysis is also quite standard.

Regression Analysis

The statistical problem of finding a least squares fit to a set of data is dealt with in most statistics texts; the particular problem here is not significantly different from those discussed in the texts except that we use relatively high order (4th) polynomials. If one redefines higher order terms as auxiliary linear terms such as

$$
\begin{aligned}
Z_1 &= x\ y \\
Z_2 &= x^2 \\
Z_3 &= y^2 \\
&\text{etc.}
\end{aligned}
$$

then any high order polynomial can be reduced to a linear expansion problem. This is the way many software statistics packages deal with the multinomial regression problem.

Tables A2, A2, and A3 tabulate the coefficients for the best quartic regressions in the form

$$PCT\ (°k) = \sum_{i,j,k,\ell = o}^{I,J,K,L} a_{ijk\ell}\ X_i\ X_j\ X_k\ X_\ell$$

with I = J = K = L = 7 and $X_o = 1$

i	=	1	↔	peaking factor variation
i	=	2	↔	gap conductance variation
i	=	3	↔	fuel conductivity variation
i	=	4	↔	heat transfer coefficient variation
i	=	5	↔	break R_m variation
i	=	6	↔	pump head and torque curve variation
i	=	7	↔	T_{MIN} variation

The actual values of X_i are those between the limits listed in Table 3 in the body of this document (using fractions not percent, but using °C for T_{MIN}).

The specific values used for the Pump and Break variations are normalized; this means that the values entering the regressed multinomial are numbers between zero and two (for 2nd level variation). For these parameters we absorb 50% of the probability between 0 and 10^{-3} and then use a linear variation up to 2. The cumulative probability table for these parameters looks like:

Variation	:	0	0.001	1.	2.
Cumulative Probability:	:	0	0.5	0.75	1.00

The reason for absorbing the probability at zero is, as discussed in the body of this document, to reduce the total number of computor runs and is allowable because the peak clad temperature (for this NPP and this break

scenario) is as tests have shown, a nondecreasing function of the increasing positive variation of these parameters.

It is important to point out that the specific values of the pump variation are not given because they are proprietary data of the Westinghouse 1/3 scale pump.

A user may take the values of the temperatures (Tables 4, 5, 6 in the body of the document) and the values of the variations implied by Table 3 and indicated by the 3rd column and the first row in Tables 4, 5, 6 (nominal = 0, 1st level = 1, etc.) and using any regression analysis program produce the equivalent of the results given in Table A1...A3.

Monte Carlo Analysis

Monte Carlo Analysis covers a very wide range of methods and the reader should consult any text on random sampling methods. Basically, when the underlying probability distribution function is uniform a random number generator is used to generate a number between 0, 1 (or -1, 1 or a, b). The location of the number on the allowed range defines the value of the parameter being chosen. If more than one parameter is used at a time (as in a multinomial) then independent random numbers are chosen for each parameter. These values of the parameters chosen are inserted in the regression multinomial and a value of the PCT is found. This process is repeated many times (50,000 trials for example) and a table of the PCT's is collected. The values are accumulated in preselected bins (500 to 525- °K; 525 to 550 °K; 550 to 575 °F; etc.) and normalized by the total number of trials; the result is a frequency histogram which is interpreted as a probability distribution function. From this histogram we may determine the standard statistics desired (mean, mode, 95th percentile, etc.). Because of the non-deterministic nature of the process, a different choice of starting random number (the input "seed") or the use of a different random number generator or a change in the number of trials will produce a

slightly different final result. This was discussed in the body of this document and depicted in Figures 7-9.

The reader then should not expect to be able to establish a deterministically exact reproduction of the numbers in Table 9-12 but only a statistically equivalent one as implied by the results in Figures 7-9. Tables A4-A6 contain the 50,000 trial estimation of the distribution functions derived from the regression surfaces listed in Tables A1...A3.

TABLE A1

BLOWDOWN

SUMMARY OF LEAST SQUARES FIT OBTAINED FOR Pd Cld Tmp DATA -- # 1

The specified fit has a total of 70 terms and a redundancy of 2.63.

Following are fit coefficients determined by SVDFIT
Fit Normalization Constant (Quadratic offset) = 0.0000

Constant Term						0.86688E+03
Linear	Term for Param	#	1			0.12813E+02
Linear	Term for Param	#	2			-0.53412E+02
Linear	Term for Param	#	3			-0.70288E+01
Linear	Term for Param	#	4			-0.57052E+02
Linear	Term for Param	#	5			0.28762E+03
Linear	Term for Param	#	6			0.11527E+02
Linear	Term for Param	#	7			0.23213E+02
Quad	Term for Param	#	1			0.58005E+00
Quad	Term for Param	#	2			0.35337E+02
Quad	Term for Param	#	3			0.70380E+00
Quad	Term for Param	#	4			0.38992E+01
Quad	Term for Param	#	5			-0.17036E+03
Quad	Term for Param	#	6			0.23051E+02
Quad	Term for Param	#	7			-0.83715E+01
Cross	Term for Params	#	1	5		0.49428E+01
Cross	Term for Params	#	1	6		0.18896E+01
Cross	Term for Params	#	1	7		0.11819E+01
Cross	Term for Params	#	2	3		-0.66677E+01
Cross	Term for Params	#	2	4		0.20122E+02
Cross	Term for Params	#	2	5		-0.91521E+02
Cross	Term for Params	#	2	6		-0.30770E+02
Cross	Term for Params	#	2	7		-0.11027E+02
Cross	Term for Params	#	3	5		-0.20021E+02
Cross	Term for Params	#	3	6		-0.14269E+02
Cross	Term for Params	#	3	7		-0.14899E+02
Cross	Term for Params	#	4	5		0.28157E+02
Cross	Term for Params	#	4	6		-0.18322E+02
Cross	Term for Params	#	4	7		0.13235E+03
Cross	Term for Params	#	5	6		-0.19232E+02
Cubic	Term for Params	#	2	2	2	-0.15679E+02
Cubic	Term for Params	#	2	2	4	-0.14732E+02
Cubic	Term for Params	#	2	2	5	0.28346E+02
Cubic	Term for Params	#	2	2	6	0.97824E+01
Cubic	Term for Params	#	2	5	5	0.60311E+02
Cubic	Term for Params	#	2	6	6	0.18708E+02
Cubic	Term for Params	#	3	5	5	0.15098E+02
Cubic	Term for Params	#	3	6	6	0.88323E+01
Cubic	Term for Params	#	3	7	7	0.16008E+02
Cubic	Term for Params	#	4	4	4	-0.48188E+01
Cubic	Term for Params	#	4	4	5	-0.20071E+01
Cubic	Term for Params	#	4	4	7	-0.64291E+02
Cubic	Term for Params	#	4	5	5	-0.27140E+02
Cubic	Term for Params	#	4	6	6	0.15160E+02
Cubic	Term for Params	#	4	7	7	-0.14929E+03
Cubic	Term for Params	#	2	5	6	0.10196E+02
Cubic	Term for Params	#	3	5	6	0.53766E+01
Cubic	Term for Params	#	4	5	6	0.57277E+01
Cubic	Term for Params	#	5	5	6	-0.19232E+02
Cubic	Term for Params	#	5	6	6	-0.96162E+01

TABLE A (continued)

Quartic Term for Params #	2	2	4	5	0.18468E+02
Quartic Term for Params #	2	2	5	5	-0.17284E+02
Quartic Term for Params #	2	4	4	5	0.10753E+02
Quartic Term for Params #	2	4	5	5	-0.52818E+01
Quartic Term for Params #	3	3	6	6	0.16794E+01
Quartic Term for Params #	4	4	4	7	0.47280E+01
Quartic Term for Params #	4	4	5	5	0.43919E+01
Quartic Term for Params #	4	4	7	7	0.54681E+02
Quartic Term for Params #	2	2	2	6	-0.47644E+01
Quartic Term for Params #	2	2	5	6	-0.10186E+02
Quartic Term for Params #	2	5	5	6	0.10196E+02
Quartic Term for Params #	2	5	6	6	0.50979E+01
Quartic Term for Params #	3	4	5	6	0.00000E+00
Quartic Term for Params #	3	5	5	6	0.53766E+01
Quartic Term for Params #	4	4	5	6	0.36643E+01
Quartic Term for Params #	4	5	5	6	0.57277E+01
Quartic Term for Params #	4	5	6	6	0.28639E+01
Quartic Term for Params #	5	5	6	6	-0.96162E+01
Quartic Term for Params #	3	5	6	6	0.26883E+01
Quartic Term for Params #	3	4	6	6	0.00000E+00

ERROR ANALYSIS FOR LEAST SQUARES POLYNOMIAL FIT

Standard (RMS) Error of the fit = 0.540E+01 °K

TABLE A2

EARLY REFLOOD

SUMMARY OF LEAST SQUARES FIT OBTAINED FOR Pk Cld Tmp DATA -- Case # 2

The specified fit has a total of 67 terms and a redundancy of 2.75

Following are fit coefficients determined by SVDFIT
Fit Normalization Constant (Quadratic offset) = 0.0000

Constant Term						0.79213E+03
Linear	Term for Param	#	1			0.15536E+02
Linear	Term for Param	#	2			-0.45912E+02
Linear	Term for Param	#	3			-0.93189E+01
Linear	Term for Param	#	4			-0.13298E+03
Linear	Term for Param	#	5			0.40758E+03
Linear	Term for Param	#	6			-0.30644E+01
Linear	Term for Param	#	7			-0.78826E+02
Quad	Term for Param	#	1			0.94964E+01
Quad	Term for Param	#	2			0.66242E+02
Quad	Term for Param	#	3			0.11514E+02
Quad	Term for Param	#	4			0.21080E+02
Quad	Term for Param	#	5			-0.26304E+03
Quad	Term for Param	#	6			-0.19296E+01
Quad	Term for Param	#	7			-0.54986E+02
Cross	Term for Params	#	1	5		0.45994E+01
Cross	Term for Params	#	1	6		-0.77526E+00
Cross	Term for Params	#	1	7		0.16497E+00
Cross	Term for Params	#	2	3		-0.15709E+02
Cross	Term for Params	#	2	4		-0.13733E+02
Cross	Term for Params	#	2	5		-0.41316E+02
Cross	Term for Params	#	2	6		0.43679E+01
Cross	Term for Params	#	2	7		-0.27483E+02
Cross	Term for Params	#	3	5		-0.16843E+02
Cross	Term for Params	#	3	6		-0.16757E+01
Cross	Term for Params	#	3	7		-0.63822E+01
Cross	Term for Params	#	4	5		0.95489E+01
Cross	Term for Params	#	4	6		0.94540E+01
Cross	Term for Params	#	4	7		0.13394E+02
Cross	Term for Params	#	5	6		-0.22115E+02
Cubic	Term for Params	#	2	2	2	-0.51258E+02
Cubic	Term for Params	#	2	2	4	0.46036E+02
Cubic	Term for Params	#	2	2	5	-0.56437E+01
Cubic	Term for Params	#	2	2	6	0.39521E+01
Cubic	Term for Params	#	2	2	7	0.11795E+02
Cubic	Term for Params	#	2	3	7	0.33121E+02
Cubic	Term for Params	#	2	5	6	0.10658E+02
Cubic	Term for Params	#	3	3	7	-0.11053E+02
Cubic	Term for Params	#	3	5	5	0.13100E+02
Cubic	Term for Params	#	3	7	7	0.73541E+01
Cubic	Term for Params	#	4	4	5	-0.97147E+01
Cubic	Term for Params	#	4	4	7	0.40854E+02
Cubic	Term for Params	#	4	5	6	-0.12509E+02
Cubic	Term for Params	#	4	6	6	-0.83784E+01
Cubic	Term for Params	#	4	7	7	-0.54269E+02
Cubic	Term for Params	#	5	5	6	-0.22115E+02
Cubic	Term for Params	#	5	6	6	-0.11057E+02

TABLE A2 (Continued)

Quartic Term for Params #	2	2	2	2	0.12215E+02
Quartic Term for Params #	2	2	2	4	0.66851E+02
Quartic Term for Params #	2	2	2	5	0.25459E+02
Quartic Term for Params #	2	2	3	7	-0.19045E+02
Quartic Term for Params #	2	2	4	4	-0.10824E+02
Quartic Term for Params #	2	2	4	5	-0.25353E+02
Quartic Term for Params #	2	3	3	7	-0.33121E+02
Quartic Term for Params #	2	3	5	5	-0.17985E+02
Quartic Term for Params #	2	3	6	6	-0.30843E+01
Quartic Term for Params #	2	3	7	7	-0.30550E+02
Quartic Term for Params #	2	4	4	7	0.97923E+01
Quartic Term for Params #	2	4	5	5	-0.16463E+02
Quartic Term for Params #	2	4	5	6	-0.97388E+01
Quartic Term for Params #	2	4	7	7	-0.90213E+01
Quartic Term for Params #	3	3	5	6	-0.66220E+01
Quartic Term for Params #	4	4	4	7	-0.14306E+02
Quartic Term for Params #	4	4	5	6	0.10058E+02
Quartic Term for Params #	4	4	7	7	0.25945E+02
Quartic Term for Params #	4	5	6	6	-0.62547E+01
Quartic Term for Params #	4	5	5	6	-0.12509E+02

ERROR ANALYSIS FOR LEAST SQUARES POLYNOMIAL FIT

Standard (RMS) Error of the fit = 0.136E+02 °K

TABLE A3

LATE REFLOOD

SUMMARY OF LEAST SQUARES FIT OBTAINED FOR Pk Cld Tmp DATA -- CASE # 3

The specified fit has a total of 60 terms and a redundancy of 3.07

Following are fit coefficients determined by SVDFIT
Fit Normalization Constant (Quadratic offset) = 0.0000

Constant Term						0.77295E+03
Linear	Term for Param	#	1			0.17072E+02
Linear	Term for Param	#	2			-0.63157E+01
Linear	Term for Param	#	3			-0.11441E+02
Linear	Term for Param	#	4			-0.22556E+03
Linear	Term for Param	#	5			0.22298E+03
Linear	Term for Param	#	6			-0.27400E+02
Linear	Term for Param	#	7			-0.19702E+03
Quad	Term for Param	#	1			0.35255E+01
Quad	Term for Param	#	2			0.53233E+02
Quad	Term for Param	#	3			0.20924E+01
Quad	Term for Param	#	4			-0.23777E+01
Quad	Term for Param	#	5			-0.11037E+03
Quad	Term for Param	#	6			0.27266E+02
Quad	Term for Param	#	7			-0.48828E+02
Cross	Term for Params	#	1	5		0.44219E+01
Cross	Term for Params	#	1	6		0.34157E+00
Cross	Term for Params	#	1	7		-0.89018E+01
Cross	Term for Params	#	2	3		-0.86315E+01
Cross	Term for Params	#	2	4		0.22588E+02
Cross	Term for Params	#	2	5		-0.22435E+02
Cross	Term for Params	#	2	6		-0.11149E+02
Cross	Term for Params	#	2	7		0.10767E+03
Cross	Term for Params	#	3	5		-0.34379E+01
Cross	Term for Params	#	3	6		0.66447E+01
Cross	Term for Params	#	3	7		-0.59781E+02
Cross	Term for Params	#	4	5		-0.47766E+02
Cross	Term for Params	#	4	6		-0.24133E+02
Cross	Term for Params	#	4	7		-0.18513E+02
Cross	Term for Params	#	5	6		0.77327E+01
Cubic	Term for Params	#	2	2	2	-0.49421E+02
Cubic	Term for Params	#	2	2	3	0.49630E+01
Cubic	Term for Params	#	2	2	7	0.35897E+02
Cubic	Term for Params	#	2	4	7	0.29150E+02
Cubic	Term for Params	#	2	7	7	-0.10200E+03
Cubic	Term for Params	#	4	4	4	0.28640E+02
Cubic	Term for Params	#	4	4	7	0.12186E+03
Cubic	Term for Params	#	4	5	5	0.34805E+02
Cubic	Term for Params	#	2	5	6	0.63182E+01
Cubic	Term for Params	#	4	5	6	0.14840E+02
Cubic	Term for Params	#	3	7	7	0.69969E+02
Cubic	Term for Params	#	3	5	5	0.83087E+01
Cubic	Term for Params	#	3	5	6	-0.67988E+01
Cubic	Term for Params	#	4	6	6	0.20335E+02

TABLE A3 (Continuted)

Quartic Term for Params #	2	2	2	7	-0.67295E+02
Quartic Term for Params #	2	2	4	4	-0.51319E+01
Quartic Term for Params #	4	4	4	4	-0.43012E+01
Quartic Term for Params #	4	4	4	5	-0.78349E-01
Quartic Term for Params #	4	4	4	6	0.49327E+01
Quartic Term for Params #	4	4	6	6	-0.15001E+02
Quartic Term for Params #	4	4	4	7	-0.38516E+02
Quartic Term for Params #	4	4	7	7	0.19959E+02
Quartic Term for Params #	2	3	5	6	-0.68423E+01
Quartic Term for Params #	2	4	5	6	0.10338E+02
Quartic Term for Params #	2	5	5	6	0.63183E+01
Quartic Term for Params #	3	3	5	5	0.49197E+01
Quartic Term for Params #	3	3	5	6	-0.22670E+02
Quartic Term for Params #	3	3	6	6	0.10564E+02
Quartic Term for Params #	4	4	5	6	-0.16605E+02
Quartic Term for Params #	5	5	6	6	0.38664E+01

ERROR ANALYSIS FOR LEAST SQUARES POLYNOMIAL FIT

Standard (RMS) Error of the fit = 0.237E+02 °K

TABLE A4

BLOWDOWN DISTRIBUTION FUNCTIONS

Statistics for Pk Cld Tmp (°K) based on 50000 histories:

Sample Mean Value	=	901.02594
Sample Standard Deviation	=	89.32980
Prob Pk Cld Tmp > 1000.00	=	0.13502
Prob Pk Cld Tmp > 1059.41	=	0.05000
Prob Pk Cld Tmp > 1130.21	-	0.01000

Pk Cld Tmp DISTRIBUTION PREDICTED BY FIT AND MONTE CARLO

Index	Pk Cld Tmp °K	PDF /°K	CDF
1	688.00	0.75000E-05	0.18000E-03
2	712.000	0.95000E-04	0.24600E-02
3	736.00	0.56583E-03	0.16040E-01
4	760.00	0.12942E-02	0.47100E-01
5	784.00	0.19642E-02	0.94240E-01
6	808.00	0.23700E-02	0.15112E+00
7	832.00	0.29400E-02	0.22168E+00
8	856.00	0.38216E-02	0.31340E+00
9	880.00	0.45891E-02	0.42354E+00
10	904.00	0.46366E-02	0.53482E+00
11	928.00	0.44408E-02	0.64140E+00
12	952.00	0.38241E-02	0.73317E+00
13	976.00	0.31408E-02	0.80855E+00
14	1000.00	0.23433E-02	0.86479E+00
15	1024.00	0.18008E-02	0.90801E+00
16	1048.00	0.12733E-02	0.93857E+00
17	1072.00	0.89834E-03	0.96013E+00
18	1096.00	0.66167E-03	0.97601E+00
19	1120.00	0.43083E-03	0.98635E+00
20	1144.00	0.31250E-03	0.99385E+00
21	1168.00	0.17833E-03	0.99813E+00
22	1192.00	0.64167E-04	0.99967E+00
23	1216.00	0.13333E-04	0.99999E+00
24	1240.00	0.00000E+00	0.99999E+00
25	1264.00	0.00000E+00	0.99999E+00

TABLE A5

EARLY REFLOOD DISTRIBUTION FUNCTIONS

Statistics for Pk Cld Tmp (°K) based on 50000 histories:

Sample Mean Value	=	798.62964
Sample Standard Deviation	=	128.35620
Prob Pk Cld Tmp > 1000.00	=	0.07597
Prob Pk Cld Tmp > 1032.74	=	0.05000
Prob Pk Cld Tmp > 1128.96	=	0.01000

Pk Cld Tmp DISTRIBUTION PREDICTED BY FIT AND MONTE CARLO

Index	Pk Cld Tmp °K	PDF /°K	CDF
1	524.00	0.61111E-05	0.22000E-03
2	560.00	0.19389E-03	0.72000E-02
3	596.00	0.65445E-03	0.30760E-01
4	632.00	0.14611E-02	0.83360E-01
5	668.00	0.21444E-02	0.16056E+00
6	704.00	0.26439E-02	0.25574E+00
7	740.00	0.30405E-02	0.36520E+00
8	776.00	0.30089E-02	0.47352E+00
9	812.00	0.28444E-02	0.57592E+00
10	848.00	0.25733E-02	0.66855E+00
11	884.00	0.22744E-02	0.75043E+00
12	920.00	0.19678E-02	0.82127E+00
13	956.00	0.15456E-02	0.87691E+00
14	992.00	0.10983E-02	0.91645E+00
15	1028.00	0.83945E-03	0.94667E+00
16	1064.00	0.63834E-03	0.96965E+00
17	1100.00	0.38667E-03	0.98357E+00
18	1136.00	0.21278E-03	0.99123E+00
19	1172.00	0.14056E-03	0.99629E+00
20	1208.00	0.65000E-04	0.99863E+00
21	1244.00	0.28889E-04	0.99967E+00
22	1280.00	0.77778E-05	0.99995E+00
23	1316.00	0.11111E-05	0.99999E+00
24	1352.00	0.00000E+00	0.99999E+00
25	1388.00	0.00000E+00	0.99999E+00

TABLE A6

LATE REFLOOD DISTRIBUTION FUNCTIONS

Statistics for Pk Cld Tmp (°K) based on 50000 histories:

Sample Mean Value	=	676.86517
Sample Standard Deviation	=	176.71304
Prob Pk Cld Tmp > 1000.00	=	0.04828
Prob Pk Cld Tmp > 997.47	=	0.05000
Prob Pk Cld Tmp > 1087.12	=	0.01000

Pk Cld Tmp DISTRIBUTION PREDICTED BY FIT AND MONTE CARLO

Index	Pk Cld Tmp °K	PDF /°K	CDF
1	388.00	0.83333E-06	0.40000E-04
2	436.00	0.53750E-03	0.25840E-01
3	484.00	0.19117E-02	0.11760E+00
4	532.00	0.30008E-02	0.26164E+00
5	580.00	0.26934E-02	0.39092E+00
6	628.00	0.20050E-02	0.48716E+00
7	676.00	0.16346E-02	0.56562E+00
8	724.00	0.14171E-02	0.63364E+00
9	772.00	0.13166E-02	0.69684E+00
10	820.00	0.12583E-02	0.75724E+00
11	868.00	0.12050E-02	0.81508E+00
12	916.00	0.12162E-02	0.87346E+00
13	964.00	0.10725E-02	0.92494E+00
14	1012.00	0.72792E-03	0.95988E+00
15	1060.00	0.48834E-03	0.98332E+00
16	1108.00	0.21500E-03	0.99364E+00
17	1156.00	0.84583E-04	0.99770E+00
18	1204.00	0.37500E-04	0.99950E+00
19	1252.00	0.95833E-05	0.99996E+00
20	1300.00	0.83333E-06	0.10000E+01

NRC FORM 335 (2-89) NRCM 1102, 3201, 3202

U.S. NUCLEAR REGULATORY COMMISSION

BIBLIOGRAPHIC DATA SHEET

(See instructions on the reverse)

1. REPORT NUMBER (Assigned by NRC. Add Vol., Supp., Rev., and Addendum Numbers, if any.)

NUREG/CR-5249
EGG-2552

2. TITLE AND SUBTITLE

Quantifying Reactor Safety Margins: Application of Code Scaling, Applicability, and Uncertainty Evaluation Methodology to a Large-Break, Loss-of-Coolant Accident

3. DATE REPORT PUBLISHED

MONTH	YEAR
December	1989

4. FIN OR GRANT NUMBER

A6868

5. AUTHOR(S)

B. Boyack, R. Duffey, P. Griffith, G. Lellouche, S. Levy, U. Rohatgi, G. Wilson, W. Wulff, N. Zuber, K. Katsma, D. Hall, R. Shaw, C. Fletcher, K. Boodry

6. TYPE OF REPORT

Research

7. PERIOD COVERED (Inclusive Dates)

8. PERFORMING ORGANIZATION – NAME AND ADDRESS (If NRC, provide Division, Office or Region, U.S. Nuclear Regulatory Commission, and mailing address; if contractor, provide name and mailing address.)

Idaho National Engineering Laboratory
EG&G Idaho, Inc.
Idaho Falls, ID 83415

9. SPONSORING ORGANIZATION – NAME AND ADDRESS (If NRC, type "Same as above"; if contractor, provide NRC Division, Office or Region, U.S. Nuclear Regulatory Commission, and mailing address.)

Division of Systems Research
Office of Nuclear Regulatory Research
U. S. Nuclear Regulatory Commission
Washington, D.

10. SUPPLEMENTARY NOTES

11. ABSTRACT (200 words or less)

The U.S. Nuclear Regulatory Commission (NRC) has issued a revised rule for loss-of-coolant accident/emergency core cooling system (ECCS) analysis of light water reactors to allow the use of best-estimate computer codes in safety analysis as an option. To support the revised ECCS rule and illustrate its application, the NRC and its contractors and consultants have developed and demonstrated an uncertainty evaluation methodology called code scaling, applicability, and uncertainty (CSAU).

The CSAU methodology and an example application described in this report demonstrate that uncertainties in complex phenomena can be quantified. The methodology is systematic and comprehensive as it addresses and integrates the scenario, experiments, code, and plant to resolve questions concerned with: (a) code capability to scale-up processes from test facility to full-scale nuclear power plants; (b) code applicability to safety studies of a postulated accident scenario in a specified nuclear power plant; and (c) quantifying uncertainties of calculated results. The methodology is able to address both uncertainties for which bias and distribution are quantifiable and uncertainties for which only a bounding value is quantifiable.

12. KEY WORDS/DESCRIPTORS (List words or phrases that will assist researchers in locating the report.)

code scaling, applicability, and uncertainty (CSAU)
large-break, loss-of-coolant accident (LBLOCA)

13. AVAILABILITY STATEMENT

Unlimited

14. SECURITY CLASSIFICATION

(This Page)
Unclassified

(This Report)
Unclassified

15. NUMBER OF PAGES

16. PRICE